

Pacific Northwest National Laboratory

Operated by Battelle for the
U.S. Department of Energy

Estimating Retained Gas Volumes in the Hanford Tanks using Waste Level Measurements

P.D. Whitney
G. Chen
P.A. Gauglitz

P.A. Meyer
N.E. Miller

RECEIVED
OCT 10 1997
OSTI

September 1997

Prepared for the U.S. Department of Energy
under Contract DE-AC06-76RLO 1830

PNNL-11693

DISCLAIMER

This report was prepared as an account of work sponsored by an agency of the United States Government. Neither the United States Government nor any agency thereof, nor Battelle Memorial Institute, nor any of their employees, makes any warranty, express or implied, or assumes any legal liability or responsibility for the accuracy, completeness, or usefulness of any information, apparatus, product, or process disclosed, or represents that its use would not infringe privately owned rights. Reference herein to any specific commercial product, process, or service by trade name, trademark, manufacturer, or otherwise does not necessarily constitute or imply its endorsement, recommendation, or favoring by the United States Government or any agency thereof, or Battelle Memorial Institute. The views and opinions of authors expressed herein do not necessarily state or reflect those of the United States Government or any agency thereof.

PACIFIC NORTHWEST NATIONAL LABORATORY

operated by

BATTELLE

for the

UNITED STATES DEPARTMENT OF ENERGY

under Contract DE-AC06-76RLO 1830

Printed in the United States of America

Available to DOE and DOE contractors from the
Office of Scientific and Technical Information, P.O. Box 62, Oak Ridge, TN 37831;
prices available from (615) 576-8401.

Available to the public from the National Technical Information Service,
U.S. Department of Commerce, 5285 Port Royal Rd., Springfield, VA 22161



The document was printed on recycled paper.

DISCLAIMER

**Portions of this document may be illegible
in electronic image products. Images are
produced from the best available original
document.**

Estimating Retained Gas Volumes in the Hanford Tanks using Waste Level Measurements

P.D. Whitney
G. Chen
P.A. Gauglitz

P.A. Meyer
N.E. Miller

September 1997

DISTRIBUTION OF THIS DOCUMENT IS UNLIMITED *ph*

MASTER

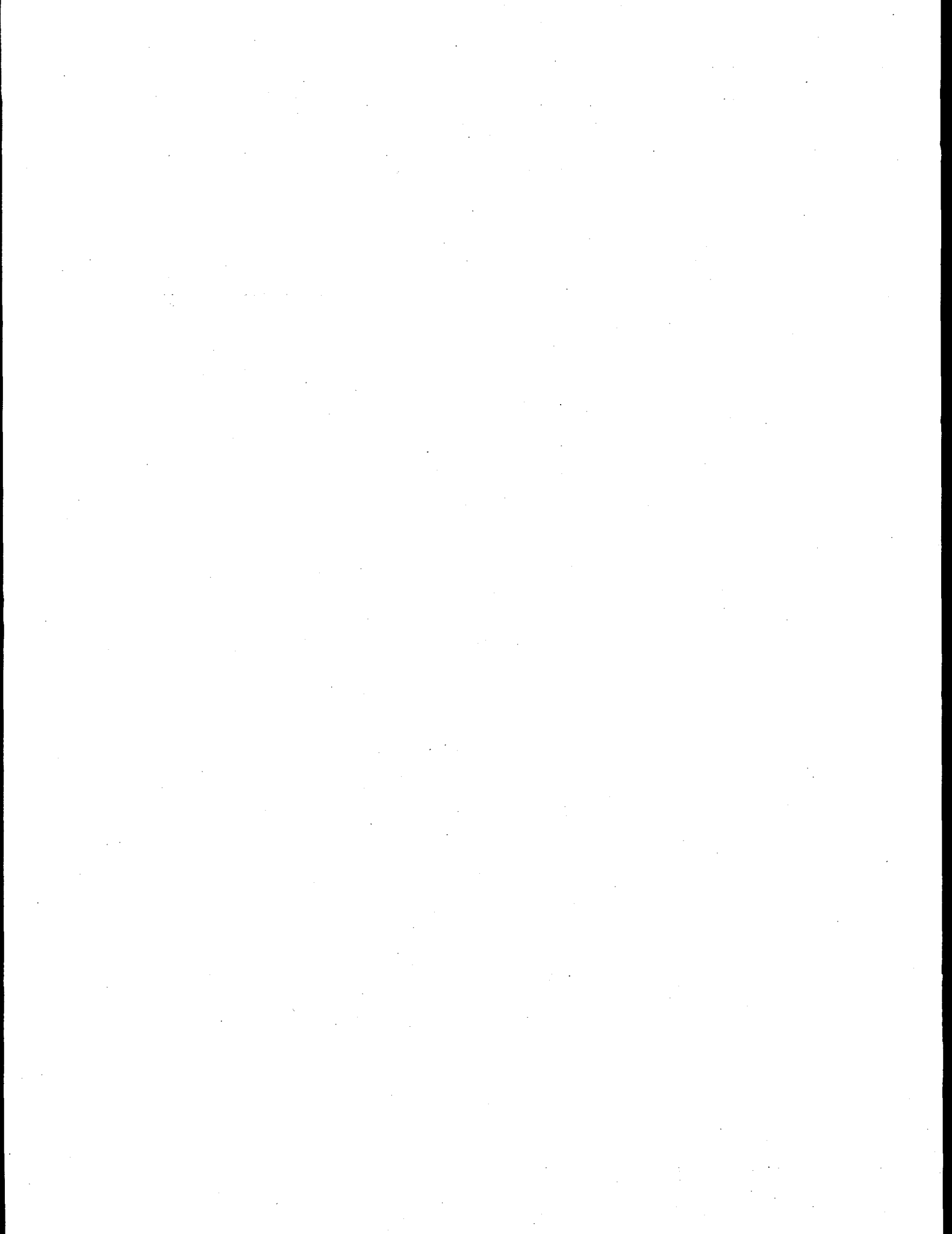
Prepared for the U.S. Department of Energy
under Contract DE-AC06-76RLO 1830

Summary

The Hanford site is home to 177 large, underground nuclear waste storage tanks. Safety and environmental concerns surround these tanks and their contents. One such concern is the propensity for the waste in these tanks to generate and trap flammable gases. This report focuses on understanding and improving the quality of retained gas volume estimates derived from tank waste level measurements. While direct measurements of gas volume are available for a small number of the Hanford tanks, the increasingly wide availability of tank waste level measurements provides an opportunity for less expensive (than direct gas volume measurement) assessment of gas hazard for the Hanford tanks.

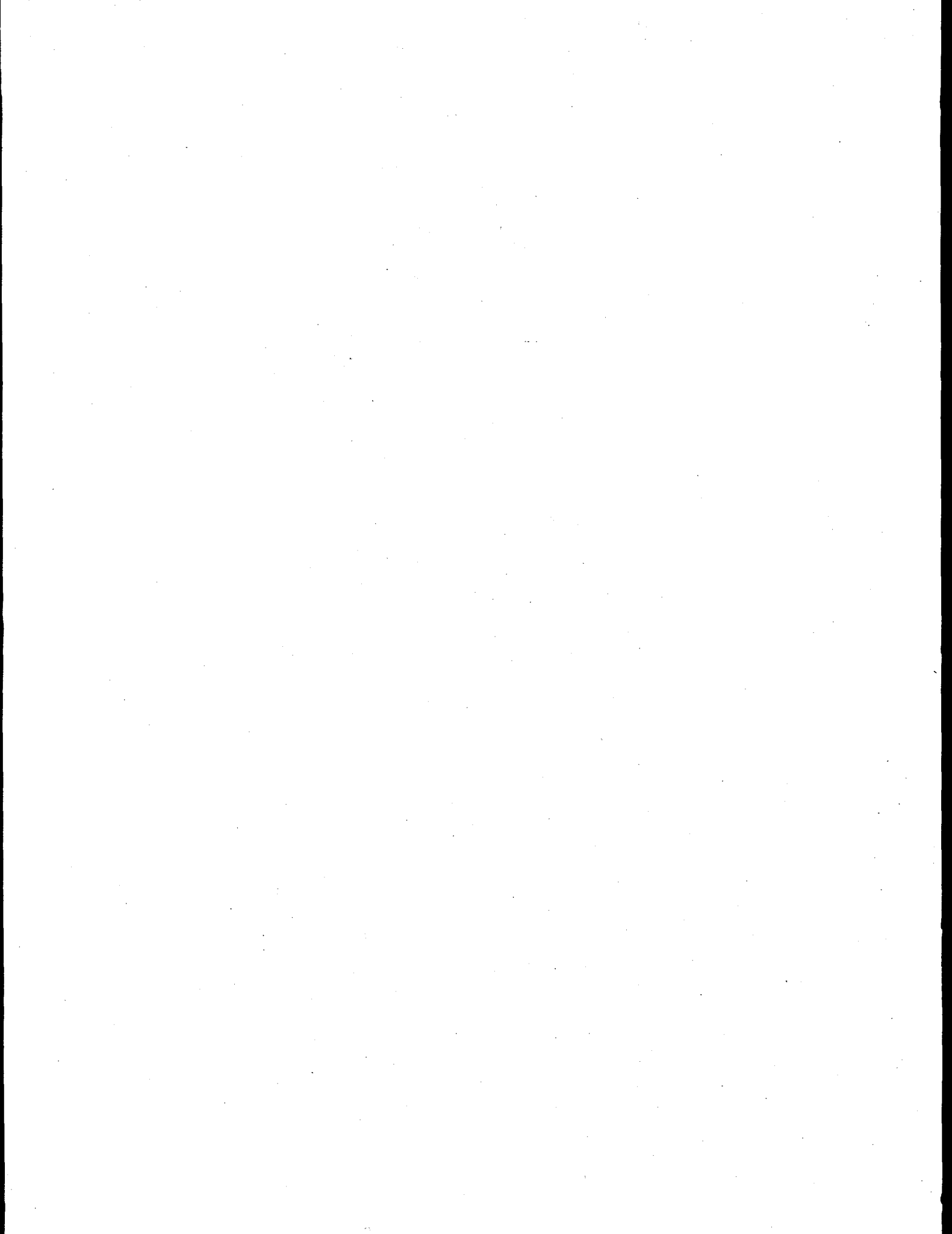
Retained gas in the tank waste is inferred from level measurements -- either long-term increase in the tank waste level, or fluctuations in tank waste level with atmospheric pressure changes. This report concentrates on the latter phenomena. As atmospheric pressure increases, the pressure on the gas in the tank waste increases, resulting in a level decrease (as long as the tank waste is "soft" enough). Tanks with waste levels exhibiting fluctuations inversely correlated with atmospheric pressure fluctuations were catalogued in an earlier study. Additionally, models incorporating ideal-gas law behavior and waste material properties have been proposed. These models explicitly relate the retained gas volume in the tank with the magnitude of the waste level fluctuations, dL/dP . This report describes how these models compare with the tank waste level measurements. Additionally, this report contains:

- New methodology for calculating dL/dP from tank waste levels -- the methodology is applied to tanks with suitably available level measurements, and incorporates aspects of waste strength. The estimates are compared with previous estimates, which were based solely on the ideal gas law.
- Experimental work -- Waste simulants containing retained gas were created, subjected to various pressure changes, and the waste levels recorded. For some experimental configurations, the behavior of the simulant tank waste was observed to be consistent with the simpler gas-law model. For waste simulants with sufficiently large shear strength, the level fluctuations were less than expected under the model. The level/pressure hysteresis that is observed in some tanks' waste levels was not evident in the experiments.
- Work towards evaluating the uncertainty of tank gas volume estimates from direct measurements -- For Tank A-101, the retained gas sampler measurements are compared with waste-level-based estimates related to retained gas volume. The two measurements compare well with each other for this tank.
- Comparison of dL/dP estimates from atmospheric pressure readings at weather stations around the Hanford site -- Atmospheric pressure measurements from weather stations surrounding the tank farms are used to calculate dL/dP summaries like those used to evaluate tanks for flammable gas hazard. The choice of weather station has a very small effect on dL/dP .
- Tank data summaries-- Detailed summaries of analyses provided for tank evaluations during the past year are gathered together in this report.



Acknowledgments

Discussions with Kevin Anderson of PNNL led to the linear methodology for estimating dL/dP_{STEEP} . Lenna Mahoney graciously provided detailed descriptions of the retained gas sampler data and calculation procedures. As always, thanks to the critical reviewers: Joe Brothers, Roger Bauer, Jerry Johnson, Blaine Barton, Kirk Remund and Frank Ryan.



Contents

Summary.....	iii
Acknowledgments	v
1. Introduction	1
1.1 Data Analysis and Modeling.....	2
1.2 Experimental Work.....	2
1.3 Report Outline	3
2. Inferring the Presence of Retained Gas via Fluctuations in Waste Level.....	5
2.1 Explanations of Tank Waste Level Fluctuations in Hanford Tanks.....	5
2.2 Refining the Model and Estimating Retained Gas Volume.....	7
2.3 Data.....	10
3. Estimating the Parallelogram Model Parameters from Tank Data	13
3.1 Nonlinear Parallelogram Parameter Estimation Methodology.....	13
3.2 Linear Parallelogram Parameter Estimation Methodology	14
3.3 Comparison of the Linear and Nonlinear Methodologies.....	17
3.4 Estimating dL/dP_{STEEP} with Daily Level Data	18
4. Estimating dL/dP Using Retained Gas Sampler (RGS) Data	21
4.1 Input Variables for Tank A-101.....	22
4.2 The Calculation Procedure.....	24
4.3 Results	26
4.4 Discussion of dL/dP Uncertainty Estimates.....	27
5. Data Analyses and Results	29
5.1 Summary of dL/dP_{STEEP} Calculations	29
5.2 Lag Between Pressure Change and Level Response.....	32
6. Experimental Study of Pressure/Level Response of Bubble Simulants.....	41
6.1 Experimental Apparatus and Method.....	41
6.2 Experimental Results and Discussion	45
6.3 Summary of Experimental Findings.....	49
7. Summary Findings and Recommendations	51
7.1 Results	51
7.2 Relevant Unexplained or Unstudied Phenomena.....	51
7.3 Miscellaneous Observations	52
8. References	53
Appendix A: Weather Station Location Effect on dL/dP	57
Appendix B: Effect of Small Gas Releases on Waste Level in SSTs	61
Procedure to Test Hypothesis.....	61
Discussion of Results	61
Appendix C: Information Provided for Tank Evaluations for FY97	65
Evaluation of Tank 241-BY-103.....	65
Evaluation of Tank 241-S-112	68
Evaluation of Tank 241-SX-106	70

Evaluation of Tank 241-T-108	72
Evaluation of Tank 241-T-111	73

List of Figures

Figure 2.1: Tank waste level measurements for Feb 97 for selected Hanford waste tanks. See Table 2.1 for a complete listing of the tanks.	6
Figure 2.2: Level and pressure phase space for the parallelogram model.....	8
Figure 2.3: Simulated tank waste level data.....	9
Figure 3.1: Tank waste level data (cm), atmospheric pressure data (kPa), and model fits.....	14
Figure 3.2: Pressure data used to determine time intervals in which the tank waste is in state S+ or S-.....	15
Figure 3.3: U-107 level (solid line) and HMS atmospheric pressure (dashed line) data over an interval used to estimate dL/dP_{STEEP}	16
Figure 3.4: U-107 data from Figure 3.3 with levels and pressures plotted against each other. The slopes of the lines estimate dL/dP_{STEEP}	17
Figure 3.5: Tank S-111 dL/dP_{STEEP} estimates from the nonlinear and linear estimation methodologies.	18
Figure 3.6: Comparison of dL/dP calculated from TMACS data with dL/dP calculated from daily (SACS) data. The data for this plot are listed in Table 3.2. The line plotted is $y=x$	19
Figure 4.1: A-101 gamma probe 3/16/95.....	22
Figure 4.2: RGS gas volume fraction estimates.....	23
Figure 4.3: Estimates of $-dL/dP$ from Tank A-101 RGS and tank surveillance data.....	25
Figure 5.1: Summary of dL/dP_{STEEP} estimates from the linear parallelogram method (solid boxes) compared with gas model dL/dP estimates (dashed boxes).....	32
Figure 5.2: Tank S-106 level compared with atmospheric pressure. The levels and pressures are shown as the solid and dashed lines, respectively.	33
Figure 5.3: Tank S-106 level (solid line) and corresponding atmospheric pressure (dashed line) data. The region shown in thicker lines will enter a dL/dP_{STEEP} calculation. The plot shows a time lag of about 5 hours between the pressure reversal and the corresponding level response.....	34
Figure 5.4: Tank S-106 dL/dP_{STEEP} estimates.....	38
Figure 5.5: Tank TY-102 dL/dP_{STEEP} estimates.....	39
Figure 6.1: Schematic of apparatus for measuring pressure/level response of bubbly sludges and slurries.	42
Figure 6.2: Level change during a series of pressure cycles for a 147 Pa bentonite clay with 10% gas (Experiment 1). The level/pressure response is nearly identical to the predicted ideal behavior.	46
Figure 6.3: Level pressure results for bubbly bentonite clays in the 4 in. ID test vessel, with a range of shear strengths and with known retained gas volumes (Experiments 1, 2, and 3).....	47
Figure 6.4: Level pressure results for bubbly bentonite clays in the 1 in. ID test vessel, with a range of shear strengths and with known gas contents (Experiments 4, 5, and 6).....	48
Figure 6.5: Level pressure results for bubbly slurry of 90 μ m glass beads in the 1 inch ID test vessel with a known gas content.....	49
Figure A.1: HMS weather station locations (from Hoitink 1994).....	57
Figure A.2: HMS barometric pressure measurements compared.....	58
Figure C.1: Comparison of Enraf level measurements and HMS atmospheric pressure for Tank BY-103.	66
Figure C.2: Summary dL/dP calculation for Tank 241-BY-103 neutron interstitial liquid levels. The units for dL/dP are inches per inches Hg.....	66
Figure C.3: Estimated dL/dP (cm per kPa) for Tank BY-103 based on the ILL data from November 1, 1995 through January 1, 1997.....	67
Figure C.4: Summary ILL calculation for Tank 241-S-112. The units for dL/dP are inches per inches Hg.....	68
Figure C.5: Estimated dL/dP (cm per kPa) for Tank S-112 based on the ILL data from the beginning of 1994 through February 1997.....	69
Figure C.6: Summary ILL calculation for Tank 241-SX-106.....	70
Figure C.7: Summary Enraf calculation for Tank 241-SX-106.....	71
Figure C.8: Summary FIC calculation for Tank 241-SX-106.....	71
Figure C.9: Summary Enraf calculation for Tank 241-T-108.....	72
Figure C.10: Summary Enraf calculation for Tank 241-T-111.....	73
Figure C.11: Summary ILL calculation for Tank 241-T-111.....	74

List of Tables

Table 2.1: Data used in this study. The data for tanks in TY and U farms were hourly interpolated before dL/dP estimation.....	11
Table 3.1: Comparison of $(dL/dP)_{STEEP}$ estimates for Tank S-111.....	18
Table 3.2: dL/dP from SACS and TMACS data for selected tanks.....	20
Table 4.1: Comparison of dL/dP estimates for Tank A-101.....	26
Table 4.2: In-situ gas volume fraction estimates in Tank A-101.....	26
Table 5.1: Summary of linear fitting of parallelogram model. The quantities in the dL/dP estimates columns are in units of inches per inches Hg.....	31
Table 5.2: Summary from simulated tank data.....	35
Table 5.3: Tank S-106 dL/dP _{STEEP} estimates for various time lags and 2τ values.....	36
Table 5.4: Tank S-107 dL/dP _{STEEP} estimates for various time lags and 2τ values.....	37
Table 5.5: Tank S-111 dL/dP _{STEEP} estimates for various time lags and 2τ values.....	37
Table 5.6: Tank TX-102 dL/dP _{STEEP} estimates for various time lags and 2τ values.....	38
Table 6.1: Bubbly simulants used in testing.....	44
Table 6.2: Comparison of estimated and measured gas volumes.....	48
Table A.1: dL/dP estimates for selected tanks and weather stations.....	58
Table B.1: Time windows centered at pressure low.....	61
Table B.2: Comparison of waste level model fits for gas release and non-gas release time periods.....	62

1. Introduction

The Hanford site is home to 177 large, underground nuclear waste storage tanks. Safety and environmental concerns surround these tanks and their contents. One such concern is the propensity for the waste in these tanks to generate and trap flammable gases. An overview of the flammable gas safety issue for the Hanford tanks is provided in Johnson et al (1997).

This report focuses on understanding and improving the quality of retained gas volume estimates derived from tank waste level measurements. The physical basis for the relationship between tank waste level estimates and retained gas volumes is discussed in detail in Whitney et al (1996), Whitney (1995) and Stewart et al (1996). The basis for the potential improvement over previous efforts is 1) the increasing availability of better tank waste level data and 2) a corresponding refinement in our understanding of the phenomena that relate waste level behavior and gas retained in the tank waste. In all of these models, a summary of the tank waste level response to atmospheric pressure changes, dL/dP , is estimated. This quantity is useful to estimate since it's directly related to the quantity of retained gas in the tank waste. Accurate estimates of retained gas from the level/pressure relationship are valuable because direct in-tank measurement of retained gas is expensive. This report includes a discussion of tank waste level data in light of recent developments in models relating retained gas volume to tank waste level; and a discussion of experimental work undertaken to examine these models.

The scientific basis for using tank waste level to detect retained gas in the tank waste is strong, and is supported by the following:

- Data: Tank waste levels fluctuate with atmospheric pressure changes (Whitney 1995).
- Physically based models: The fluctuations of the level measurements are consistent with physics based on the ideal gas law and, for some tanks, with the properties of the tank waste material (Whitney 1995, Whitney et al 1996, Stewart et al 1996).
- Experiments: This report documents the results of simple experiments with waste simulants, which show that waste levels change with atmospheric pressure in a manner consistent with the ideal gas law model.
- Validation from other measurements: The tanks for which a direct gas volume measurement has been taken (SY-101, SY-103, AN-103, AN-104, AN-105, A-101, U-103) show both a significant gas volume as measured directly, and a detectable gas volume via the dL/dP estimate.

The models also provide formulas for calculating retained gas volume from dL/dP . For double shell tanks 241-AN-103, 241-AN-104, 241-AN-105, 241-AW-101 and 241-SY-103, a comparison between the estimated retained gas volume obtained via level data and via direct measurements is reported in Meyer et al (1997). The two measurements were within 30% for in-situ retained gas volumes for these tanks and within 40% for standard volumes of retained gas.

This report contains a comparison for Tank 241-A-101 (A-101): the directly measured and level-based values of dL/dP are within 10% of each other and the gas volume fractions are within 15%.

1.1 Data Analysis and Modeling

The data analyses in this report focus on tanks with high-resolution surface level data; namely, those tanks with Enraf¹ level gauges connected to the Tank Monitoring and Control System (TMACS) data acquisition system. The following summarizes the work and findings of these analyses:

- New methodologies were derived to estimate dL/dP based on recent modeling developments. One of these estimation schemes, the "linear parallelogram estimation method," was tested and applied to the data from the 54 Hanford waste tanks for which suitable data were available.
- The methodology was tested by comparing results with similar methods for estimating dL/dP , and by applying the estimation methodology to model generated data. In the latter case, since the "true" dL/dP was known, the correctness of the methodology could be directly assessed. The dL/dP estimation methodology passed both tests.
- For tanks with a dL/dP noticeably different from zero (zero means no retained gas), the nominal value of the dL/dP estimate was larger in magnitude than the currently used estimate. Everything else being equal, a larger dL/dP results in a larger retained gas volume estimate; see Equation 2.1. See Table 5.1 and Figure 5.1 for details on this comparison of dL/dP estimates for the two methodologies.
- Deviations from the proposed model are evident in the data; both a time lag between the pressure change and the level response and some nonlinear behavior are observed. The effects of these deviations on retained gas volume estimation need to be assessed.
- A methodology is outlined for calculating gas volumes and dL/dP estimates from retained gas sampler (RGS) data, but this method omits some contributions to the uncertainty (see Section 4.4).

1.2 Experimental Work

A series of simple experiments were conducted to determine the level response of bubbly bentonite clay simulants to changes in pressure. The strength of the simulants ranged from 14 to 10,700 Pa, and the gas content, which was measured independently for each experiment, was about 10% gas volume. A single experiment was also conducted with a bubbly slurry (particulate simulant) composed of 90 μm glass beads in water. In all of the experiments, the retained gas was generated by incorporating a small amount of hydrogen peroxide that would decompose to generate bubbles of retained oxygen.

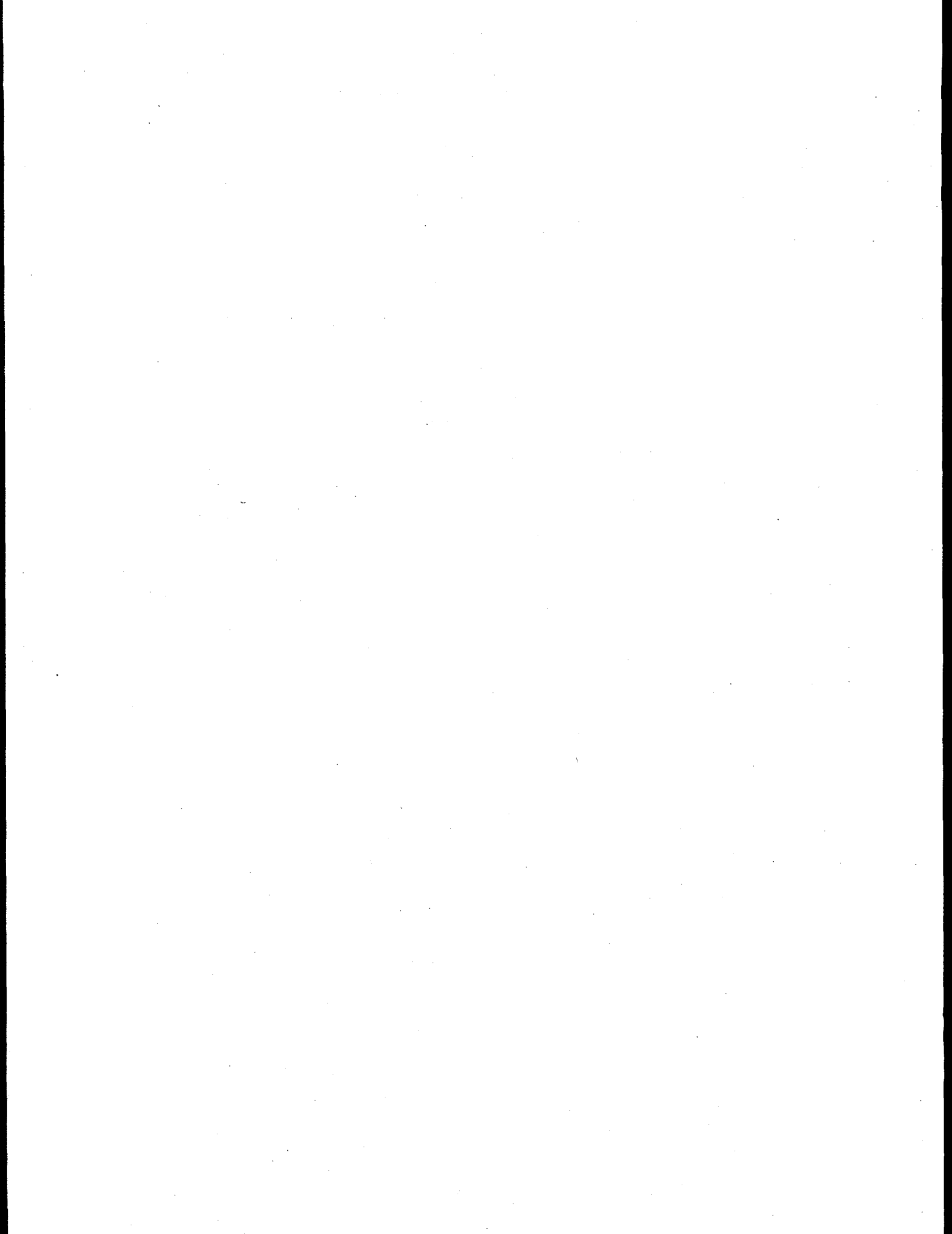
The results were:

- For most cases in the experiment, the pressure/level response provided an accurate estimate of retained gas volume.
- Material properties of the simulated sludge can mask the quantity of gas present. However, in these experiments the masking may be a wall effect (the simulated waste sticking to the wall of the container) and not a gas bubble/waste interaction phenomenon.
- No level/pressure hysteresis was observed for the simulants. A likely reason for this is that the simulants were not stiff enough for the hysteresis to be measurable.

¹ The Enraf 854 ATG level detector manufactured by Enraf Incorporated

1.3 Report Outline

Section 2 contains an overview of the phenomena used to infer and estimate retained gas volume from tank waste level measurements. Section 3 discusses the estimation procedures and algorithms used to extract the relevant parameter estimates from the level data. Section 4 presents methodology to estimate dL/dP and associated uncertainties from retained gas sampler data. Section 5 presents results of applying the methodology to the 54 Hanford tanks with suitable data and examines the lag observed between pressure changes and the level responses. Section 6 reviews the experimental work and the results of studies conducted to assess the effects of waste strength on retained gas volume estimation. Section 7 summarizes key (and miscellaneous) findings; discusses weaknesses of the current methodologies, and proposes how the weaknesses might be addressed. Section 8 is a list of references. Appendix A discusses the effect of weather station location on the dL/dP estimates. Appendix B considers the effects of small gas releases on the SST waste levels. Appendix C contains the data that were analyzed for the tank evaluations.



2. Inferring the Presence of Retained Gas via Fluctuations in Waste Level

This section presents an overview of how the presence of retained gas and retained gas volumes are inferred and estimated from tank waste level measurements. Section 2.1 briefly describes the estimation model based on the ideal gas law. Section 2.2 briefly describes how the model has been augmented with waste material properties. Section 2.3 contains details about the data used in this study.

2.1 *Explanations of Tank Waste Level Fluctuations in Hanford Tanks*

Synchronous fluctuations that are observed in the waste level data for some Hanford tanks are also inversely synchronous with atmospheric pressure fluctuations at Hanford. Figure 2.1 shows Hanford tank waste levels during February 1997 for the tanks examined in this report. The relative scales are the same for the level measurements shown. For a few of the tanks, the levels were spliced together for times at which the Enraf level instrument was recalibrated; the splice points are shown as "♦". Synchronous fluctuations in the level measurements are evident in some of these tanks (see Whitney (1995) for additional detail on other tanks). A natural explanation of these fluctuations is that the waste in these tanks contained trapped material in the gaseous phase, and that some of the waste in these tanks is "soft" enough to yield under atmospheric pressure changes. That is, as the atmospheric pressure increases, the retained gas in the tank waste decreases in volume, resulting in a level decrease. When the pressure decreases, the retained gas in the tank waste increases in volume, resulting in a level increase.

This phenomenology, in addition to Boyle's law, is sufficient to yield the following quantitative relation between retained gas volume and a summary value, dL/dP , of the waste level fluctuations that occur in conjunction with atmospheric pressure fluctuations:

$$\alpha = (P_{eff} / L) dL/dP, \quad (2.1)$$

where α is the gas volume fraction in the tank waste, P_{eff} is the effective pressure at which the gas is held in the tank waste, and L is the total depth of the tank waste. Variants of this equation relate retained gas volume, at either tank conditions or at standard temperature and pressure (STP), to dL/dP ; see Stewart et al (1996).

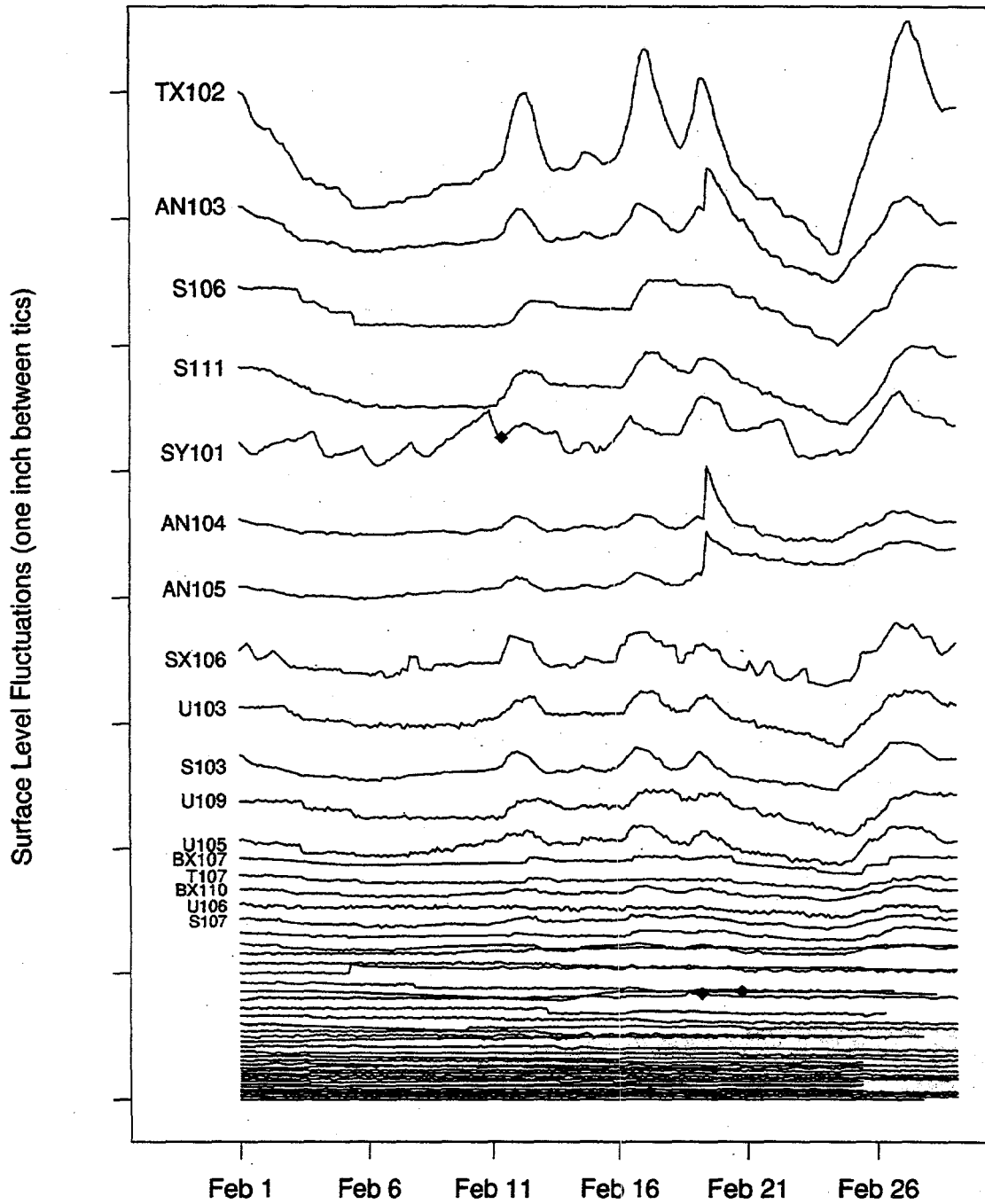


Figure 2.1: Tank waste level measurements for Feb 97 for selected Hanford waste tanks. See Table 2.1 for a complete listing of the tanks.

The quantity dL/dP has been estimated in a variety of ways. However, all the estimates are based on the following procedures:

1. The tank waste level data are extracted for the time interval of interest. The atmospheric pressures matching the times of the level measurements are also obtained.
2. The waste levels and pressures from Step 1 are paired according to the times of the observations, and a relation between the level and pressure is estimated (e.g., a linear regression of tank waste level on pressure). An estimate of dL/dP (the change in level corresponding to a unit change in pressure) is extracted from the estimated relation (e.g., the slope of the fitted linear regression).

2.2 *Refining the Model and Estimating Retained Gas Volume*

As better waste level data became available, it was evident that the model described in the previous subsection was not adequate to describe the behavior of waste levels in some of the tanks². In particular, comparisons of tank waste level with atmospheric pressure, which under the gas law model would show a linear relation, consistently showed more complicated (i.e., nonlinear) behavior. Figures 2.2 and 3.1 show this nonlinear behavior, as modeled and as seen in the data, respectively. Additional phenomenology was described in Whitney et al (1996) to account for some of this behavior in terms of the material properties of the tank waste.

Overview of the refined model

The model assumes that gas is present in the waste in the form of small, spherical bubbles. The waste is assumed to exhibit a linear elasticity with an elastic modulus E (in units of inches Hg) and a Poisson's ratio of η (dimensionless). When the pressure far from a bubble is increased or decreased, stresses are transmitted within the elastic waste that deform the bubble. If the surrounding pressure field is hydrostatic, then the deformations are radial. If pressure changes are large enough, circumferential stresses at the bubble walls can become large enough to break or fail the waste material. This failure is assumed to happen when induced stresses exceed the yield strength of the waste, τ . The bubble geometry, together with the assumed waste material properties, implies that yielding of the waste occurs after a total (external) pressure change of 2τ .

Once yielding has occurred, it is likely that plastic flow takes place. While this flow is a rate-dependent phenomenon that is, in general, complex, the model simply assumes free flow of the waste after yielding, as long as the pressure gradient does not reverse. Once the pressure gradient reverses, the model assumes that the waste "sets up" again, and flow does not occur until the net pressure change since the reversal again exceeds 2τ .

Figure 2.1 shows how the pressure and level can vary together according to this model. Three pressure decreases of the same magnitude are shown, along with the corresponding level changes. The first (rightmost) pressure change occurs at a reversal in the direction of the pressure gradient: (the pressure just changed from increasing to decreasing). The total pressure change shown is less than 2τ , the width of the parallelogram, and so the corresponding level change is determined by waste material properties. The next (middle) pressure change includes the point at which the waste yields. The final pressure change occurs in the region at which the waste has

² Flammable Gas Data Evaluation Progress Report, WTSFG96.1. P.D. Whitney, N.E. Wilkins, N.E. Miller, P.A. Meyer and M.E. Brewster.

yielded and is flowing freely. The corresponding level changes are indicated on the y-axis; the magnitude of the level change varies for the same magnitude of pressure change, depending on the initial state of the tank waste. According to the model, the level change corresponding with the leftmost pressure change satisfies Equation 2.1.

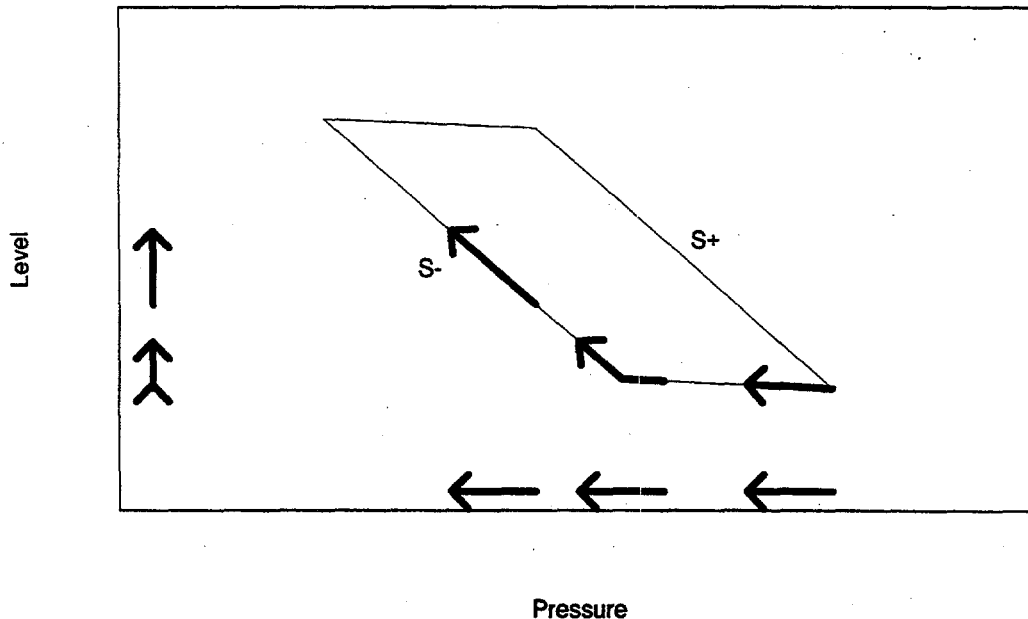


Figure 2.2: Level and pressure phase space for the parallelogram model.

Simulating tank level data from the parallelogram model

In the work reported here, simulated levels were used to test various aspects of the estimation schemes for retained gas volume. Additionally, the simulated levels are needed for the nonlinear parallelogram estimation methodology described in Section 3.1.

The model parameters required to generate the level response to pressure changes are:

- The steep slope common to both sides of the parallelogram is referred to as dL/dP_{STEP} . This slope is zero or negative; positive slopes have no physical interpretation. The waste is modeled as flowing freely in states S+ and S-. The states are distinguished from each other by the direction of the pressure gradient (see Section 3.2).
- The shallow slope for the base of the parallelogram. This slope is also zero or negative.
- 2τ , the width of the parallelogram, where τ is the yield strength.
- The starting positions for level and pressure on the parallelogram: These are the starting level and the initial pressure (or horizontal distance (in units of pressure) from the starting point to either S+ or S-).

Given the above parameters and an atmospheric pressure history, the model can generate a waste level history in response. Figure 2.3 shows simulated levels for input parameters $2\tau=0.3$, $dL/dP_{STEP} = -1$ (inches Hg), a shallow slope = -0.001 (inches Hg), initial level = 100 (inches), and initial position on S+. Additionally, a 5-hour time lag was inserted between the level response to pressure changes and the changes themselves. While such a lag does not appear explicitly in the

model, there is empirical evidence that some lag exists between pressure changes and the corresponding level changes; see Section 5.2 for a discussion of the lag. These simulated levels shown in Figure 2.3 strongly resemble Hanford tank waste level behaviors.

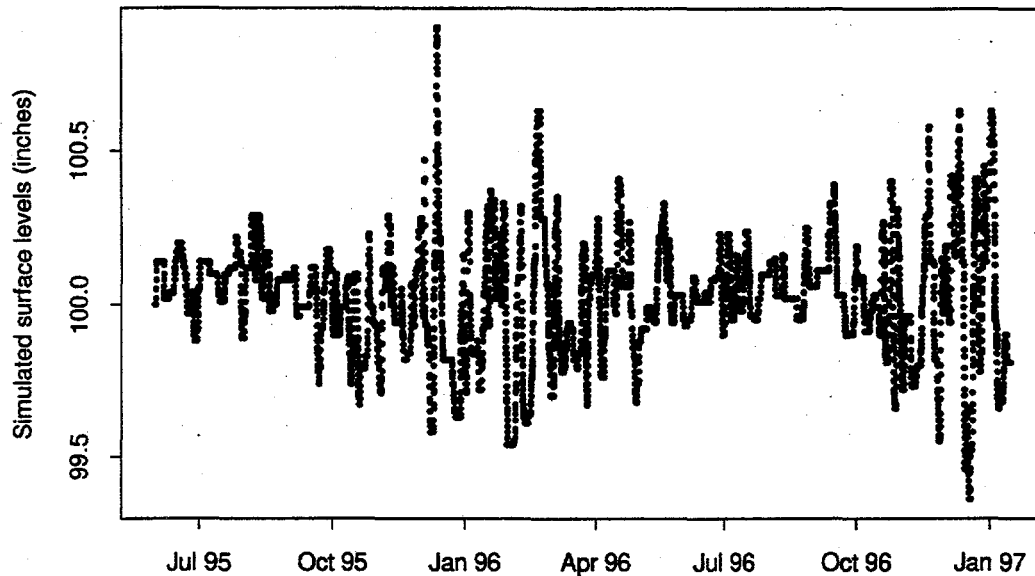


Figure 2.3: Simulated tank waste level data.

Apparent weaknesses in the model

There are still observed deviations of the data from model behavior. One of these deviations is an observed time lag. Another is the fact that the residuals in the nonlinear model never appear as white noise; that is, there is structure in the data which is not accounted for by any existing models. Both of these deviations from the model strongly suggest that more phenomena in the tank waste levels remain unexplained.

While we have attempted to correct for the time lag, and while the model does a good job of explaining many features of the tank waste level data, the lack of fit (in the details) of the model to the data remains, and can be seen in Figure 3.1. The lack of fit is also evident in the dL/dP_{STEEP} plots of Figures 5.4 and 5.5. The 95% error bars on the dL/dP_{STEEP} estimates of Figures 5.4 and 5.5 are derived by assuming that the model is correct, up to the limit of statistical noise. The error bars would be expected to overlap if 1) the model is correct and 2) the retained gas volume in the waste is approximately constant over a relatively long time (say a month or so). Since the error bars clearly fail to overlap, one of these assumptions is wrong. We interpret these poor fits as indicating that we do not have the phenomenology entirely correct. However, the parallelogram model does explain the data better than the gas law model for tanks showing a hysteresis in the level/pressure relation.

2.3 Data

The data used in this study are the Enraf level measurements available from TMACS³ through SACS⁴. These data were chosen because the Enraf level measurements are the most accurate waste level measurements available, and the frequency of observations is high.

While suitable measurements are available, waste levels in Tanks 241-SY-101 (SY-101) and 241-C-106 (C-106) were not considered for gas retention estimates in this report; because the waste in both tanks is constantly disturbed. The waste in Tank SY-101 is stirred every three days or so, and the waste in Tank C-106 undergoes a periodic (~60 day) water addition followed by a fairly rapid evaporation. Note that the effects of the stirring on SY-101 are evident as cusps that appear approximately every three days in Figure 2.1.

In the TMACS system, a measurement (and its time) is recorded when the current measurement differs from the previous recorded measurement by at least a "delta-band" amount. The delta-band is an input quantity. For instance, if the previous level measurement were 154.667, and the delta-band for this particular measurement stream is 0.01, then the next recorded measurement would occur when the measurement differs from 154.667 by at least 0.01.

The level data were "cleaned" by discarding large outliers. Finally, the level data for tanks in the TY and U tank farms were linearly interpolated to hourly readings (from the original more frequent readings), so that the computer program would not fail due to limitations in data processing. The use of the delta-band makes linear interpolation a fairly natural procedure: if measurements L_1 and L_2 are recorded at times T_1 and T_2 with a delta-band of $\delta=L_2-L_1$, then for any time T between T_1 and T_2 , we know that the level measurement device read between L_2 and L_1 . Linear interpolation of the level at time T using the data (T_1, L_1) and (T_2, L_2) results in an appropriate choice of L between L_1 and L_2 .

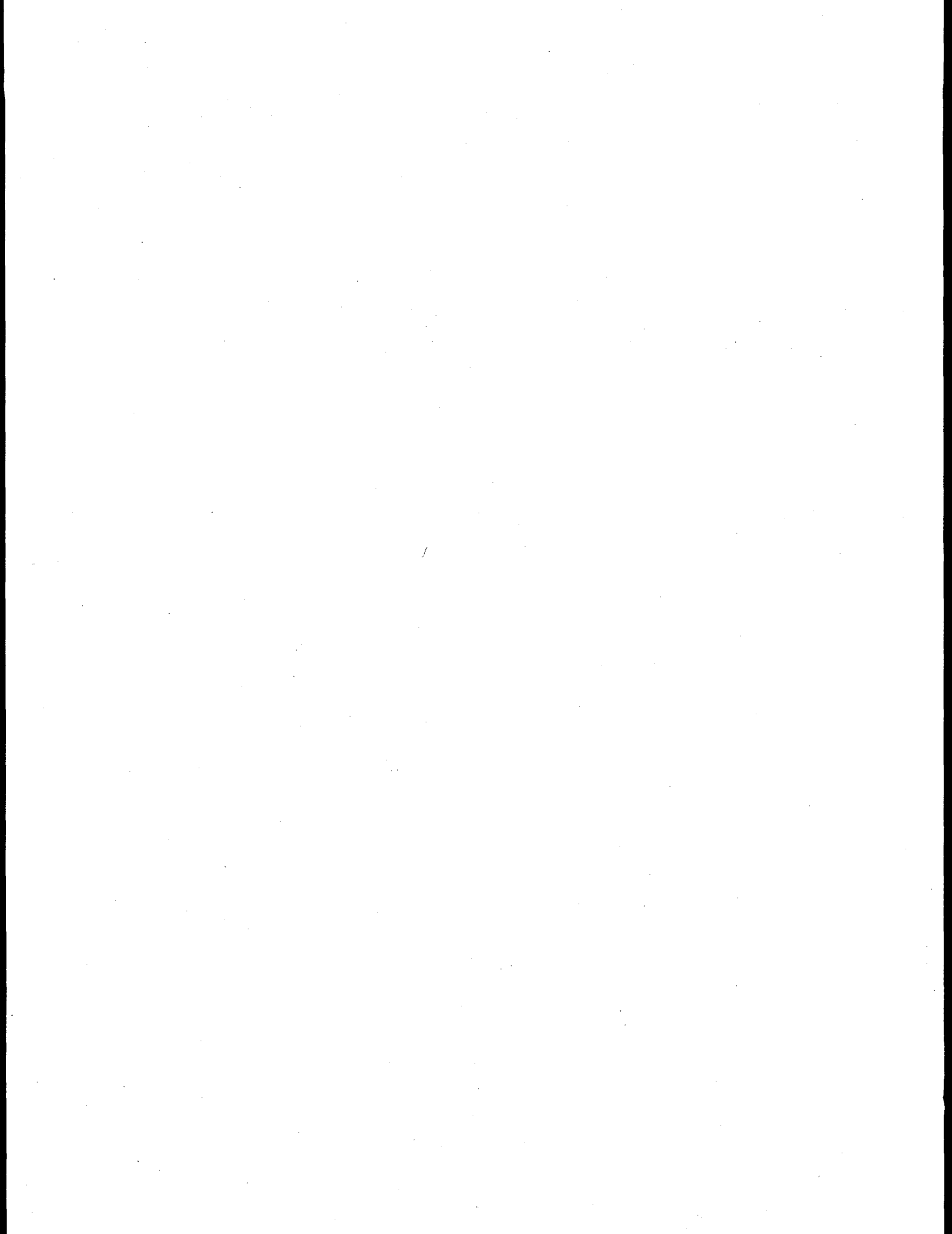
Table 2.1 summarizes the data used in this study. The columns under the heading "Data from TMACS" show the basic properties of the data as acquired from TMACS through SACS. The next three columns show the properties of the data after removal of outliers and, where necessary, linear interpolation. Linear interpolation is indicated by *italics* in the table.

³ Tank Monitoring and Control System

⁴ Surveillance Analysis Computer System, the database in which the tank waste level data are stored

Table 2.1: Data used in this study. The data for tanks in TY and U farms were hourly interpolated before dL/dP estimation.

Tank	Data from TMACS			Data after cleaning/interpolation		
	From	To	# of obs.	From	To	# of obs.
AN101	1/23/97	3/7/97	6,037	1/28/97	3/7/97	5,990
AN103	1/23/97	3/7/97	2,611	1/28/97	3/7/97	2,585
AN104	1/23/97	3/7/97	2,548	1/28/97	3/7/97	2,498
AN105	1/23/97	3/7/97	4,248	1/28/97	3/7/97	4,213
BX101	5/22/96	3/6/97	66,204	7/1/96	3/6/97	65,378
BX102	5/22/96	3/6/97	50,103	7/1/96	3/6/97	50,065
BX103	5/22/96	3/6/97	24,425	7/1/96	3/6/97	24,349
BX104	5/22/96	3/7/97	27,716	7/1/96	3/7/97	27,551
BX105	5/22/96	3/6/97	15,104	7/2/96	3/6/97	15,066
BX106	6/20/95	3/6/97	58,364	7/1/96	3/6/97	54,806
BX107	5/22/96	3/6/97	29,108	7/1/96	3/6/97	28,410
BX108	5/22/96	3/6/97	13,673	7/1/96	3/6/97	12,798
BX109	5/22/96	3/6/97	63,875	7/1/96	3/6/97	62,914
BX110	5/22/96	3/7/97	62,477	7/1/96	3/7/97	61,665
BX111	5/22/96	3/7/97	59,970	7/2/96	3/7/97	59,936
BX112	5/22/96	3/7/97	48,654	7/1/96	3/7/97	46,833
C103	5/10/95	3/7/97	161,953	10/2/95	3/7/97	161,893
C107	6/2/95	2/13/97	15,574	10/2/95	2/13/97	15,571
S103	6/2/95	3/7/97	22,930	8/15/95	3/7/97	22,923
S106	6/2/95	3/7/97	14,758	8/15/95	3/7/97	14,749
S107	6/2/95	3/7/97	16,177	8/15/95	3/7/97	16,170
S111	6/2/95	3/7/97	19,729	8/15/95	3/7/97	19,723
SX106	6/2/95	3/7/97	13,354	8/15/95	3/7/97	13,319
T102	6/12/95	3/7/97	30,211	6/12/95	3/7/97	30,210
T107	6/19/95	3/7/97	24,425	6/19/95	3/7/97	24,409
TX101	5/22/96	3/7/97	50,470	6/28/96	3/7/97	50,468
TX102	5/22/96	3/7/97	32,369	6/27/96	3/7/97	32,361
TX103	5/22/96	3/7/97	33,114	9/1/96	3/7/97	23,292
TX104	5/22/96	3/6/97	32,659	9/10/96	3/6/97	21,256
TX105	5/22/96	3/6/97	36,970	8/13/96	3/6/97	36,910
TX106	5/22/96	3/6/97	31,170	8/20/96	3/6/97	31,168
TX107	5/22/96	3/7/97	37,650	6/27/96	3/7/97	37,648
TX108	5/22/96	3/7/97	13,985	7/23/96	3/7/97	8,793
TX109	5/22/96	3/7/97	7,483	7/1/96	3/7/97	7,473
TX110	5/22/96	3/7/97	18,023	7/1/96	3/7/97	18,021
TX111	5/22/96	3/6/97	9,378	7/3/96	3/6/97	9,080
TX112	5/22/96	3/6/97	24,866	6/27/96	3/6/97	24,861
TX113	5/22/96	3/6/97	43,207	7/1/96	3/6/97	43,204
TX114	5/22/96	3/7/97	48,806	7/1/96	3/7/97	48,800
TX115	5/22/96	3/7/97	12,310	6/27/96	3/7/97	12,304
TX116	5/22/96	3/7/97	90,703	7/1/96	3/7/97	90,701
TX117	5/22/96	2/25/97	7,815	7/1/96	2/25/97	7,808
TX118	5/22/96	3/7/97	35,029	6/27/96	3/7/97	35,027
TY101	12/19/95	3/6/97	96,116	12/28/95	3/6/97	10,427
TY102	12/19/95	3/6/97	72,074	12/28/95	3/6/97	10,427
TY103	12/19/95	3/7/97	70,991	12/22/95	3/7/97	10,591
TY104	12/19/95	2/13/97	158,531	12/22/95	2/13/97	10,050
TY105	12/19/95	3/7/97	139,071	12/22/95	3/7/97	10,591
TY106	12/19/95	3/7/97	32,639	12/22/95	3/7/97	10,580
U103	6/12/95	3/7/97	43,116	6/12/95	3/7/97	15,218
U105	6/14/95	3/7/97	37,720	6/14/95	3/7/97	15,186
U106	6/14/95	3/7/97	55,303	6/14/95	3/7/97	15,191
U107	6/14/95	3/7/97	55,871	6/14/95	3/7/97	15,185
U109	6/14/95	3/7/97	35,890	6/14/95	3/7/97	15,185



3. Estimating the Parallelogram Model Parameters from Tank Data

Two approaches to estimating the model parameters are presented here. The two methodologies, referred to as the Nonlinear and the Linear parallelogram estimation methods, are presented respectively in Sections 3.1 and 3.2. The nonlinear approach has the potential to estimate all the model parameters, while the linear method estimates only the steep slope in the parallelogram. The results from the two estimation schemes are compared in Section 3.3. Additionally, Section 3.3 discusses other comparisons (data requirements, etc.) between the two methods.

The nonlinear methodology is discussed primarily for the sake of completeness and documentation: the results from this methodology were presented to the Sub-Panel on Tank Waste Chemical Reactions/Characterization/Retrieval on Dec 4, 1996⁵. However, the linear methodology is currently considered the prime candidate for providing dL/dP estimates to be used to calculate retained gas volumes, because it turned out to be more cost-effective, resulted in comparable retained-gas estimates (see section 3.3) and has greater utility (see section 3.4).

3.1 Nonlinear Parallelogram Parameter Estimation Methodology

The overall estimation strategy is referred to as nonlinear least-squares regression; there are numerous general references to it (see for instance, Gallant (1987)). This strategy is outlined in the remainder of this subsection.

The calculation in Section 2.2 describes how the model can be used to obtain predicted surface levels, given the input parameter values listed in that section. A sum of squares criterion for the parameters is:

$$\sum_{\text{data in the interval}} (\text{observed level} - \text{predicted level})^2 \quad (3.1)$$

where the *observed levels* are the actual level measurements from the SACS database and the *predicted levels* depend on the selected parameters. The parameters can be estimated by selecting parameter values that minimize Equation 3.1. A standard numerical optimization strategy was used to obtain the estimates. Typically, the estimates were obtained with the shallow slope parameter fixed to a small number (0.001 inches Hg) and with the initial level as the value of the first level measurement in an interval.

The estimation algorithm consists of the following steps:

1. Isolate a time window of the data. Typically, we selected windows of data corresponding to a single major pressure cycle.
2. Set initial parameter values, and choose which parameters are fixed (such as the steep slope) and which are estimated from the data in the interval.
3. Do the nonlinear least-squares calculation; the code used in the prototype system is based on Dennis and Schnabel (1983).

⁵ Letter FDH-9753233A R2 from A.M. Umek to J.K. McClusky, D.O.E. The Sub-Panel expressed concerns about the utility of using tank waste level measurements to quantify retained gas volumes. The letter pointed out that comparisons (such as those made in Meyer et al 1997) showed level-based retained gas volume estimates compared well with more direct measurements for the DSTs that are in the Flammable Gas Watch List.

The results from the algorithm are parameter estimates for the data in that particular time interval.

For a large enough pressure swing, we typically see that the nonlinear least-squares algorithm converges to a reasonable fit of the data, but that the fit misses some of the details! Figure 3.1 shows typical “good” fits. The pressure and level data are plotted as points, and the model fits are shown as lines. While the steep slopes estimated from the fits are consistent with trends in the data, there are details in the data that the model fits do not capture.

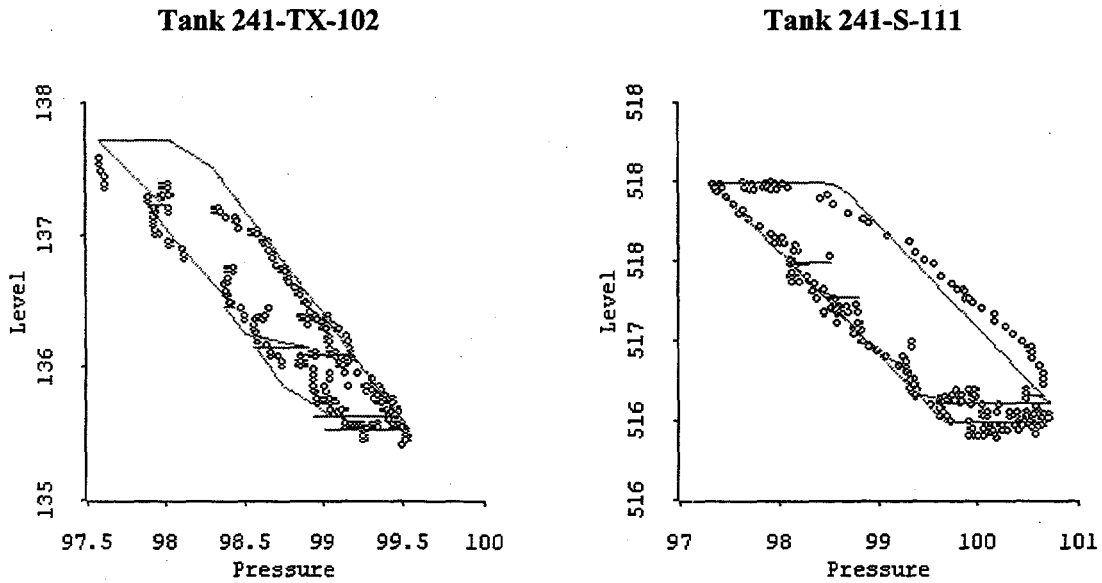


Figure 3.1: Tank waste level data (cm), atmospheric pressure data (kPa), and model fits.

3.2 Linear Parallelogram Parameter Estimation Methodology

The second methodology is based on the observation that the system is in either of the states S+ or S- just after a cumulative pressure change larger than 2τ has occurred (see Figure 2.2). In a time interval during which the system is in either state S+ or S-, a slope in the level vs. pressure relation is a dL/dP estimate that can be used in conjunction with the model described in Section 2 to estimate the retained gas in the tank waste. Figure 3.1 shows how the time intervals can be obtained from atmospheric pressure data.

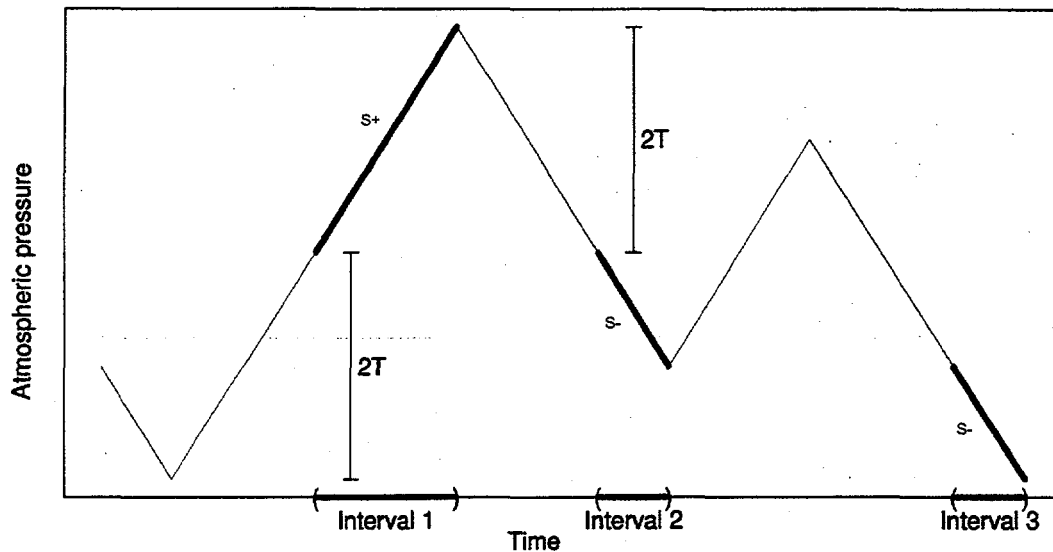


Figure 3.2: Pressure data used to determine time intervals in which the tank waste is in state S+ or S-.

The figure shows a fictitious sequence of pressure swings, and indicates when the tank waste must be in state S+ or S-; depending on the parameter 2τ . The pressure starts by decreasing a small amount and then increasing. When the total pressure increase since the last reversal is greater than 2τ , the tank waste must be in phase S+. The subsequent thicker line tracing the pressure history, and the corresponding times on the time axis, indicate that the waste is in this state. Next, the pressure begins to decrease. Once the total decrease since the last reversal exceeds 2τ , the tank waste is (according to the model) assumed to yield and to be in state S-. The subsequent, smaller, pressure excursion up and then back down places the tank waste in a state between S+ and S- (elastic yield). However, once the eventual pressure decrease gets back to the previous low, the waste returns to state S-.

The logic outlined above is used to isolate the time interval during which the waste has yielded, and thus for which the level pressure relationship satisfies Equation 2.1. In particular, levels and pressures for Interval 1 would be used to provide a dL/dP_{STEEP} estimate. The level and pressure data from Intervals 2 and 3 could also be used (or perhaps the union of these two intervals, if they're close enough together in time). These time intervals are those at the end of large pressure swings.

Figure 3.3 shows such an interval for Tank 241-U-107 (U-107) data. The figure shows both the level and time-matched atmospheric pressure data (from Hanford Meteorological Station, HMS) for one of the intervals. The bold portions for both level and pressure show the data actually in the selected interval; the data surrounding the time period of interest are also presented to provide context. Figure 3.4 shows the levels and pressures for this interval plotted against each other. Two linear fits are shown: the solid line is an ordinary least-squares fit of level against pressure data. The slope from this fit is a dL/dP_{STEEP} estimate. The dashed line is a "robust" linear

fit⁶. We considered using the robust fit because we anticipated that the potential time lag effects and misspecified 2τ parameters might cause some deviation from linearity in the relation between level and pressure, especially for the low or high pressures in the interval. Robust linear fits are designed to accommodate this kind of deviation from linearity. It turned out that the robust and least-squares fits provide the same overall summary (see Tables 5.2 to 5.6 later in the report). So the summary and analyses presented here are based on the commonly available and well-understood least-squares linear fits. Future analyses will include both the least-squares and robust slope estimates.

Tank 241-U-107 data from 8-7-95 to 8-8-95

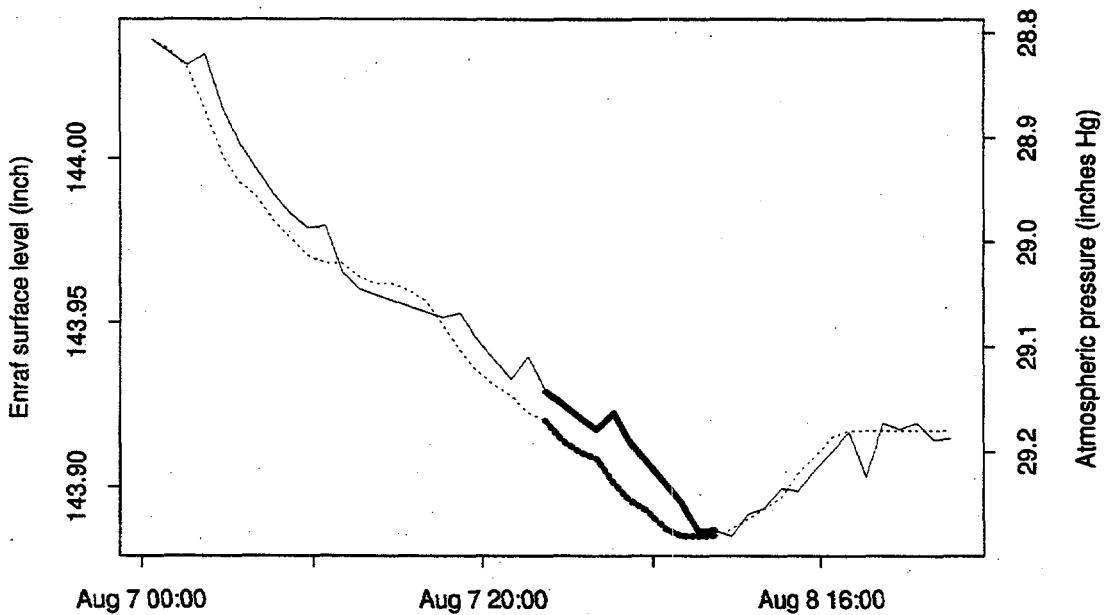


Figure 3.3: U-107 level (solid line) and HMS atmospheric pressure (dashed line) data over an interval used to estimate dL/dP_{STEEP} .

⁶ This particular robust linear fitting procedure was discussed and applied in Neerchal, N. and Whitney, P. 1995 Letter Report "Measurement Responses to Gas Release Events in Tank 241-SY-103"

Tank 241-U-107 data from 8-7-95 to 8-8-95

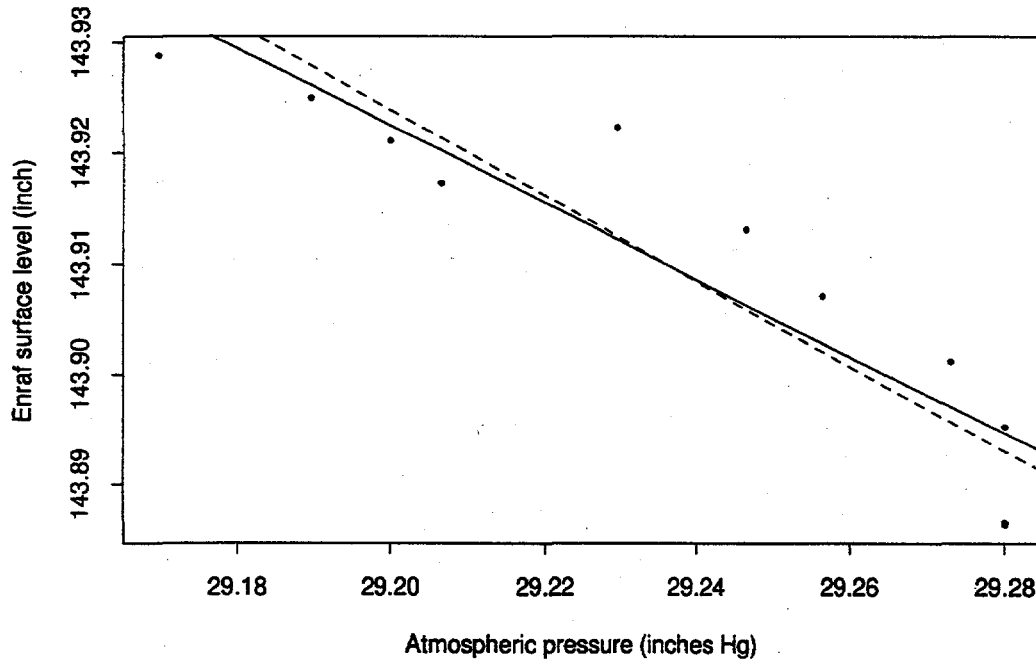


Figure 3.4: U-107 data from Figure 3.3 with levels and pressures plotted against each other. The slopes of the lines estimate dL/dP_{STEEP}

3.3 Comparison of the Linear and Nonlinear Methodologies

First a numerical comparison, based on Tank 241-S-111 (S-111) Enraf level data, is presented. Then, the algorithmic properties of the two estimation methodologies are compared. The nonlinear estimates were obtained by first breaking the data into 7-day intervals, and then fitting the model via nonlinear least-squares regression to each interval. The value of 7 days was chosen because it is a reasonably small interval but still tends to include the durations of significant pressure swings at Hanford. A fixed 2τ value of 0.2 inches Hg was used. The (nonlinear methodology) estimated steep slopes for each 7-day interval are plotted in Figure 3.5 with the character "N".

The linear estimates were obtained using the same underlying data. Values of $2\tau = 0.2$ and $2\tau = 0.4$ inches Hg were used. The estimates for $2\tau = 0.4$ are plotted in Figure 3.5 with the character "L". A more complete discussion of the choice of parameters for this and some other tanks appears in Section 5.2. Figure 3.5 shows that the two estimation schemes provide broadly the same view of this tank's dL/dP_{STEEP} estimates over time.

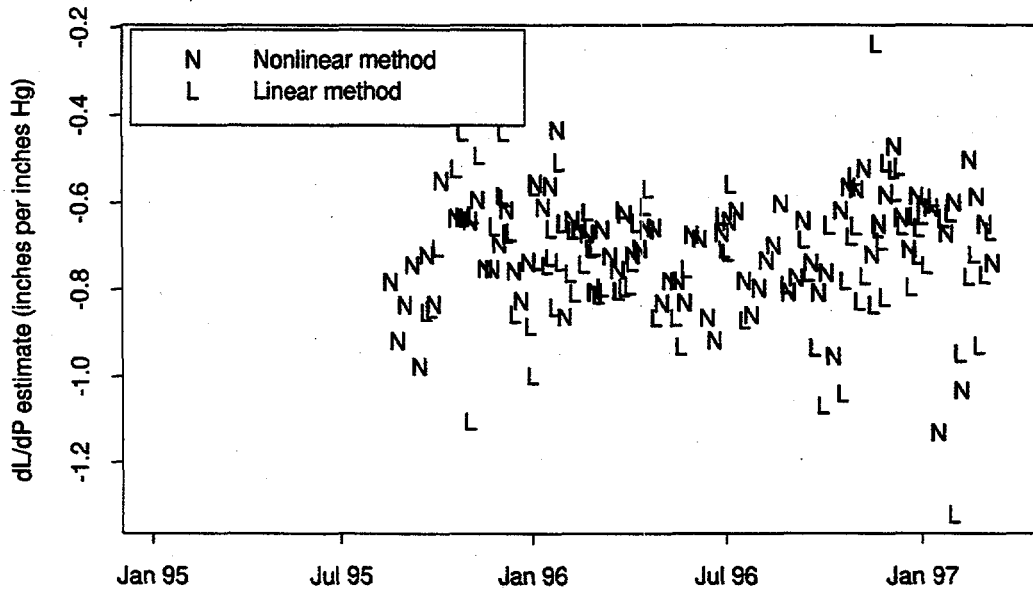


Figure 3.5: Tank S-111 dL/dP_{STEEP} estimates from the nonlinear and linear estimation methodologies.

Table 3.1 summarizes the two collections of estimates. Not only do the medians of the estimates obtained from the two methodologies agree well, so do the 25th and 75th percentile values. The agreement is better between the linear and nonlinear methods when the linear method uses the input parameter $2\tau=0.4$.

Table 3.1: Comparison of $(dL/dP)_{STEEP}$ estimates for Tank S-111.

Method	Min.	25%	Median	75%	Max.
Nonlinear	-1.13	-0.78	-0.70	-0.62	-0.43
Linear ($2\tau=0.2$)	-2.52	-0.72	-0.66	-0.57	-0.21
Linear ($2\tau=0.4$)	-1.32	-0.80	-0.71	-0.63	-0.24

As algorithms, the estimation methodologies differ significantly. The key differences are that the nonlinear method has the potential to provide estimates for all the model parameters, while the linear method provides estimates only of dL/dP_{STEEP} ; and computing the estimates using the nonlinear method is more problematic, due to standard issues in nonlinear optimization.

3.4 Estimating dL/dP_{STEEP} with Daily Level Data

The linear estimation strategy for obtaining dL/dP under the hysteresis model was initially conceived and tested on the TMACS level data. It turns out that the strategy is also applicable to the daily data available from the SACS database. It sometimes happens that a large pressure swing extends over several days, and so pairs or triplets of daily level measurements can occur in the intervals of interest. For tanks with both types of level data, TMACS-based and SACS-based dL/dP estimates were obtained and compared, Table 3.2. Note that only the Enraf level measurements are used in this comparison. Figure 3.6 compares the dL/dP values derived from

SACS and TMACS data for selected tanks with both data types. The line drawn on the plot is where the points would lie if the calculated values were identical. That the points do not deviate far from this line indicates that the daily values are adequate to obtain estimates of dL/dP under the hysteresis model.

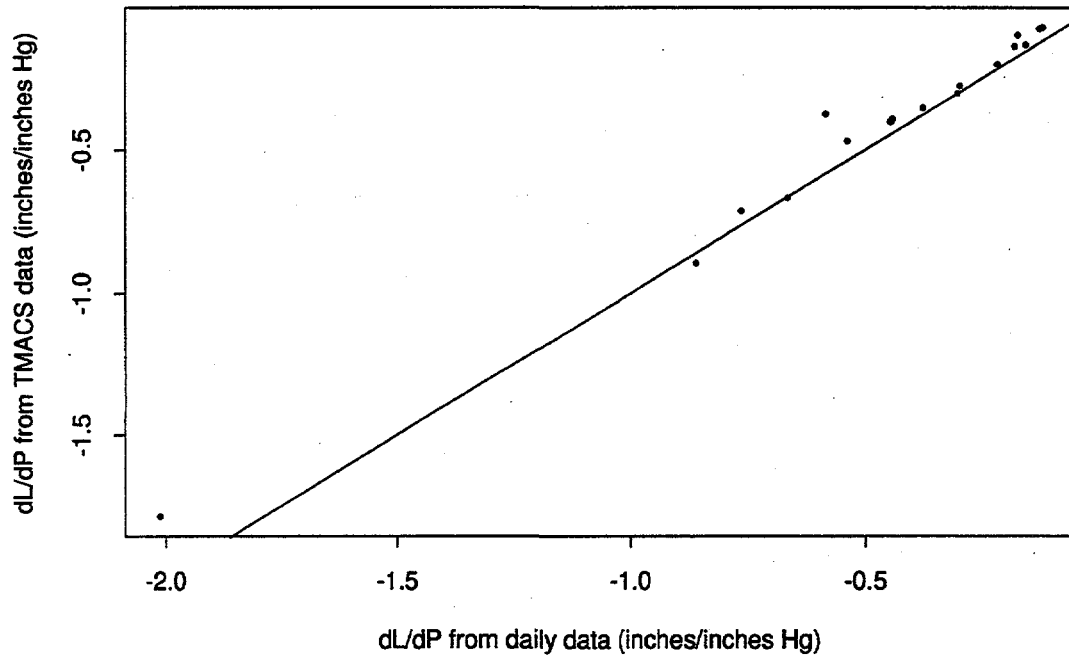


Figure 3.6: Comparison of dL/dP calculated from TMACS data with dL/dP calculated from daily (SACS) data. The data for this plot are listed in Table 3.2. The line plotted is $y=x$.

Table 3.2: dL/dP from SACS and TMACS data for selected tanks.

Tank	SACS Data dL/dP (inches/inches Hg)			TMACS Data dL/dP (inches/inches Hg)		
	1 st Quartile	Median	3rd Quartile	1 st Quartile	Median	3rd Quartile
AN103	-0.74	-0.66	-0.66	-0.88	-0.67	-0.65
AN104	-0.36	-0.30	-0.25	-0.46	-0.28	-0.24
AN105	-0.23	-0.22	-0.21	-0.28	-0.20	-0.16
BX104	-0.12	-0.12	-0.09	-0.11	-0.07	-0.04
BX107	-0.23	-0.17	-0.08	-0.16	-0.10	0.00
S103	-0.48	-0.44	-0.36	-0.42	-0.39	-0.33
S106	-1.05	-0.86	-0.56	-1.11	-0.89	-0.71
S107	-0.19	-0.16	-0.13	-0.16	-0.13	-0.11
S111	-0.82	-0.76	-0.64	-0.80	-0.71	-0.63
SX106	-0.57	-0.45	-0.36	-0.44	-0.40	-0.31
TX102	-2.12	-2.01	-1.78	-1.90	-1.79	-1.51
TX103	-0.19	-0.18	-0.14	-0.17	-0.14	-0.11
U103	-0.63	-0.54	-0.41	-0.56	-0.47	-0.38
U105	-0.47	-0.38	-0.29	-0.40	-0.36	-0.25
U106	-0.18	-0.13	-0.04	-0.13	-0.08	-0.01
U107	-0.39	-0.30	-0.26	-0.33	-0.30	-0.27
U109	-0.68	-0.58	-0.36	-0.45	-0.38	-0.24

4. Estimating dL/dP Using Retained Gas Sampler (RGS) Data

Gas volume in parts of the tank waste can be measured directly with the gas volume fraction instrument (VFI) or the retained gas sampler (RGS) (Stewart, et al., 1996, Shekarriz, et al., 1997). These measurements can be used to calculate dL/dP, which is then compared with dL/dP as estimated using waste surface level, to calibrate the use of dL/dP to estimate gas volume. The comparison of dL/dP for the two independent measurement sets translates directly to a comparison of retained gas volumes *assuming that the same effective pressure is used for the surface-level and RGS based dL/dP estimates*. This is because $\alpha = -dL/dP P_{eff}/L$ (Stewart et al 1996); the effective pressure enters into the comparison as a proportionality constant. Comparing RGS-based and level-based dL/dP is more straightforward than comparing the estimated gas volumes, since in comparing volumes the effective pressure must be taken into account. This section describes how dL/dP can be calculated from the RGS data. Additionally, in Section 4.3, a comparison of gas volume fractions estimated from RGS and from level measurements is given; the two are 15% apart.

It is assumed that the compressibility of tank waste is negligible compared with the compressibility of retained gas. Therefore, the volume of retained gas in a tank, or the gas volume fraction of the tank waste, is directly related to the magnitude of fluctuations of the waste surface level with respect to the changes in atmospheric pressure. The relationship between gas volume fraction and dL/dP is:

$$\frac{dL}{dP} = - \int_0^{Slvl} \frac{\alpha(l)}{P_{hyd}(l)} dl \quad (4.1)$$

where $\alpha(l)$ and $P_{hyd}(l)$ are the gas volume fraction and hydrostatic pressure at the elevation l , respectively, and $Slvl$ is the elevation of the waste surface. The data used in this calculation are basically independent of the observed surface level changes and independent of the atmospheric pressure. Therefore, a comparison of the dL/dP estimates based on this calculation with the estimates based on the observed surface level data can indicate whether it is appropriate to estimate the volume of retained gas in a tank using the surface level data.

A Monte Carlo simulation technique was employed to implement this estimation. The basic idea is to simulate a tank condition -- including the waste configuration, waste density, temperature, and gas volume fraction; and then calculate the dL/dP under the simulated condition. The distributions of these tank conditions are derived based on sampling or monitoring data. A series of such simulation runs will result in an empirical distribution of dL/dP. Both the mean and the uncertainty of the dL/dP values can be estimated from the distribution. The estimated uncertainty reflects the impacts of uncertainties associated with all tank conditions under consideration. It is difficult to assess this uncertainty analytically due to the complexity of the calculation process.

The estimation and comparison were conducted for Tank A-101, which is one of the two single-shell tanks with gas volume fraction measurements available. Section 4.1 describes the input variables used in the simulation. Section 4.2 discusses the calculation process. The results are summarized in Section 4.3. Some issues and potential improvements are discussed in Section 4.4.

4.1 *Input Variables for Tank A-101*

Four major factors were considered in simulating a tank condition. These factors are: waste configuration, waste density, temperature, and gas volume fraction. Each factor includes one or more variables, as discussed below.

Waste Configuration

This factor includes waste surface level and the boundaries between waste layers. Shekarriz et al. (1997) used temperature data to infer two distinct layers in the tank waste. The gamma log, shown in Figure 4.1, also suggests two distinct layers. Accordingly, the model contains two variables to describe this configuration: waste surface level, and layer boundary.

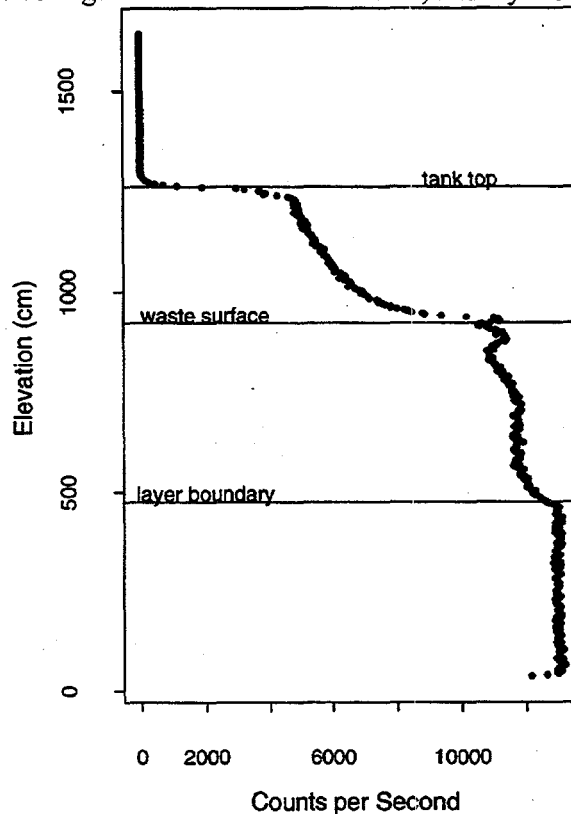


Figure 4.1: A-101 gamma probe 3/16/95

a) waste surface level: assumed to have a uniform distribution between 880 cm and 940 cm (measured from the bottom of the tank). This distribution was derived using surface level measurements, gamma logging data and the report on the Shekarriz, et al. (1997) study.

b) layer boundary: assumed to have a uniform distribution between 465cm and 498cm. The range of the boundary was estimated using gamma-logging data.

Waste Density

The waste density is considered to be homogeneous within each layer. The density in the upper layer is assumed to have a normal distribution, with mean 1.62 (g/cc) and standard deviation 0.08. The density in the lower layer is also assumed to have a normal distribution, with mean 1.7 (g/cc) and standard deviation 0.1. The two distributions are assumed to be independent. The values of the distribution parameters are based on the Shekarriz (1997) report and on other tank sample data from TWINS (PNL 1994).

Temperature

The temperature data are used in calculating in-situ gas volume fractions at each sample location. Therefore, only temperatures at the seven sample locations are needed. The temperature at each location is assumed to have a normal distribution, with a mean and standard deviation at the values used in Shekarriz et al. (1997). These distributions are considered to be independent.

Gas Volume Fraction

Seven sample segments were taken from Tank A-101 using the retained gas sampler. The in-situ gas volume fraction estimates provided in the Shekarriz et al. (1997) are plotted in Figure 4.2. These results can be used directly to simulate the realizations of the gas volume fractions at these sample locations. However, the in-situ gas volume fractions depend on the tank temperatures, waste densities and waste configuration. It is more appropriate to simulate a realization of gas volume fractions using the simulated tank condition along with the measured retained gas volume in each sample at standard conditions. According to the gas volume fraction calculation procedure used in Shakarriz et al (1997), the retained gas volume in each sample is measured in terms of the number of moles per liter of waste for each gas constituent. These mole numbers are used as the input variables for the gas volume fraction factor. It is assumed that the mole number for each species has a normal distribution, with mean and standard deviation values as reported in Shakarriz et al (1997).

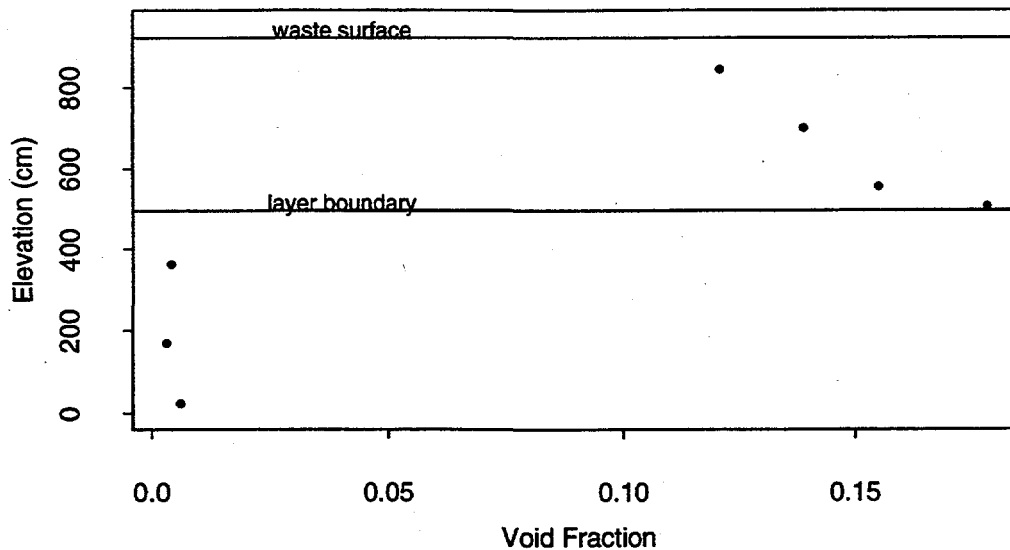


Figure 4.2: RGS gas volume fraction estimates

4.2 The Calculation Procedure

In each simulation run, dL/dP is calculated based on Equation 4.1. The integration is carried out numerically. Specifically, the tank waste is divided into many thin slices, and the local gas volume fraction and hydrostatic pressure are calculated. Both gas volume fraction and hydrostatic pressure are assumed to be homogeneous within each slice. Horizontal spatial variability is not taken into account, because there is not enough information to support its assessment. The contribution of each slice can then be obtained using the formula, and the dL/dP of the waste surface is estimated by summing the contributions of all the slices. The two quantities that need to be calculated for each slice are gas volume fraction and hydrostatic pressure. Further calculation details for these two quantities are given below.

a) Gas Volume Fraction Calculation

The gas volume fraction for each slice of the waste is obtained in two steps. First, the gas volume fraction of each sample is calculated from the moles of gas extracted from the tank waste. Second, an extrapolation is conducted to estimate the gas volume fraction for each slice.

1) Gas volume fraction of each sample

The in-situ gas volume fraction of each sample is calculated using the same procedure as in the RGS gas volume fraction calculation. Specifically, the following non-linear equation set is solved:

$$p_i = \frac{n_{i,tot} / V_{tot}}{\frac{\alpha}{RT} + (1-\alpha) * K_{H,i}}, \quad i = 1, 2, \dots, 8 \quad (4.2)$$

and

$$p_{hyd} = p_{H_2O} + \sum_i p_i \quad (4.3)$$

where

- p_i : partial pressure of the i th gas constituent, unknown
- $n_{i,tot}$: total number of moles of the i th gas constituent
- V_{tot} : sample volume
- $K_{H,i}$: Henry's law constant for the i th gas constituent
- p_{H_2O} : water vapor pressure
- p_{hyd} : hydrostatic pressure at sample location
- R : ideal gas law constant
- T : temperature (K)

Among these quantities, the p_i values are unknown and are solved for along with the gas volume fraction. V_{tot} is considered to be constant for each sample and its uncertainty is negligible. $K_{H,i}$ and p_{H_2O} are estimated based on the waste composition, and are also considered to be constant for each sample. These values are obtained from the spreadsheet of RGS calculations for Tank A-101 (Mahoney 1997). p_{hyd} is actually a function of the gas volume fraction, and its calculation is discussed later in this section.

The gas volume fractions of seven samples are estimated in each simulation run. The result is an empirical distribution of gas volume fraction for each sample. These distributions provide a useful check for comparison with the results of the RGS gas volume fraction calculation.

2) Gas volume fraction for each slice of waste

Several ways of conducting the extrapolation are possible. For instance, a model may be fitted as a function of elevation, based on the sample gas volume fractions. The model predictions can then be used for each slice. The reported RGS gas volume fraction results (see Figure 4.2) show small magnitudes and little variation in the lower layer of the waste. Therefore, the choice of extrapolation method will not have much impact on the result. In the upper layer, however, the gas volume fraction shows an apparent curve over the elevation. A quadratic model would also be a reasonable choice if the model fitting method were used for extrapolation.

Considering the small number of observations available, a simple method is chosen for the extrapolation, as follows. For any slice of the waste, the gas volume fraction takes the value of the nearest sample gas volume fraction. In other words, the gas volume fraction is assumed to be a step function of the elevation, with the estimated sample gas volume fractions as the step values, and the midpoint of two successive sample locations as the breakpoint.

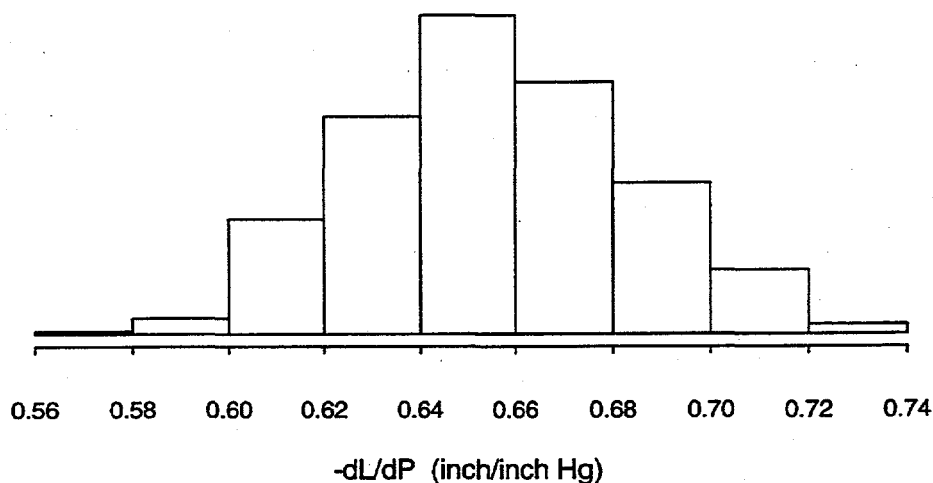


Figure 4.3: Estimates of $-dL/dP$ from Tank A-101 RGS and tank surveillance data

b) Hydrostatic Pressure Calculation

The hydrostatic pressure, p_{hyd} , at elevation l is calculated using Equation 4.4:

$$p_{hyd} = p_{atm} + \int_L^{S/l} (1 - \alpha(l)) \rho(l) dl \quad (4.4)$$

where P_{atm} is the standard atmospheric pressure, Δ is waste density, and l is elevation. This indicates that P_{hyd} is a function of gas volume fraction α . For the gas volume fraction calculation, P_{hyd} and the unknown α values are found by applying Equation 4.3. For the dL/dP calculation, P_{hyd} is evaluated using the gas volume fraction for each slice.

4.3 Results

A simulation with 500 runs yielded a dL/dP estimate for Tank A-101 with a mean of -0.65 (inch/inch-Hg) and a standard deviation of 0.028 (inch/inch-Hg). The standard deviation estimate appears unreasonably low (less than 5% of the mean estimate). The histogram of the simulation outputs is shown in Figure 4.3. Possible reasons for the small calculated uncertainty will be discussed later.

This result is compared with the dL/dP estimates based on waste level data, i.e., with the Enraf data for Tank A-101 with a two-hour lag. The results from both methods are shown in Table 4.1. The table indicates that the estimates are in reasonable agreement. The magnitude of the median from RGS estimates is slightly larger than the median from waste level estimates, with a relative difference of about 10%. The ranges between the first and third quartiles, however, are quite different for the two methods. The range for the RGS method is only about 1/3 of the range for the waste level method.

Table 4.1: Comparison of dL/dP estimates for Tank A-101

Method	1st Quartile (inch/inch Hg)	Median (inch/inch Hg)	3rd Quartile (inch/inch Hg)
RGS	-0.67	-0.65	-0.62
Waste Level	-0.63	-0.59	-0.50

Other results of the simulation study are the estimates of sample gas volume fractions and associated uncertainties. These results, along with the gas volume fraction estimates from Shekarriz et al. (1997), are listed in Table 4.2.

Table 4.2: In-situ gas volume fraction estimates in Tank A-101

Segment	Shekarriz et al (1997)	Simulation
24-2	0.121±0.0090	0.121±0.0085
15-5	0.139±0.0110	0.140±0.0047
15-8	0.155±0.0150	0.155±0.0059
24-9	0.178±0.0110	0.182±0.0071
15-12	0.004±0.0004	0.004±0.0004
24-16	0.003±0.0004	0.004±0.0003
24-19	0.006±0.0005	0.006±0.0004

The mean gas volume fraction estimates by both methods agree quite well for all segments. This agreement is evidence that the simulation-based calculation procedure for gas volume fraction is consistent with the RGS calculation procedure. This, in turn, provides more confidence in the mean estimate of dL/dP . However, the uncertainty estimates for the two methods show substantial differences for Segments 15-5, 15-8, and 24-9, which are all in the upper waste layer. The uncertainty estimates from the simulation are 35% to 60% smaller than those from the Shekarriz et al. (1997) report. A possible cause for these discrepancies is that a different procedure was used for uncertainty estimation in the spreadsheet calculation. In that procedure, the ideal gas law (see Equation 3.3.4 in the Shekarriz et al. (1997) report) was used to estimate the uncertainty, without phase partitioning. In other words, the uncertainty was assessed assuming that all gases are in the vapor phase and that there is no condensation. However, the mean gas volume fractions were estimated with phase partitioning taken into account (see Equation 4.2). The simulation procedure, on the other hand, propagates the uncertainties from input variables in exactly the same way as the mean gas volume fractions were estimated. Therefore, the resulting simulation-based uncertainties represent the uncertainties associated with only the vapor phase portion of retained gas, and are expected to be smaller than the uncertainties associated with both phases. However, it is not clear at this point whether this procedural difference would be expected to result in such large differences in uncertainty.

An estimated gas-volume-fraction for Tank A-101 is available from information independent of the RGS. The Tank A-101 characterization report (Field et al 1997) contains the observation that A-101 tank waste has an upper "solid" and lower liquid layer. We assume that almost all of the retained gas is in the upper layer. An effective pressure is calculated using the average density of the upper layer and the assumption that the gas is contained at a level in the solid layer 75% from the top. The density used, 1.69 g/mL, was obtained by averaging the density measurements from segments 1-9 in table B2-53 of Field et al (1997). These segments were identified as being in the upper layer by using the estimated layer boundary of 4.72m from the A-101 report, and the core segment elevations available from Shekarriz et al (1997). The assumption that the gas is contained at about 75%-level is consistent with earlier analyses (Hodgson et al, 1996). The resulting gas volume fraction in the upper layer is calculated as $(-dL/dP) P_{eff}/L = 0.59 * (29.92 + 15.12)/(412/2.54) = 0.164$. The identification between the formula and the calculation is that $dL/dP = -0.59$ inches per inches Hg, $P_{eff} = (29.92 + 15.12)$ inches Hg (atmospheric + waste pressure), and L , the thickness of the upper layer, is 412/2.54 inches. By comparison, Shekarriz et al (1997) reports 0.142 as the gas volume fraction in the upper layer. These two estimates are about 15% apart.

4.4 *Discussion of dL/dP Uncertainty Estimates*

The uncertainty estimates of dL/dP calculated in this report from the RGS data seem unreasonably low. The following contributing factors to these low uncertainties have been identified:

- The horizontal spatial variability of gas volume fractions is not included in the calculation of uncertainty, because not enough gas volume fraction observations were available for Tank A-101 to estimate their contribution to overall uncertainty.
- The current RGS calculation procedures assume that the gas constituents in a sample are distributed independently, but they are actually correlated (i.e., they sum to one mole). A

further study would be required to assess and incorporate the correlation structure, which would benefit the uncertainty assessment for both gas volume fraction and dL/dP work.

- The Henry's law constants used in gas volume fraction calculations are estimated based on waste compositions. The uncertainties associated with these constants are not included in the RGS calculations.

5. Data Analyses and Results

Estimates of dL/dP_{STEEP} were calculated for each Hanford waste tank with Enraf measurements available from TMACS. Section 5.1 summarizes the dL/dP_{STEEP} estimates and compares them with dL/dP estimates obtained previously, without the benefit of the refined model and the high frequency Enraf data. Section 5.2 presents a study of the time lag between level response and pressure changes for Tanks S-106, S-107, S-111, and TX-102. Additionally, the simulated data shown previously is analyzed, providing some verification that the estimation techniques are accurate and correctly implemented.

5.1 Summary of dL/dP_{STEEP} Calculations

Figure 5.1 and Table 5.1 present summaries of the dL/dP_{STEEP} calculations for the tanks with suitable data. Both the figure and the table additionally present summaries of similar quantities as currently calculated (using daily level measurements and the model based only on the ideal gas law). The comparisons are not exactly fair, since they are based on different data sets. The linear parallelogram dL/dP_{STEEP} estimation methodology requires data from TMACS, while the gas law methodology accepts data from daily or even weekly readings. Additionally, the linear parallelogram methodology for dL/dP_{STEEP} aggregates information over much shorter time periods (often less than a day) than the gas law method (typically aggregating over 15 days).

Summaries of dL/dP_{STEEP} (in units of inches of level per inches Hg) from the linear parallelogram model are shown in columns 2 through 4 of Table 5.1. The column labeled "Median" contains the median of all the dL/dP_{STEEP} estimates calculated for each interval. The column labeled "25%" contains the lower quartile of all the dL/dP_{STEEP} estimates calculated for each interval (25% of the calculated dL/dP_{STEEP} estimates are less than that value, and the remaining 75% are greater than that value). The column labeled "75%" contains the upper quartile of all the dL/dP_{STEEP} estimates calculated for each interval (75% of the calculated dL/dP_{STEEP} estimates are less than that value, and the remaining 25% are greater than that value). The next three columns contain analogous summaries for the estimates by the current method. The values in each of these six columns are plotted for each tank in Figure 5.1.

The remaining columns in the table provide additional information concerning the calculation and results from the linear methodology:

- The **ARMSE** column lists the Average Root Mean Square Error from the linear regressions used to obtain the dL/dP_{STEEP} estimates. This quantity can be taken as an estimate of measurement-to-measurement accuracy of the Enraf for that particular tank. The units are inches.
- The **n.int** column lists the number of intervals for which a regression line was calculated and used to obtain estimates of dL/dP_{STEEP} and the summary information in columns 2-4.
- The column labeled "**lag**" lists the number of hours of time lag between the reported HMS atmospheric pressure and the measured surface level. For a few tanks (241-AN-103, 104, and 105; 241-S-106, 107, and 111; and 241-TX-112), several values were considered for the lag and 2τ parameters. As described in Section 5.2, we chose the values that minimized the overall ARMSE to obtain dL/dP_{STEEP} summaries.
- The column labeled 2τ lists the input values of the 2τ parameter in the calculation (units are inches Hg).

- The column labeled "**min. press.**" lists a parameter value used to determine whether or not to estimate the dL/dP_{STEEP} for an interval. An estimate was calculated only if the range of pressures in the interval exceeded this minimum. This parameter has not been studied extensively.

The dL/dP_{STEEP} estimates are best discussed in the context of Figure 5.1. The figure shows both the dL/dP_{STEEP} estimates (from the linear parallelogram model) as well as the estimates currently used for each tank. The plot shows precisely the same data as in columns 2-4 and columns 5-7 of Table 5.1. For each tank, the solid outlined box shows the 25%, median, and 75% estimates (corresponding to the leftmost, middle, and rightmost vertical lines in the boxplot). So, for instance, the figure readily shows that the most extreme (outlying) dL/dP_{STEEP} estimate for the tanks in this study is for Tank TX-102. The dashed box shows the same information, but for the gas law model estimates. In cases where the magnitudes of the estimates are (visually) significantly larger than zero, the dL/dP_{STEEP} estimates are larger in magnitude than the currently calculated estimates. The largest difference occurs for Tank S-106, where the two intervals do not overlap. The gas volume estimated by dL/dP_{STEEP} is twice that estimated using the gas law model. On a tank-by-tank basis, the interquartile ranges (the difference between the 75% and the 25% estimates) appear to be similar for both distributional summaries.

Table 5.1: Summary of linear fitting of parallelogram model. The quantities in the dL/dP estimates columns are in units of inches per inches Hg.

Tank	Linear parallelogram dL/dP estimates			Gas Model dL/dP estimates			ARMSE (inch)	n.int	lag (hours)	2 τ (inches Hg)	min press (inches Hg)
	25%	Median	75%	25%	Median	75%					
241-AN-101	0.00	0.00	0.00	-0.01	0.00	0.02	4.8E-03	6	0	0.4	0.1
241-AN-103	-0.70	-0.63	-0.54	-0.61	-0.52	-0.41	1.7E-02	13	2	0.2	0.1
241-AN-104	-0.27	-0.23	-0.21	-0.25	-0.20	-0.16	1.3E-02	13	2	0.2	0.1
241-AN-105	-0.26	-0.22	-0.18	-0.24	-0.20	-0.15	6.8E-03	13	0	0.2	0.1
241-BX-101	-0.03	-0.01	0.00	-0.03	-0.02	0.00	5.6E-03	17	0	0.4	0.2
241-BX-102	0.00	0.00	0.00	-0.01	0.00	0.01	5.0E-03	8	0	0.4	0.2
241-BX-103	0.00	0.00	0.00	-0.02	-0.01	0.00	5.0E-03	8	0	0.4	0.2
241-BX-104	-0.11	-0.08	-0.04	-0.10	-0.08	-0.05	7.0E-03	18	0	0.4	0.2
241-BX-105	-	-	-	-0.01	0.00	0.00	-	-	-	-	-
241-BX-106	0.00	0.00	0.00	-0.01	0.00	0.01	5.0E-03	10	0	0.4	0.2
241-BX-107	-0.16	-0.10	0.00	-0.15	-0.12	-0.08	1.2E-02	17	0	0.4	0.2
241-BX-108	0.00	0.00	0.00	-0.02	0.00	0.01	5.1E-03	5	0	0.4	0.2
241-BX-109	0.00	0.00	0.00	-0.02	0.00	0.01	5.7E-03	21	0	0.4	0.2
241-BX-110	-0.13	-0.12	-0.11	-0.11	-0.10	-0.08	6.8E-03	27	0	0.4	0.2
241-BX-111	0.00	0.00	0.00	-0.01	0.00	0.01	5.2E-03	16	0	0.4	0.2
241-BX-112	0.00	0.00	0.00	-0.02	-0.01	0.00	5.0E-03	16	0	0.4	0.2
241-C-103	0.00	0.00	0.00	-0.01	0.00	0.01	1.1E-02	18	0	0.4	0.2
241-C-107	-0.04	-0.02	-0.01	-0.02	-0.01	0.01	7.5E-03	13	0	0.4	0.2
241-S-103	-0.42	-0.40	-0.34	-0.43	-0.39	-0.35	1.0E-02	53	0	0.4	0.2
241-S-106	-1.15	-0.91	-0.75	-0.63	-0.44	-0.23	2.4E-02	65	2	0.5	0.1
241-S-107	-0.15	-0.13	-0.11	-0.13	-0.11	-0.08	9.9E-03	86	0	0.3	0.1
241-S-111	-0.76	-0.67	-0.61	-0.63	-0.54	-0.44	1.6E-02	118	0	0.3	0.1
241-SX-106	-0.44	-0.41	-0.34	-0.47	-0.41	-0.34	2.0E-02	38	0	0.4	0.2
241-T-102	0.00	0.00	0.00	-0.01	0.00	0.01	3.8E-01	42	0	0.4	0.2
241-T-107	-0.16	-0.07	-0.01	-0.08	-0.03	-0.01	4.3E-01	45	0	0.4	0.2
241-TX-101	0.00	0.00	0.00	-0.02	-0.01	0.00	5.0E-03	11	0	0.4	0.2
241-TX-102	-1.88	-1.63	-1.46	-1.72	-1.59	-1.35	3.3E-01	32	2	0.5	0.1
241-TX-103	-0.17	-0.14	-0.11	-0.13	-0.11	-0.09	6.2E-03	22	0	0.4	0.2
241-TX-104	0.00	0.00	0.00	0.00	0.01	0.02	5.1E-03	11	0	0.4	0.2
241-TX-105	0.00	0.00	0.00	0.00	0.00	0.01	5.0E-03	12	0	0.4	0.2
241-TX-106	0.00	0.00	0.00	0.00	0.00	0.01	5.0E-03	13	0	0.4	0.2
241-TX-107	0.00	0.00	0.00	-0.01	0.00	0.00	5.0E-03	12	0	0.4	0.2
241-TX-108	0.00	0.00	0.00	-0.01	0.00	0.01	5.0E-03	3	0	0.4	0.2
241-TX-109	0.00	0.00	0.00	-0.01	0.00	0.01	5.0E-03	5	0	0.4	0.2
241-TX-110	0.00	0.00	0.00	-0.01	0.00	0.01	5.0E-03	4	0	0.4	0.1
241-TX-111	0.00	0.00	0.00	-0.02	0.00	0.01	5.0E-03	2	0	0.4	0.2
241-TX-112	0.00	0.00	0.00	0.00	0.00	0.01	5.1E-03	5	0	0.4	0.2
241-TX-113	0.00	0.00	0.00	-0.01	0.00	0.01	2.3E-02	12	0	0.4	0.2
241-TX-114	0.00	0.00	0.00	0.00	0.00	0.01	5.0E-03	18	0	0.4	0.2
241-TX-115	0.00	0.00	0.00	-0.02	0.00	0.01	5.0E-03	6	0	0.4	0.2
241-TX-116	0.00	0.00	0.00	-0.01	0.00	0.00	5.0E-03	22	0	0.4	0.2
241-TX-117	-0.02	0.04	0.10	-0.06	0.00	0.12	3.8E-02	6	0	0.4	0.2
241-TX-118	0.00	0.00	0.00	-0.01	0.00	0.00	5.2E-03	14	0	0.4	0.2
241-TY-101	0.00	0.00	0.01	-0.01	0.00	0.01	1.0E-02	48	0	0.4	0.2
241-TY-102	-0.05	-0.01	0.00	-0.03	-0.01	0.01	4.7E-03	46	0	0.4	0.2
241-TY-103	-0.01	0.00	0.01	-0.02	-0.01	0.00	4.9E-03	50	0	0.4	0.2
241-TY-104	-0.01	0.00	0.01	-0.01	0.00	0.01	6.5E-01	49	0	0.4	0.2
241-TY-105	-0.01	-0.01	0.00	-0.02	-0.01	0.00	3.2E-03	52	0	0.4	0.2
241-TY-106	0.00	0.00	0.01	0.00	0.00	0.01	2.3E-03	44	0	0.4	0.2
241-U-103	-0.56	-0.48	-0.38	-0.46	-0.37	-0.27	3.9E-01	60	0	0.4	0.2
241-U-105	-0.40	-0.36	-0.28	-0.38	-0.32	-0.26	4.0E-01	60	0	0.4	0.2
241-U-106	-0.13	-0.08	-0.01	-0.09	-0.06	-0.03	4.0E-01	58	0	0.4	0.2
241-U-107	-0.33	-0.30	-0.27	-0.32	-0.29	-0.27	4.2E-01	60	0	0.4	0.2
241-U-109	-0.46	-0.38	-0.27	-0.30	-0.21	-0.12	4.1E-01	62	0	0.4	0.2

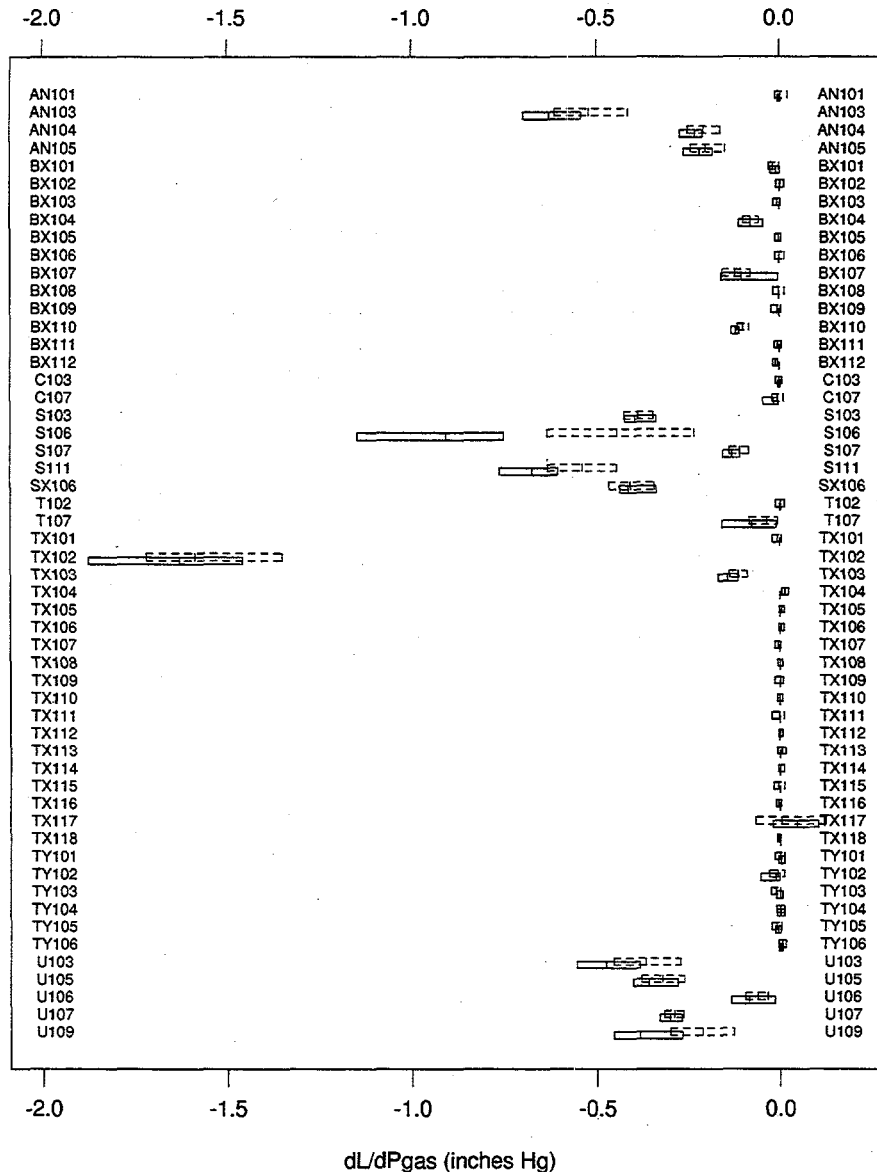


Figure 5.1: Summary of dL/dP_{STEEP} estimates from the linear parallelogram method (solid boxes) compared with gas model dL/dP estimates (dashed boxes).

5.2 Lag Between Pressure Change and Level Response

The lag observed between pressure change and level response is partially explained by hysteresis, when it is present. The model predicts that the level response is initially suppressed, and then a large level response is observed when the pressure change continues. Figure 5.2 shows an overlay of Tank S-106 level and atmospheric pressure data. A cursory glance at the figure suggests a lag on the order of a day or more between pressure changes and the level responses (the vertical lines are drawn at midnight for each day on the plot). A more careful look suggests hysteresis as the “cause” of the large apparent lag; the nearly flat levels on Feb 1 and on Feb 8-11, which occur during the beginning of the pressure changes, give rise to much of the apparent lag.

Tank 241-S-106 data from 2-1-97 to 2-15-97

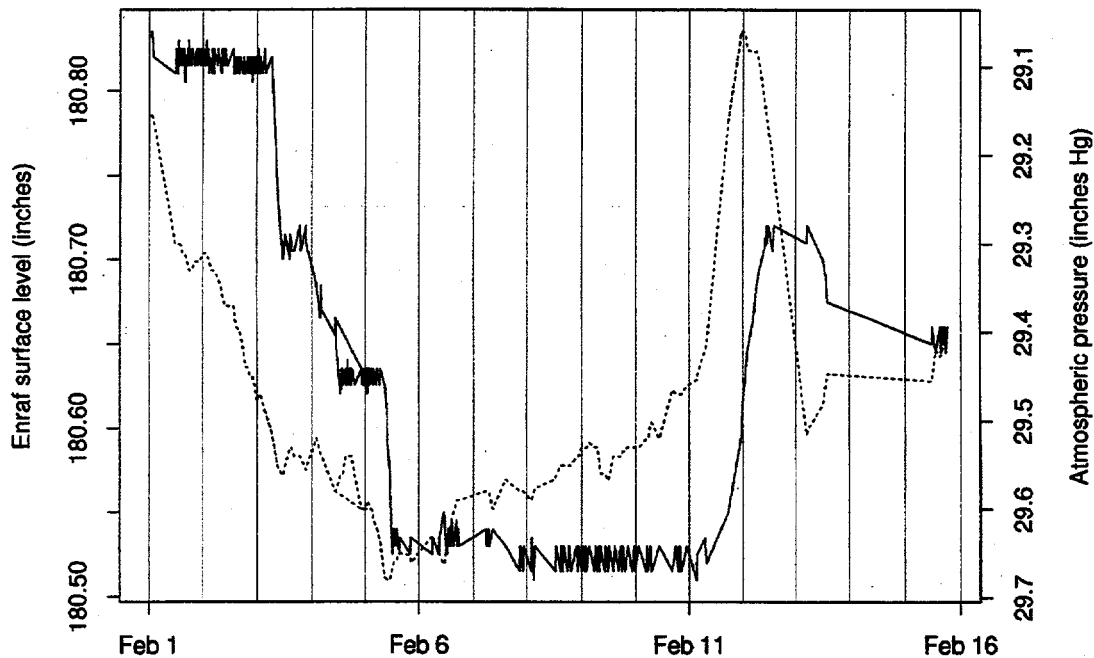


Figure 5.2: Tank S-106 level compared with atmospheric pressure. The levels and pressures are shown as the solid and dashed lines, respectively.

We can look at the lag data in a way that corrects for the modeled hysteresis. Figure 5.3 shows a segment of Tank S-106 data; the level bottoms out about 5 hours after the cusp in the atmospheric pressure. The bolded portions of the level and pressure data are used to estimate dL/dP_{STEPP} in this time interval. Note that the highlighting used to demonstrate the estimation interval also facilitates the visual comparison of the data, and makes the lag more obvious. It's tedious to look through many intervals of data (However, a 5-hour lag was observed in multiple inspections of the interval data for Tanks S-111 and S-106). So we created a procedure to help estimate the lag. The procedure is to combine and summarize the goodness of fit for the linear regression (as measured by ARMSE) used to relate level and pressure for each interval, and to select control parameters to optimize the summary goodness of fit.

Tank 241-S-106 data from 8-17-95 to 8-18-95

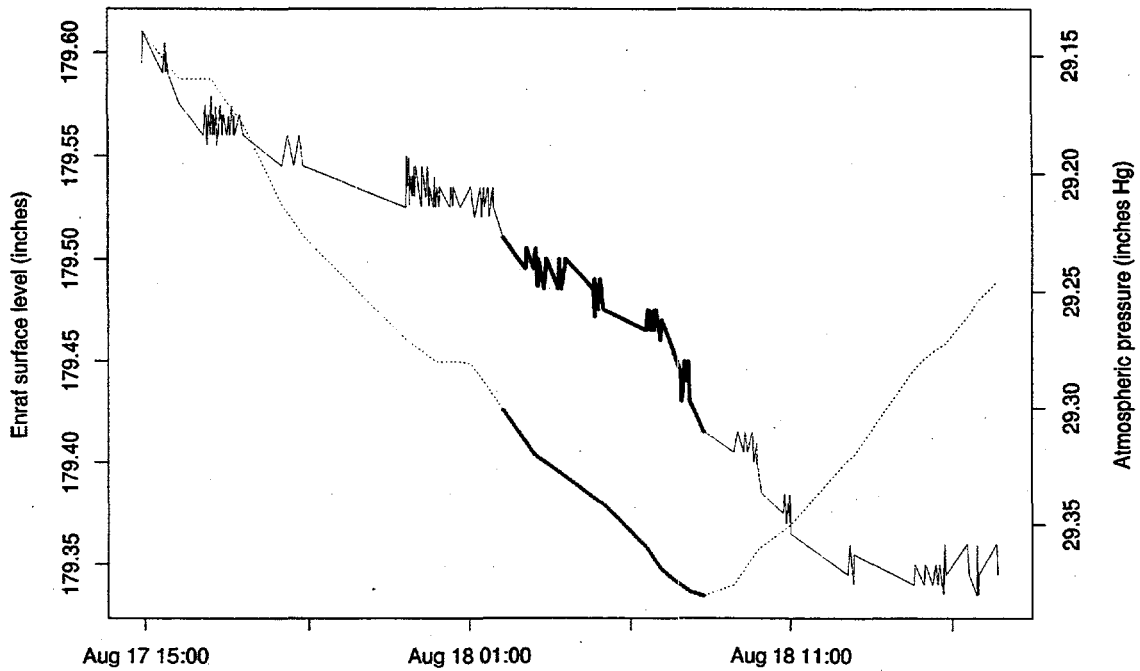


Figure 5.3: Tank S-106 level (solid line) and corresponding atmospheric pressure (dashed line) data. The region shown in thicker lines will enter a dL/dP_{STEEP} calculation. The plot shows a time lag of about 5 hours between the pressure reversal and the corresponding level response.

Table 5.2 summarizes these calculations for the simulated data shown previously. We also varied the parameter 2τ . Looking at the simulated data in Table 5.2, the first two columns show the input lag (in hours) and 2τ (in inches Hg), used as input in the linear methodology.

Table 5.2: Summary from simulated tank data

Lag	2τ	25% _{LS}	Median _{LS}	75% _{LS}	ARMSE _{LS}	n.int _{LS}	Median _{Robust}
0	0.2	-0.86	-0.69	-0.51	4.27E-02	129	-0.71
0	0.3	-1.03	-0.93	-0.79	4.11E-02	96	-0.97
0	0.4	-1.24	-1.06	-0.96	3.91E-02	63	-1.10
0	0.5	-1.21	-1.07	-0.96	3.86E-02	45	-1.10
2	0.2	-0.91	-0.79	-0.64	3.48E-02	129	-0.83
2	0.3	-1.04	-0.98	-0.92	2.96E-02	96	-1.00
2	0.4	-1.17	-1.06	-0.99	2.68E-02	63	-1.07
2	0.5	-1.20	-1.06	-0.96	2.75E-02	45	-1.06
5	0.2	-0.95	-0.89	-0.80	1.59E-02	129	-1.00
5	0.3	-1.00	-1.00	-1.00	5.45E-07	96	-1.00
5	0.4	-1.00	-1.00	-1.00	5.50E-07	63	-1.00
5	0.5	-1.00	-1.00	-1.00	5.44E-07	45	-1.00
10	0.2	-0.88	-0.76	-0.65	3.31E-02	129	-0.78
10	0.3	-0.90	-0.83	-0.66	3.46E-02	96	-0.79
10	0.4	-0.88	-0.74	-0.55	3.23E-02	63	-0.71
10	0.5	-0.90	-0.74	-0.58	3.11E-02	45	-0.73

The next three columns are summaries of the least-squares dL/dP_{STEEP} estimates (units are inches per inches Hg). The median is the proposed “best estimate”. The mean was not used, since it is sometimes thrown off by slopes estimated during intervals containing Enraf calibrations, or by wildly outlying level values. In the column of median dL/dP_{STEEP} estimates, the extreme values are highlighted in bold. For comparison, the medians of the robust slopes are presented at the far right of the table; and inspection shows that they are always close to the least-squares estimates. This observation holds for the actual tank data (see Tables 5.3-5.6), as well as for the simulated data here.

The $ARMSE_{LS}$ column shows the Average of the Root Mean Squared Errors for each least-squares regression calculation, and is an overall indicator of model fit (smaller is better). For the simulated data, the estimates that minimize $ARMSE_{LS}$ are exactly correct for a lag of 5 hours and $2\tau \geq 0.3$ inches Hg, as expected (recall that the simulated data had $2\tau = 0.3$ inches Hg and lag=5 hours). $ARMSE_{LS}$ is proposed as a guideline for selecting the input parameters. We expect it to be better for choosing lag than for choosing 2τ , since the decreasing number of points with increasing 2τ will decrease the reliability of $ARMSE_{LS}$ as a goodness of fit indicator.

The $n.int_{LS}$ column shows the number of intervals for which regressions are calculated. The decreasing number of intervals as 2τ increases is expected: the number of pressure swings larger than 2τ decreases with increasing 2τ .

Tables 5.3-5.5 show the results of applying the same “design” of estimation runs to the S farm tanks. For these three tanks, the largest magnitude dL/dP_{steep} estimates correspond with the minimum $ARMSE_{LS}$. Only for Tank S-106 does the minimum $ARMSE_{LS}$ occur for lags greater than 0 hours. Additionally, for these three tanks, the larger magnitude dL/dP_{STEEP} estimates occur for the larger values of 2τ . Recall that looking at intervals with large 2τ is the same as looking at time intervals near the end of large pressure swings.

Finally, the behavior of Tank TX-102, shown in Table 5.6, is very different from that of the S-farm tanks: Here, 2τ doesn't have much effect on $ARMSE_{LS}$ or on dL/dP_{STEEP} for lags of 0, 2, and 5 hours. Perhaps this difference in behavior is related to the observation that this tank's levels don't show much hysteresis.

These data observations suggest the following strategies for estimation: as a rule, run with large values of 2τ ; and the best fits (according to $ARMSE_{LS}$) tend to occur at the end of large pressure swings. Note that this last suggestion is beyond the scope of the model.

Table 5.3: Tank S-106 dL/dP_{STEEP} estimates for various time lags and 2τ values.

<i>Lag</i>	2τ	$25\%_{LS}$	<i>Median</i> _{LS}	$75\%_{LS}$	$ARMSE_{LS}$	$n.int_{LS}$	<i>Median</i> _{Robust}
0	0.2	-0.91	-0.69	-0.53	0.0333	121	-0.78
0	0.3	-1.00	-0.82	-0.61	0.0309	105	-0.91
0	0.4	-1.15	-0.91	-0.71	0.0290	82	-0.98
0	0.5	-1.18	-0.92	-0.73	0.0292	65	-1.03
2	0.2	-0.92	-0.73	-0.60	0.0288	122	-0.80
2	0.3	-1.07	-0.83	-0.71	0.0262	104	-0.88
2	0.4	-1.09	-0.90	-0.74	0.0255	84	-0.98
2	0.5	-1.15	-0.91	-0.75	0.0242	65	-0.96
5	0.2	-0.98	-0.80	-0.58	0.0265	128	-0.80
5	0.3	-1.03	-0.85	-0.66	0.0252	116	-0.87
5	0.4	-1.09	-0.95	-0.67	0.0253	86	-0.96
5	0.5	-1.15	-0.92	-0.68	0.0259	66	-0.93
10	0.2	-0.88	-0.72	-0.55	0.0289	133	-0.77
10	0.3	-0.93	-0.77	-0.54	0.0297	101	-0.82
10	0.4	-0.95	-0.85	-0.60	0.0308	73	-0.85
10	0.5	-1.02	-0.83	-0.51	0.0306	61	-0.83

Table 5.4: Tank S-107 dL/dP_{STEEP} estimates for various time lags and 2τ values.

Lag	2τ	25% _{LS}	Median _{LS}	75% _{LS}	ARMSE _{LS}	n.int _{LS}	Median _{Robust}
0	0.2	-0.14	-0.12	-0.10	0.0101	114	-0.12
0	0.3	-0.15	-0.13	-0.11	0.0100	86	-0.12
0	0.4	-0.15	-0.13	-0.10	0.0102	70	-0.12
0	0.5	-0.16	-0.14	-0.11	0.0102	49	-0.14
2	0.2	-0.14	-0.12	-0.08	0.0105	112	-0.11
2	0.3	-0.14	-0.12	-0.09	0.0103	86	-0.11
2	0.4	-0.15	-0.13	-0.10	0.0107	58	-0.12
2	0.5	-0.16	-0.13	-0.10	0.0108	43	-0.12
5	0.2	-0.13	-0.10	-0.05	0.0107	107	-0.09
5	0.3	-0.13	-0.11	-0.06	0.0111	77	-0.10
5	0.4	-0.14	-0.12	-0.08	0.0113	58	-0.11
5	0.5	-0.15	-0.11	-0.06	0.0117	42	-0.10
10	0.2	-0.12	-0.08	-0.04	0.0110	104	-0.07
10	0.3	-0.13	-0.09	-0.05	0.0115	76	-0.07
10	0.4	-0.13	-0.09	-0.03	0.0120	57	-0.07
10	0.5	-0.13	-0.08	-0.03	0.0125	41	-0.07

Table 5.5: Tank S-111 dL/dP_{STEEP} estimates for various time lags and 2τ values.

Lag	2τ	25% _{LS}	Median _{LS}	75% _{LS}	ARMSE _{LS}	n.int _{LS}	Median _{Robust}
0	0.2	-0.72	-0.66	-0.57	0.018	143	-0.66
0	0.3	-0.76	-0.67	-0.61	0.016	118	-0.68
0	0.4	-0.80	-0.71	-0.63	0.016	91	-0.72
0	0.5	-0.86	-0.74	-0.67	0.016	66	-0.74
2	0.2	-0.71	-0.63	-0.56	0.137	145	-0.64
2	0.3	-0.71	-0.64	-0.57	0.114	120	-0.65
2	0.4	-0.76	-0.68	-0.59	0.109	89	-0.69
2	0.5	-0.79	-0.70	-0.59	0.112	64	-0.69
5	0.2	-0.69	-0.59	-0.52	0.142	131	-0.60
5	0.3	-0.69	-0.62	-0.52	0.118	107	-0.61
5	0.4	-0.72	-0.64	-0.51	0.111	80	-0.65
5	0.5	-0.75	-0.65	-0.54	0.113	61	-0.66
10	0.2	-0.58	-0.48	-0.34	0.162	121	-0.50
10	0.3	-0.62	-0.48	-0.35	0.147	94	-0.50
10	0.4	-0.64	-0.48	-0.32	0.143	72	-0.49
10	0.5	-0.65	-0.50	-0.37	0.150	53	-0.50

Table 5.6: Tank TX-102 dL/dP_{STEEP} estimates for various time lags and 2τ values.

Lag	2τ	25% _{LS}	Median _{LS}	75% _{LS}	ARMSE _{LS}	n.int _{LS}	Median _{Robust}
0	0.2	-1.81	-1.68	-1.53	0.421	75	-1.68
0	0.3	-1.87	-1.72	-1.57	0.422	60	-1.73
0	0.4	-1.94	-1.79	-1.56	0.406	46	-1.77
0	0.5	-1.97	-1.81	-1.54	0.398	32	-1.82
2	0.2	-1.76	-1.62	-1.45	0.330	76	-1.61
2	0.3	-1.77	-1.62	-1.41	0.331	60	-1.59
2	0.4	-1.83	-1.66	-1.47	0.326	47	-1.63
2	0.5	-1.88	-1.63	-1.46	0.326	32	-1.56
5	0.2	-1.61	-1.42	-1.24	0.430	72	-1.43
5	0.3	-1.65	-1.42	-1.26	0.419	56	-1.40
5	0.4	-1.71	-1.49	-1.25	0.418	43	-1.43
5	0.5	-1.61	-1.40	-1.02	0.435	30	-1.40
10	0.2	-1.27	-0.79	-0.28	1.019	39	-0.77
10	0.3	-1.22	-0.69	-0.38	0.951	34	-0.63
10	0.4	-1.19	-0.69	-0.29	0.888	27	-0.39
10	0.5	-1.11	-0.69	-0.37	0.930	19	-0.63

Figures 5.4 and 5.5 show dL/dP_{STEEP} estimates for Tanks 241-S-106 (S-106) and 241-TY-102 (TY-102) respectively. Two plotting characters are used in these figures: the "■" are estimates based on S+ data and the "◆" are estimates based on S- data. The vertical lines through these characters indicate 95% error bars from the standard linear regression calculations; however, as discussed earlier, these intervals do not contain sufficient common overlap to be 95% confidence intervals for the same quantity. The relative widths do provide a summary of the relative goodness of fit of the model for each interval.

Tank 241-S-106 data from 8-15-95 to 3-7-97

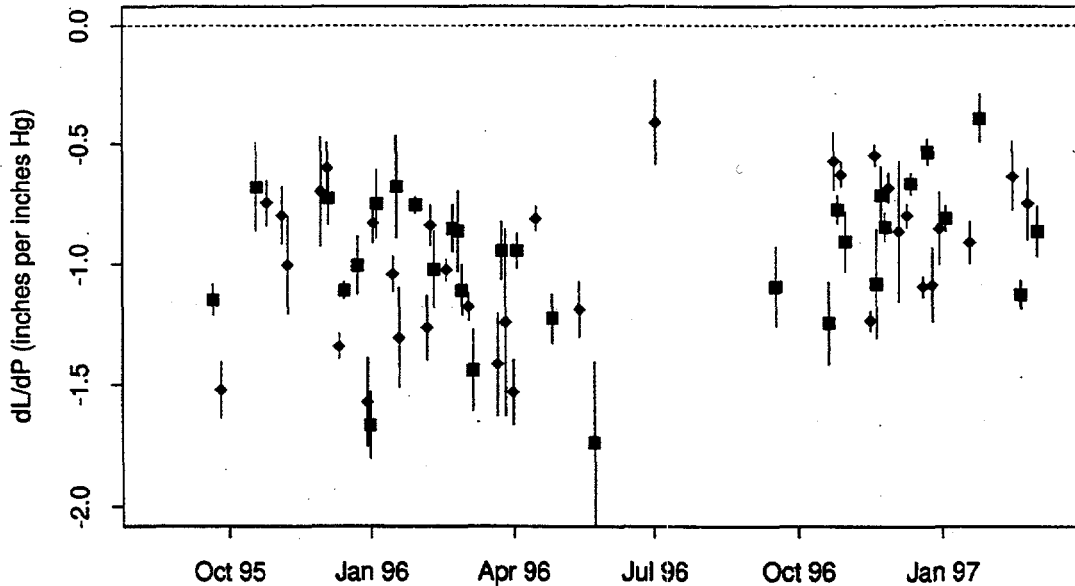


Figure 5.4: Tank S-106 dL/dP_{STEEP} estimates.

Tank 241-TY-102 data from 12-28-95 to 3-6-97

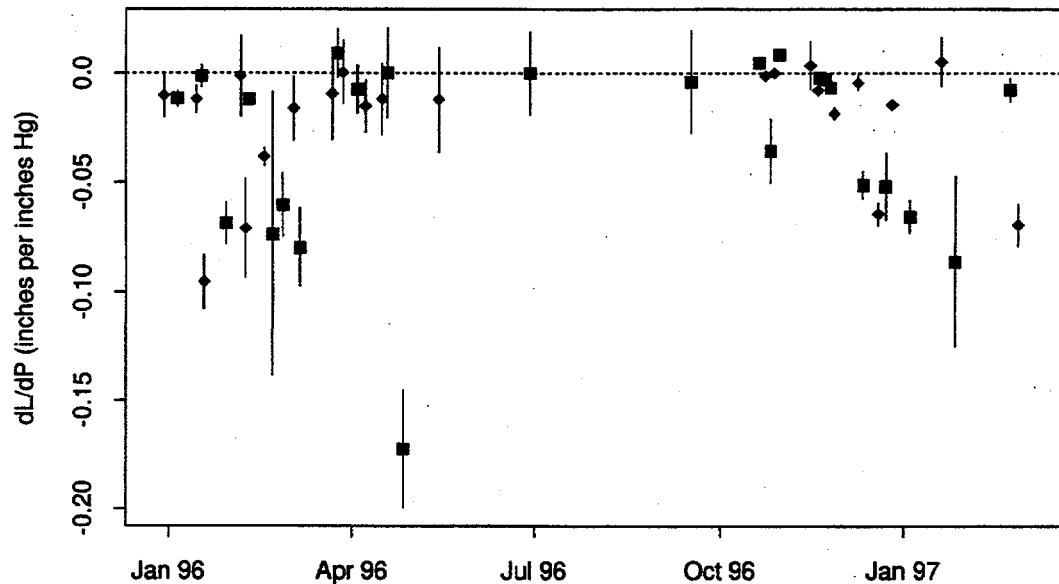
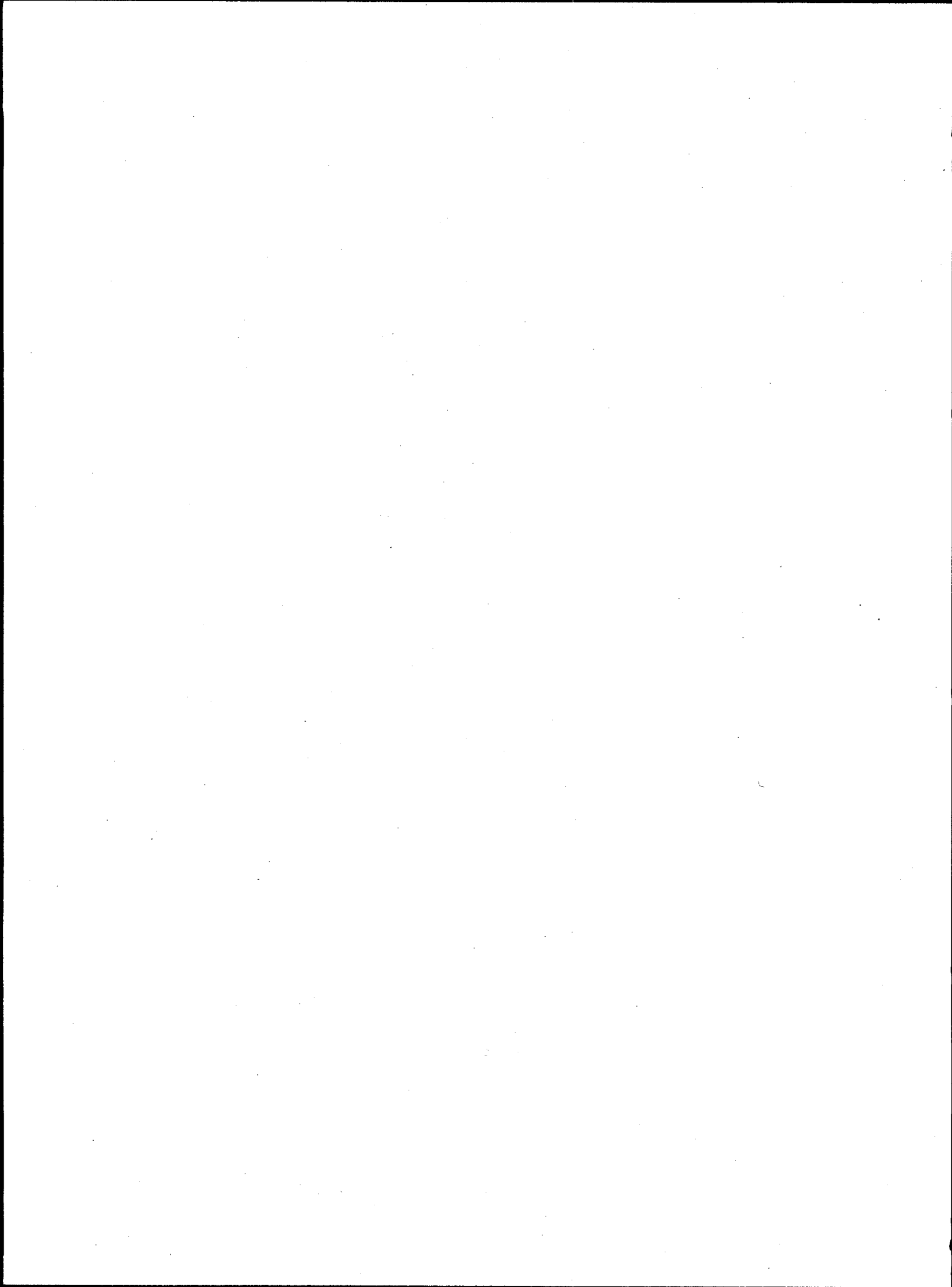


Figure 5.5: Tank TY-102 dL/dP_{STEEP} estimates.

The frequency of estimates is less during the summer than during the winter, since more large pressure swings are observed at Hanford during the winter. The dL/dP_{STEEP} estimates for Tank S-106 appear to be decreasing in magnitude. This observation is consistent with the calculations for Tank S-106 reported previously⁷. The dL/dP_{STEEP} estimates for Tank TY-102 appear to clump into either a cluster near zero or a cluster between -0.05 and -0.10. Upon further examination of the data, the explanation for the clustering can be seen from the level series: there are large segments of time (ranging from a week to a few weeks) during which the measured level is constant, and other times during which the level measurements fluctuate more freely. We were unable to correlate this behavior with the size of the pressure swing for the estimate, and recommend using the more extremely negative cluster elements for retained gas volume calculations.

⁷ "Flammable Gas Data Evaluation Progress Report", WTSFG96.1. P.D. Whitney, N.E. Wilkins, N.E. Miller, P.A. Meyer and M.E. Brewster, Feb. 2, 1996.



6. Experimental Study of Pressure/Level Response of Bubble Simulants

Previous studies have shown that the waste level responds to barometric pressure changes, that the compressibility of retained bubbles accounts for the level changes, and that the volume of retained gas can be estimated from this relationship (Whitney 1995). Accurate estimates of retained gas from the level/pressure relationship are valuable because direct in-tank measurement of retained gas is expensive and, in many single shell tanks, impossible. However, there have been no previous laboratory studies, with actual waste or waste simulants, that confirm this relationship and define pertinent limits.

The previous studies also showed that interactions between the bubbles and the waste affect the results and create inaccuracies in estimated retained gas volumes (Whitney et al. 1996). Some qualitative understanding of how these interactions affect the level/pressure relationship exists, but a complete understanding has been elusive because the interactions are complex and they vary widely. Furthermore, these interactions can completely dominate the level/pressure relationship. Previous studies focused on the hysteresis in the level/pressure relationship, because this hysteresis is observed in actual tank data and is thought to stem from the interaction of bubbles with the waste. If we knew how retained bubbles interact with the waste, and how this interaction manifests itself in the level/pressure relationship, the barometric pressure technique for estimating the volume of retained gas could be applied with more confidence and smaller uncertainties.

To help understand this behavior and define applicable limits, a series of experiments were conducted to quantify the level response to pressure changes for a range of bubbly simulants. The objectives of these experiments were to verify the use of dL/dP measurements to determine the volume of trapped gas, and to investigate the role of waste strength on these estimates. In addition, bubbly particulate simulants were also studied to gain further information on this type of material. All these experiments were conducted with known volumes of retained gas bubbles and with simulants having known physical properties. Because the volume of trapped gas is known, a direct comparison of the measured pressure level response can be made with the predicted ideal behavior.

6.1 *Experimental Apparatus and Method*

Figure 6.1 shows a schematic of the experimental apparatus. The basic component of the apparatus is a cylindrical test chamber containing the bubbly simulant, which can be pressurized. A transparent small diameter sight tube is attached to the test chamber. The bubbly simulant is covered by water, and the amount of added water is adjusted to locate the water level at an appropriate height within the sight tube. The sight tube has a smaller diameter (0.25 in.) than the test chamber to amplify the level changes of the bubbly simulant. The level measurements were always made at the sight tube, but the level data reported in the results section are calculated level changes based on the known internal diameters of the sight tube and the test chamber.

Test chambers of two different sizes were used. The main experiments were conducted in a vessel (4.00 in. internal diameter (ID)) assembled from PVC pipe components, while preliminary experiments used a transparent polycarbonate (Lexan™) tube with a 1.00 in. ID. The tall, narrow shape of the polycarbonate vessel exaggerated wall effects, which then dominated the observed behavior. In the larger diameter vessel, the depth of simulant was maintained at a level

commensurate with the vessel diameter, which minimizes the wall effects. Wall effects can be made even smaller by using even larger vessels, but this was beyond the scope of this study.

The pressure in the gas above the liquid was adjusted by metering pressurized nitrogen through a needle valve and then bleeding nitrogen through a vent valve. An alternative approach would be to set the pressure at selected values, and then close the system off with valves. We found steadier pressures could be maintained by providing an adjustable bleed flow. A Paroscientific™ Digiquartz 2100A pressure transducer (0-100 psia, accurate to $\pm 0.01\%$ of full scale) attached to a Paroscientific™ 702 Pressure Computer determined the pressure of the gas. The 75 ml reservoir was included in the system to improve system capacitance and help to maintain the set pressures.

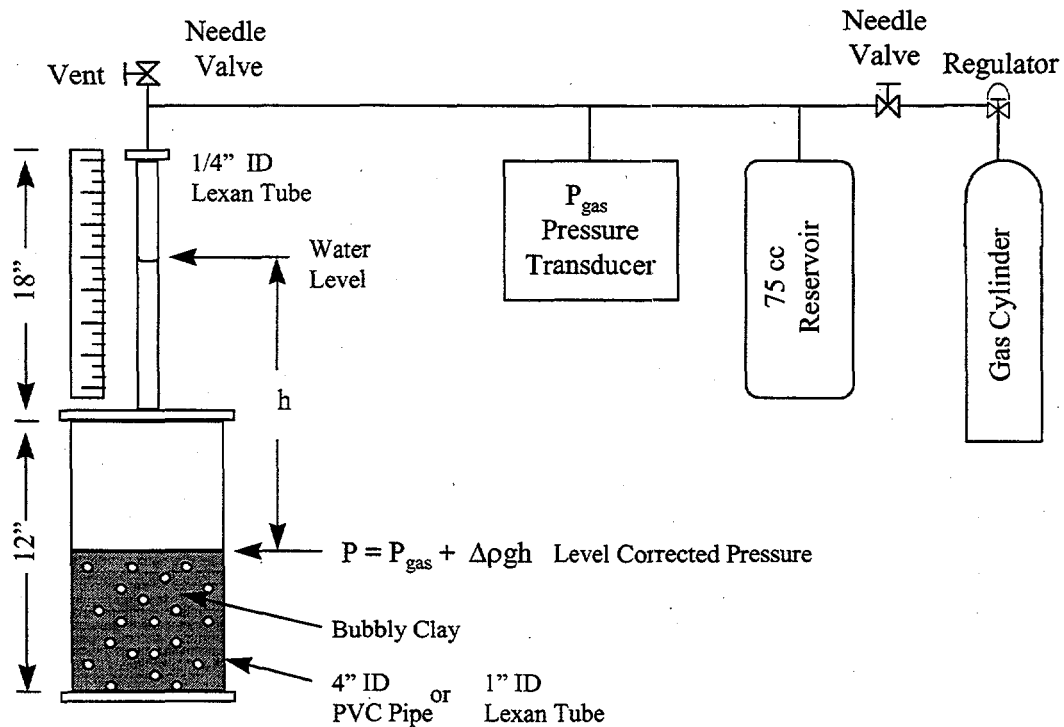


Figure 6.1: Schematic of apparatus for measuring pressure/level response of bubbly sludges and slurries

The experiment consisted of placing a bubbly simulant in the test vessel, making measurements to determine the retained gas volume, and taking level measurements during a series of pressure cycles. The pressure cycles were typically about 14 kPa (2 psi), although the level response was also recorded for smaller pressure cycles. To the extent possible, all potentially important variables were held constant during the experiments. These variables included the method of making pressure adjustments and the duration of the pressure cycles. It was apparent during initial testing that the results depended on these variables, so the results reported below would change if the duration of the pressure cycle or the pressure steps were imposed differently. In all the experiments, each pressure cycle was completed by making about ten equal step changes in pressure (1.4 kPa [0.2 psi]), both increasing and decreasing, with a three-minute duration between each step. This resulted in 60 minutes for a complete pressure cycle (30 minutes increasing, 30 minutes decreasing).

In all the experiments, the retained gas was generated by incorporating in the simulant a small amount of hydrogen peroxide, which decomposed to generate retained oxygen bubbles (Gaughlitz et al. 1996). The amount of hydrogen peroxide added was adjusted to produce a gas volume fraction of about 10 percent. While adjusting the amount of added peroxide easily controlled the gas volume fraction, the uncertainty in the retained gas volume based on controlling the peroxide addition was fairly large.

A critical aspect of these experiments was measuring the retained gas volume. The method used was based on measuring the density of the bubbly mixture and comparing this density to that of the simulant without retained gas. The difference in densities is easily related to the volume of retained gas. The actual measurements needed are the volume and the mass of the bubbly simulants. To determine the volume, the test vessels were calibrated by adding known volumes of water (from weight measurements) and noting the level in the test vessel or sight tube. When the bubbly clay was in the test vessel, its surface was typically not flat, making the level measurement uncertain. To improve these level measurements, a known mass of water was added above the bubbly simulant, producing a flat interface for level observation and thus improving the volume measurement. The relationship for determining the volume of retained gas V_{gas} , in terms of the measured quantities, is given below:

$$V_{\text{gas}} = V - \frac{W_{\text{mass}}}{\rho_{\text{water}}} - \frac{XM(1-F)}{\rho_{\text{clay}}} - \frac{XMF}{\rho_{\text{water}}} - \frac{(1-X)M}{\rho_{\text{water}}} \quad (6.1)$$

where V is the volume of bubbly clay and added water (from the vessel calibration), W_{mass} is the mass of water added to the vessel to cover the clay, M is the mass of the added clay/water mixture, X is the weight fraction of clay in the mixture (as is from the bag - the moisture content of the clay is accounted for next), F is the fraction of water moisture on the clay used to make the simulants (0.07 wt.%, LRB-BNW-55225, pg. 47, which is consistent with expectations and previous measurements), ρ_{clay} is the clay grain density (2.72 g/cm³, Gaughlitz et al. 1996), and ρ_{water} is the water density (0.9978 at 22° C, Lange 1979). In the single experiment with a bubbly slurry of glass beads, an essentially identical method was used to determine the retained gas volume. The only additional information needed to determine the retained gas volume was the density of the glass in the beads, which was determined to be 2.86 g/cm³. A conservative estimate of the uncertainty in the resulting estimates is approximately ± 3 cm³ of retained gas or roughly $\pm 0.75\%$ gas volume.

Table 6.1 lists the different simulants tested, the measured quantities, and the retained gas volumes and gas volume fractions calculated from these measured quantities. These gas volumes were compared with the pressure level measurements obtained on these systems. Also shown in Table 6.1 are the measurements and retained gas results for an experiment that had essentially no retained gas (# 7). In this experiment, an 11.25 wt.% clay simulant was prepared without any added hydrogen peroxide. Because this mixture has a quite low value of shear strength (14 Pa), essentially all entrained air bubbles were released readily. The volume and mass measurements resulted in a calculated retained gas volume of 0.55 cm³, or 0.16% gas volume fraction, which is essentially the expected value of zero gas, and is within the uncertainty estimate. This test confirms that the experimental technique for measuring the retained gas volume from mass and level measurements is reasonably accurate.

Table 6.1: Bubbly simulants used in testing

Experiment	Test Vessel (ID)	Shear Strength (Pa) ^a	X Wt. % Clay (As Is Basis)	M (g)	V (cm ³)	W _{mass} (g)	V _{gas} (cm ³)	Void (%)
1	4 in.	147	15.0	894.9	2109.9	1199.9	89.7	9.9
2	4 in.	3,760	27.25	921.9	2109.9	1236.7	94.8	10.9
3	4 in.	10,700	50.00	878.0	2110.5	1412.5	74.0	10.7
4	1 in.	14	11.25	380.6	399.3	5.11	38.0	9.6
5	1 in.	147	15.00	437.5	449.6	11.9	37.9	8.7
6	1 in.	3760	27.25	372.8	345.7	5 ^b	27.0	7.9
7 (no gas test)	1 in.	14	11.25	360.4	366.0	28.1	0.55	0.16
			Mass Water (g)	Mass Glass (g)		Slurry Vol (cm ³)		
90 μm glass beads	1 in.	-	219.9	517.6	434.6	278.6	40.2	14.4

(a) Shear strengths from Gauglitz et al. (1996), Table 4.1, column titled "Curve Fit Shear Strength"
(b) Mass of added water was estimated, actual amount not recorded

In the experiments, the pressure cycles started at ambient pressure and were typically 14 kPa gauge (2 psig); and the retained gas volumes varied between 30 and 90 cm³. For this range of pressures and gas volumes, the level in the small diameter sight tube spanned 10 to 30 cm (unless the shear strength of the simulant masked the presence of gas). This variation in level was sufficient to affect the pressure experienced by the bubbly simulants. To account for this liquid head effect, the pressure at the top of the simulant was calculated by correcting for the head of water within the test vessel and sight tube, as indicated in Figure 6.1. Finally, a pressure/level experiment was conducted with only water in the apparatus, to determine how much the components in the system would be compressed under a typical pressure variation. The level in the sight tube varied by less than 0.1 cm for a 14 kPa pressure increase, which is negligible compared to the level change associated with the retained gas.

To compare the pressure level response of the simulants to the expected ideal behavior, a relationship between the pressure and simulant level is needed. The standard relationship, which is based on ideal-gas behavior, is given as follows (see Stewart et al. [1996], for example):

$$\frac{dL}{dP} = - \frac{V_{gas}(P)}{AP} \quad (6.2)$$

where L is the level of the bubbly mixture, A is the cross sectional area, P is the pressure inside the gas bubbles, and V_{gas}(P) is the gas volume at pressure P. Integrating this equation, and again using the ideal-gas law, gives the following:

$$L = \frac{[P_0 V_{gas}(P_0)]}{AP} + L_0 \quad (6.3)$$

where L₀ is a constant of integration and V_{gas}(P₀) is the gas volume at standard temperature and pressure. The curve defined by Equation 6.3 is shown along with the test data in the figures, and is designated as the ideal behavior. Also, dL/dP in Equation 6.2 was estimated from a least-

squares fit of the data, and the volume of retained gas estimated with Equation 6.2 is compared to the measured gas volume in Table 6.2.

6.2 *Experimental Results and Discussion*

Figure 6.2 shows the pressure level response of a 147 Pa bentonite clay with 10% retained gas contained in the 4 in. ID test vessel (Experiment 1, Table 6.1). The experiment consisted of three 14 kPa pressure cycles. In Figures 6.2 - 6.5, the upper curves are for increasing pressure, and the lower curves are for decreasing pressure. The results show that the bubbly simulant compressed as the pressure increased and expanded as the pressure decreased, essentially as expected. The third pressure cycle provides the most useful data because it mimics the repeated pressure changes that the waste experiences in the actual tanks. The measured pressure/level response, or slope of the level pressure data, is essentially identical to the ideal behavior. A more quantitative comparison between the actual gas fraction and the gas fraction estimated from the dL/dP data is discussed below in relation to Figures 6.3 to 6.5.

The results in Figure 6.2 also show that the level decreased progressively after each pressure cycle. In this experiment, the simulant shear strength of 147 Pa is small compared to the pressure cycle of 14 kPa. Still, the progressive compression is most likely due to the simulant shear strength and the resistance it offers to bubble expansion (although this experiment does not prove that statement). It is important to note that in all the experiments, the bubbles released from the simulant always remained inside the test vessel and continued to compress and expand. Furthermore, bubble release was not observed for equivalent experiments done in the 1 in. ID transparent test vessel (Experiment 5, Table 6.1).

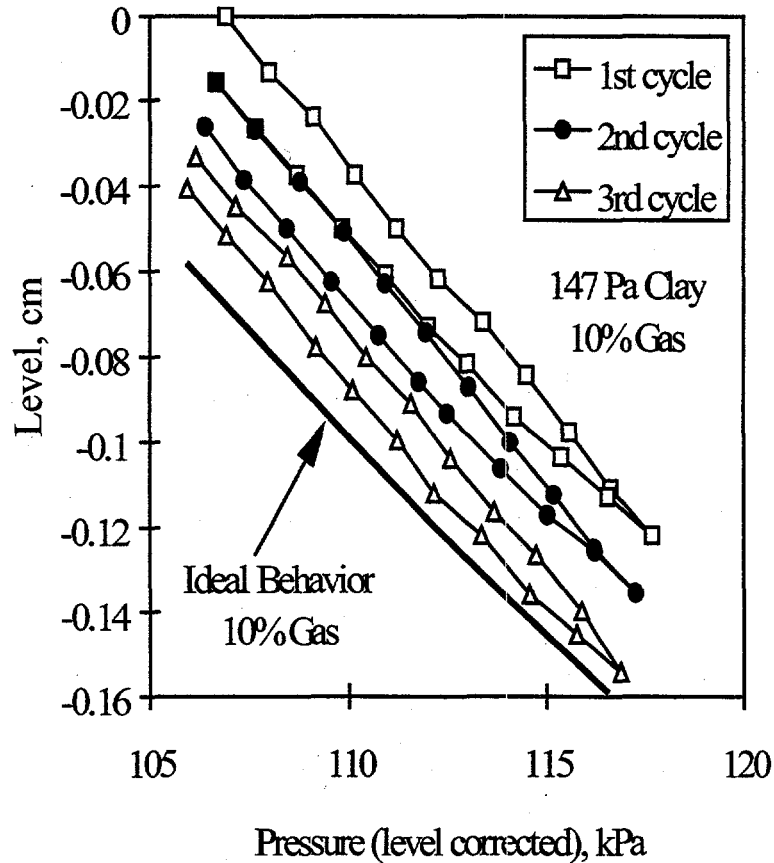


Figure 6.2: Level change during a series of pressure cycles for a 147 Pa bentonite clay with 10% gas (Experiment 1). The level/pressure response is nearly identical to the predicted ideal behavior.

Figure 6.3 compares the pressure/level response for bubbly clays with a range of strengths. These results were for the last pressure cycle of each series (typically the third cycle) taken with the 4 in. ID test vessel. The most notable observation is that the weaker clays follow essentially ideal behavior. In contrast, the strongest clay (10,700 Pa) shows a much smaller level response. For this strongest simulant, the strength of the clay masks the amount of retained gas. Table 6.2 summarizes a quantitative comparison between the measured gas volumes and the gas volumes estimated from the dL/dP data. For the two weakest simulants, the dL/dP estimates of retained gas differ from the measured gas volume fractions by less than about one percentage unit, which is good agreement. For the 10,700 Pa clay, the dL/dP estimate gives 1.9% gas volume, which is clearly smaller than the measured value of 10.7%.

The detailed mechanisms of how the waste strength masks the retained gas cannot be determined from these experiments. The mechanism could be the interaction of the clay with the vessel wall, or the interaction of the bubbles with the clay. To prove that the bubble/clay interactions are the source of this effect, experiments would need to be conducted in a series of progressively larger vessels, but maintaining the same L/D ratio to eliminate wall effects. If the level pressure response remains the same regardless of the vessel diameter, then the experiments would demonstrate that bubble/clay interactions are causing the difference between the expected ideal behavior and the actual observed behavior.

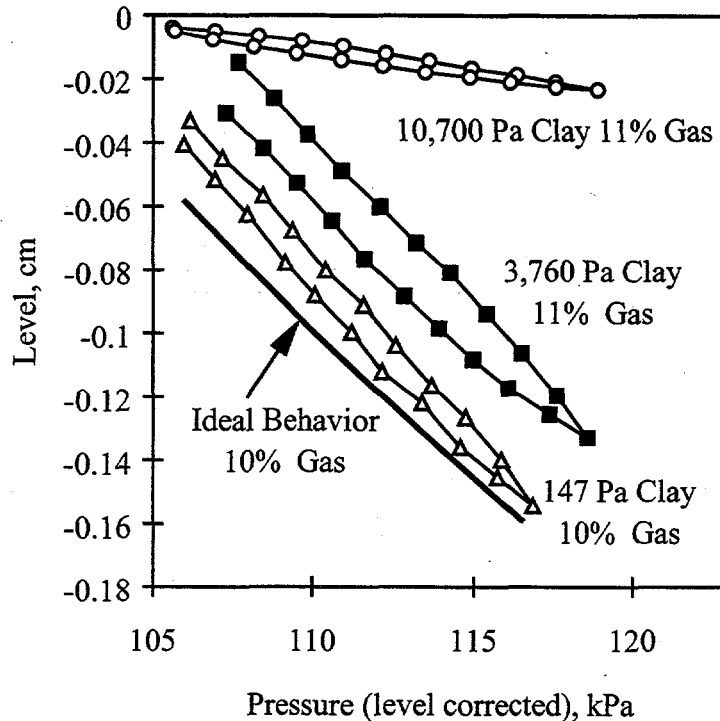


Figure 6.3: Level pressure results for bubbly bentonite clays in the 4 in. ID test vessel, with a range of shear strengths and with known retained gas volumes (Experiments 1, 2, and 3). These data are from the last pressure cycle (typically the third) of a series of experiments conducted for each clay. For the two weaker clays, the level/pressure response is nearly identical to the predicted ideal behavior.

Figure 6.4 compares the pressure/level response for bubbly clays contained in the 1 in. ID test vessel. In this apparatus, the interaction of the simulant with the tube wall played a dominant role in the level response. The results are for a range of strengths and from the last pressure cycle of each series (typically the third cycle). The most notable observation is that both the 147 Pa and 3760 Pa clays deviate substantially from the predicted ideal behavior. In contrast, both these simulants responded with essentially ideal behavior in the 4 in. ID test vessel (Figure 6.3). These results show clearly that the test vessel wall effect is dominating the observed behavior. For the weakest clay, however, the waste strength appears negligible, resulting in little or no wall effect, and the observed response is essentially identical to the ideal behavior.

Table 6.2 summarizes the quantitative comparison between the measured gas volumes and the gas volumes estimated from the dL/dP data. For the 14 Pa simulant, the dL/dP estimate of retained gas differs from the measured gas volume fraction by less than one percentage unit, which is good agreement. For the 147 Pa clay, the dL/dP estimate gives 2.8% gas volume, which is clearly smaller than the measured value of 8.7%. For the 3,760 Pa clay, the dL/dP estimate gives 0.4% gas volume, which shows nearly complete concealment of the measured gas volume of 7.9%.

Table 6.2: Comparison of estimated and measured gas volumes

Experiment	Test Vessel (ID)	Shear Strength (Pa)	Measured Gas Volume (Table 6.1)		Estimated Gas Volume from dL/dP data	
			V_{gas} (cm^3)	Void (%)	V_{gas} (cm^3)	Void (%)
1	4 in.	147	89.7	9.9	96	11
2	4 in.	3,760	94.8	10.9	90	10
3	4 in.	10,700	74.0	10.7	13	1.9
4	1 in.	14	38.0	9.6	37	9.4
5	1 in.	147	37.9	8.7	12	2.8
6	1 in.	3,760	27.0	7.9	1	0.4
90 μm glass beads	1 in.		40.2	14.4	35	13

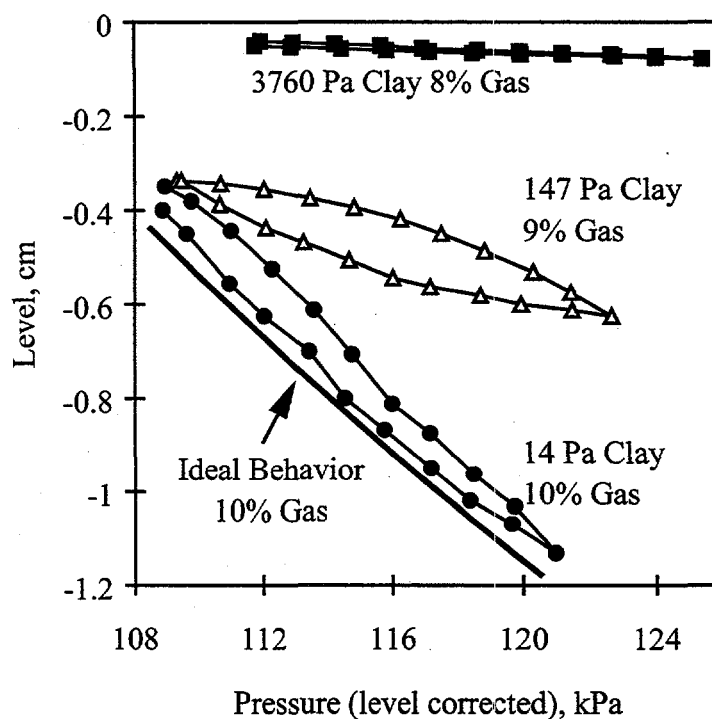


Figure 6.4: Level pressure results for bubbly bentonite clays in the 1 in. ID test vessel, with a range of shear strengths and with known gas contents (Experiments 4, 5, and 6). These data are from the last pressure cycle (typically the third) of each experiment. For the weakest clay, the level/pressure response is nearly identical to the predicted ideal behavior.

Figure 6.5 shows level pressure results for bubbly slurry made up of 90 μm glass beads (last experiment in Table 6.1). The level pressure response is nearly identical to the predicted ideal behavior. Table 6.2 compares the measured gas volume and the gas volume estimated from the dL/dP data. The dL/dP estimate of 13% gas is sufficiently close to the measured 14.4% gas volume fraction to consider this agreement good. It had been anticipated that capillary forces

acting on the bubbles within the bead pack would result in a measurable hysteresis between level and pressure. Further study is needed to explore the behavior of bubbles in particulate materials.

The experiment with the glass beads was conducted in the 1 in. ID test vessel, to make the bead pack reasonably tall. Previous studies have shown that the retained bubbles in particulate media will displace either interstitial liquid or suspended particles, depending on the particle diameter, the depth of the settled slurry, and the fluid and slurry densities (Gauglitz et al. 1996). The taller bead pack in this experiment forced the majority of the bubbles to displace interstitial liquid and to be dendritic. Because the bubbles displace the interstitial liquid primarily, the overall bubbly slurry does not expand and contract as expected. Accordingly, wall effects should be negligible, although this has not been proven.

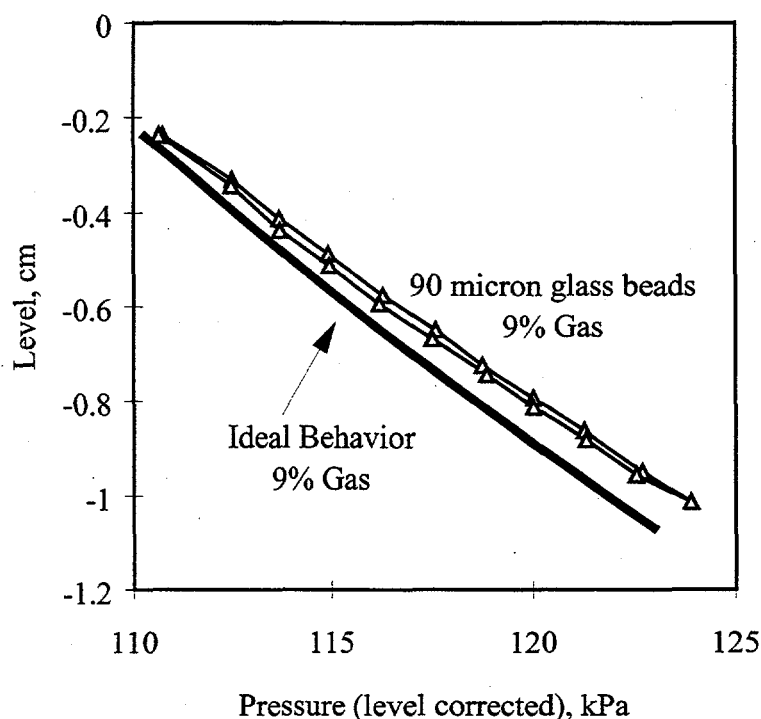


Figure 6.5: Level pressure results for bubbly slurry of 90 μm glass beads in the 1 inch ID test vessel with a known gas content. These data are from the third pressure cycle of a series of experiments. The level/pressure response is nearly identical to the predicted behavior based on an ideal gas.

6.3 Summary of Experimental Findings

The results show that the pressure level response can give an accurate estimate of the amount of retained gas in most cases. The data reported here are the first to test this relationship for simple simulants with retained gas. These experiments also confirm that the simulant strength alters the pressure/level relationship. In cases with very high waste strength, the strength can completely mask the presence of retained gas bubbles. This masking may be a wall effect. For the single experiment conducted with a particulate simulant (glass beads), the pressure/level response was

essentially identical to the expected ideal gas behavior. While these experiments have been effective at highlighting general behavior and confirming some aspects of existing models, they do not cover the full range of likely behavior. In addition, the typical pressure/level hysteresis observed in the actual tanks was not observed in the model systems of bentonite clay and glass bead slurries, although some hysteresis was certainly observed. A possible explanation is that the pressure cycling was too rapid (and we did not explore the effect of this time scale) and thus minimized the apparent hysteresis. An alternative explanation is that the simulants were not stiff enough for the hysteresis effect to be measurable (i.e., the steep slope and the shallow slope of the parallelogram were very close in value to each other).

7. Summary Findings and Recommendations

This section summarizes the major findings of these analyses and experiments, outlines the unexplained effects or other issues that should be addressed in future work, and lists some additional observations of interest.

7.1 Results

- The dL/dP_{STEEP} parameter in the waste material strength model can be estimated from the high-frequency high-resolution Hanford tank waste data contained in the TMACS database.
- The dL/dP_{STEEP} estimates tend to be larger in magnitude than the dL/dP estimates currently used to estimate the retained gas volumes in the Hanford tanks (from the daily field data).
- The experimental work showed that the gas law model held for many of the simulants and conditions tested.
- The experimental work suggests that tank waste material properties can mask the quantity of gas present; but no level/pressure hysteresis was observed for the simulants used in this small-scale experiment.
- The dL/dP_{STEEP} estimates calculated from the daily SACS data are closer to the dL/dP_{STEEP} estimates calculated from the TMACS data, than are the dL/dP estimates based on the ideal gas law model.
- For Tank A-101, the gas-law-based dL/dP estimate is within 10% of the linear dL/dP_{STEEP} estimate.

7.2 Relevant Unexplained or Unstudied Phenomena

The following unexplained or unstudied phenomena need to be documented and/or addressed by future work:

- An explanation of the observed lag in the level response to pressure changes is needed, so that the effect of the underlying phenomenology on retained gas volume estimates can be assessed. An alternative method for assessing the uncertainty of dL/dP might be based on the comparison of dL/dP from tank-waste level with dL/dP from direct measurements of gas volume.
- The relationship between the rise in level and the change in dL/dP_{STEEP} for Tank S-106 needs to be examined, to see whether a reasonable explanation can be found.
- The question of how to best synthesize multiple dL/dP_{STEEP} estimates for retained gas calculations needs to be considered carefully. While the median of these estimates will likely turn out to be a good best estimate; more thought needs to go into making the associated interval estimates (such as 95% confidence).
- The time of observation in the SACS database springs back and falls forward with Daylight Saving Time; while the time of observation of the HMS data is always Pacific Standard Time. While this discrepancy is small, we're beginning to look at the data at sufficiently small time scales that we need to apply a correction to one of these, so that the times actually match.
- There still remains a reasonable possibility that the hysteresis is instrumentation related. No hysteresis was observed in these experiments (although the lack of hysteresis might be

due to the properties of the waste simulants used), but the possible sticking (and definitely odd behavior) of the Enraf in Tank C-106⁸ suggests that instrumentation is a possible cause.

7.3 *Miscellaneous Observations*

- The double shell Tanks 241-AN-103, AN-104, and AN-105 do not exhibit much hysteresis between level and pressure.
- Tank 241-TX-102 has the largest dL/dP estimate observed for any Hanford tank, using the Enraf instrument.
- Tank 241-BX-110 Enraf data shows a small but clearly evident dL/dP. However, this tank was not flagged in the study in which the tank waste level data was used to detect retained gas in tank waste (Whitney 1995). At the time of this earlier study, no Enraf data were available for this tank and so the evaluation and flagging were based on the available Manual Tape data -- which does show a consistent rise in the level. Tanks S-112 and T-108 similarly would now be "flagged" by the methodology used in Whitney (1995); see Appendix C.

⁸ Information related to the possible sticking of the C-106 Enraf was gathered in "Flammable Gas Data Evaluation Progress Report", WTSFG96.1. P.D. Whitney, N.E. Wilkins, N.E. Miller, P.A. Meyer and M.E. Brewster.

8. References

- Andrews, GL and JW Buck, 1987. *Hanford Meteorological Station Computer Codes, Volume 6 - The SFC Computer Code*, Pacific Northwest Laboratory, PNL-6279 Vol. 6, Richland, WA.
- Dennis, JE and RB Schnabel, 1983. *Numerical Methods for Unconstrained Optimization and Nonlinear Equations*, Prentice Hall, Englewood Cliffs, NJ.
- Field, JG, DE Place and RD Cromar, 1997. *Tank Characterization Report for Single Shell Tank 241-A-101*, Lockheed Martin Hanford Corporation, HNF-SD-WM-ER-673, Rev. 0. Richland, WA.
- Gallant, RA, 1987. *Nonlinear Statistical Models*. John Wiley & Sons. New York.
- Gauglitz, PA, SD Rassat, PR Bredt, JH Konynenbelt, SM Tingey, and DP Mendoza, 1996. *Mechanisms of Gas Bubble Retention and Release: Results for Hanford Waste Tanks 241-S-102 and 241-SY-103 and Single-Shell Tank Simulants*. Pacific Northwest National Laboratory, PNNL-11298, Richland, WA.
- Glasscock, JA, 1993. *Surveillance Analysis Computer System Temperature Database Software Requirements Specification*. Westinghouse Hanford Company, WHC-SD-WM-CSRS-007, Rev. 1a, Richland WA.
- Hodgson, KM, RP Anantamula, SA Barker, KD Fowler, JD Hopkins, JA Lechelt, DA Reynolds, DC Hedengren, RE Stout, RT Winward, 1996. *Evaluation of Hanford Tanks for Trapped Gas*. Westinghouse Hanford Company, WHC-SD-WM-ER-526, Rev. 1. Richland, WA.
- Hoitink, DJ and KW Burk, 1994. *Climatological Data Summary 1993 with Historical Data*. Pacific Northwest Laboratory, PNL-9809, Richland, WA.
- Johnson, GD, WB Barton, RC Hill, JW Brothers, SA Bryan, PA Gauglitz, LR Pederson, CW Stewart and LH Stock, 1997. *Flammable Gas Project Topical Report*, Project Hanford Management Contractor. Technical report HNF-SP-1193, Rev. 2.
- Lange, NA, 1979. *Lange's Handbook of Chemistry*, McGraw Hill, New York, NY.
- Mahoney, LA. 1997. Transmittal of spreadsheet containing supporting calculations for Section 4.2 (A-101) of PNNL-11450 Rev. 1. March 1997. Pacific Northwest National Laboratory. Richland, WA.
- Meyer, PA, ME Brewster, SA Bryan, G Chen, LR Pederson, CW Stewart and G Terrones. 1997. *Gas Retention and Release Behavior in Hanford Double-Shell Waste Tanks*. PNNL-11536 Rev. 1, Richland, WA.
- PNL 1994. *TWINS User Guide: Tank Waste Information Network System, Version 4.0*, PNL-8824-2, Pacific Northwest National Laboratory, Richland, WA.
- Scaief, CC, 1994. *TMACS I/O Termination Point Listing*, Westinghouse Hanford Company, WHC-SD-WM-TI-594, Rev. 1, Richland, WA.

Shekarriz, A, DR Rector, LA Mahoney, MA Chieda, JM Bates, RE Bauer, NS Cannon, BE Hey, CG Linschooten, FJ Reitz, ER Siciliano, 1997. *Composition and Quantities of Retained Gas Measured in Hanford Waste Tanks 241-AW-101, A-101 AN-105, AN-104, and AN-103*. Pacific Northwest National Laboratory. PNNL-11450 Rev.1. Richland, WA.

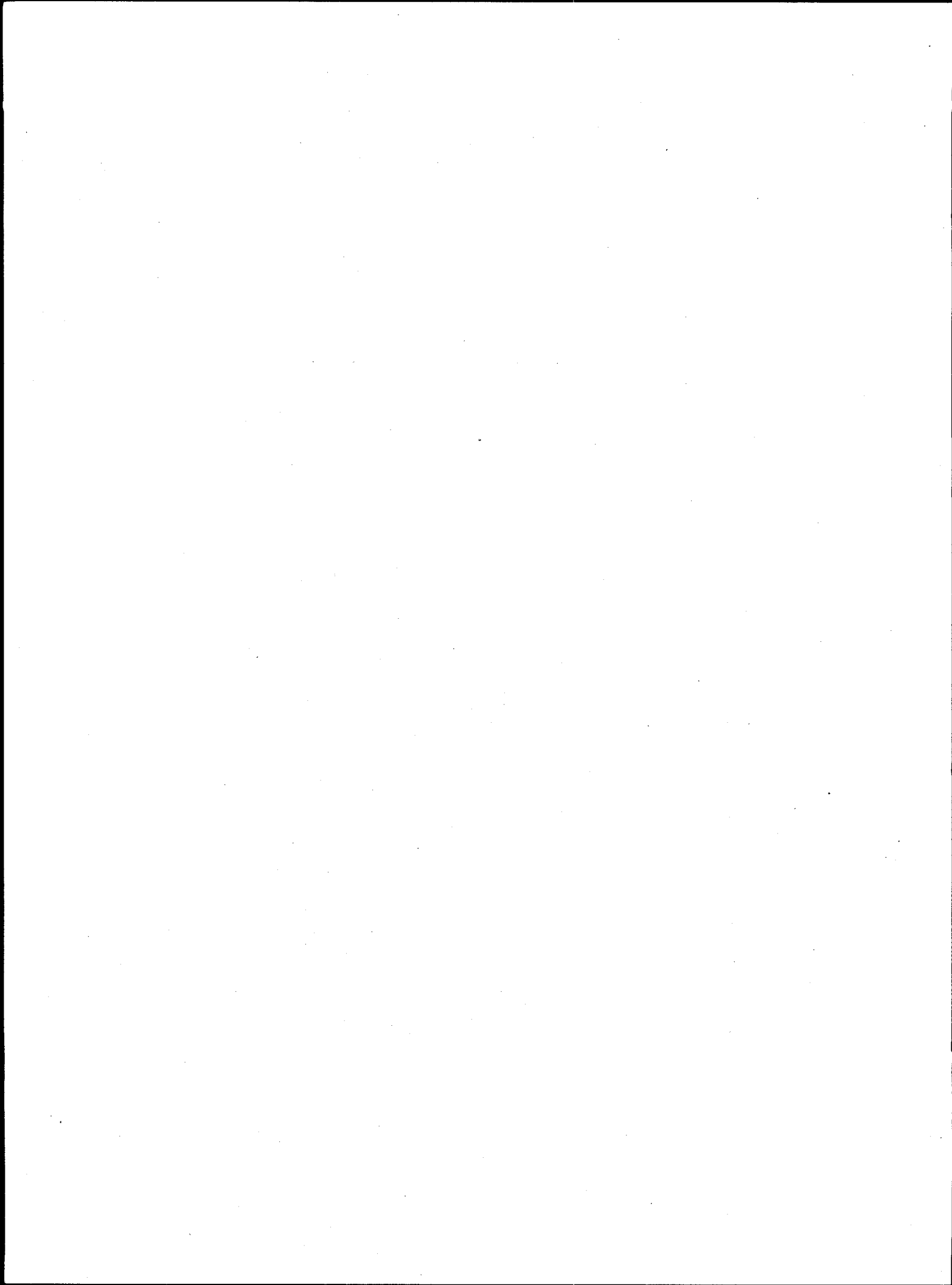
Stewart, CW, ME Brewster, PA Gauglitz, LA Mahoney, PA Meyer, KP Recknagle, HC Reed, 1996. *Gas Retention and Release Behavior in Hanford Single-Shell Tanks*, Pacific Northwest National Laboratory, PNNL-11391, Richland, WA.

Whitney, PD, PA Meyer, NE Wilkins, NE Miller, F Gao, AG Wood, 1996. *Flammable Gas Data Evaluation Progress Report*. Pacific Northwest National Laboratory, PNNL-11373, Richland, WA.

Whitney PD. 1995. *Screening the Hanford Tanks for Trapped Gas*. PNL-10821, Pacific Northwest National Laboratory, Richland, Washington.

Appendix A

Weather Station Location Effect on dL/dP



Appendix A: Weather Station Location Effect on dL/dP

The barometric pressure data from the Hanford Meteorological Station (HMS) has been compared with the waste level data from the Hanford tanks to assess the quantity of retained gas in the tank waste. The HMS is located between the 200E and 200W areas, but is not adjacent to any tank. To assess whether the station location significantly affected the dL/dP estimates, we obtained barometric pressure data from other stations around the Hanford area and calculated the usual dL/dP summary. The weather stations used were the 200E weather station, the Fast Flux Test Facility (FFTF) weather station and the Yakima Barricade (YAKB) weather station. These stations are significantly farther from the tanks than the HMS, and approximately surround the tank farms. Figure A.1 shows the station locations.

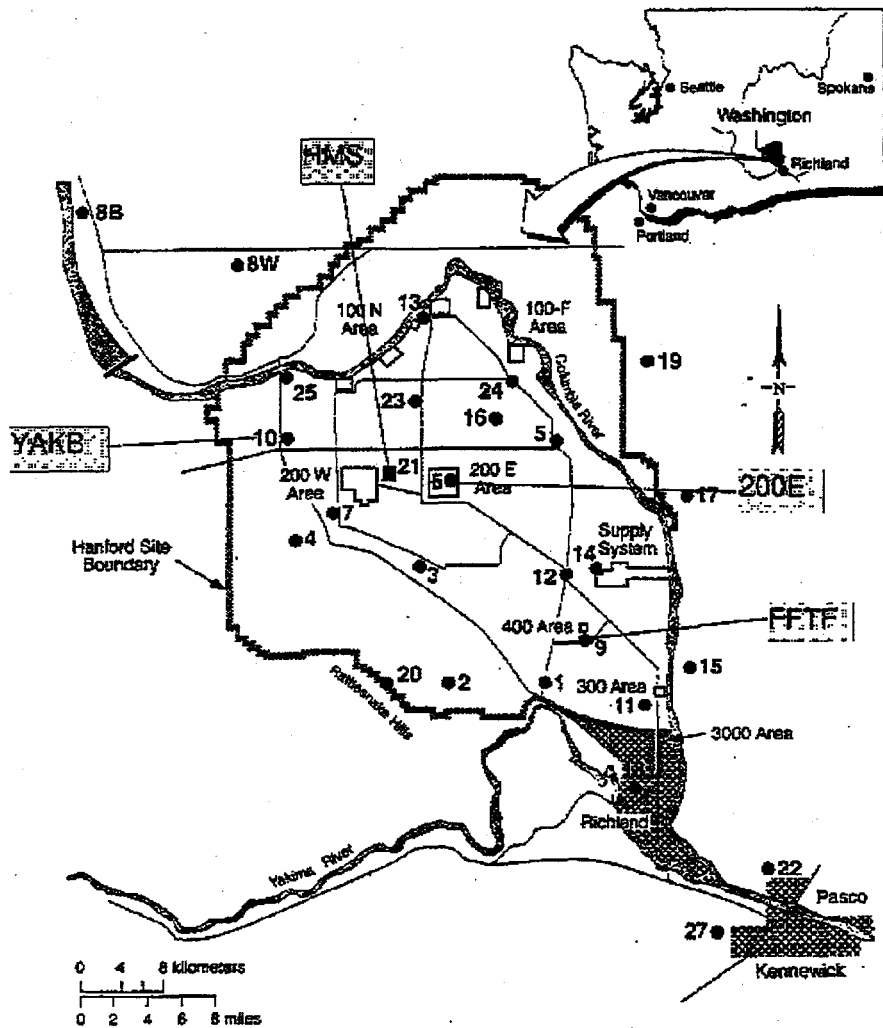


Figure A.1: HMS weather station locations (from Hoitink 1994)

There are two barometric pressure measurement devices at the HMS. Calculations of dL/dP were done for both. The devices are based on different measurement principles and their sampling patterns also differ. The HMS data is available hourly; and the HMS telemetry, 200E, FFTF and YAKB data are sporadically available (at least in the data sets used in this study); however, the

pattern of availability is the same for these 4 stations, so the same level measurements are used to calculate dL/dP.

The following table compares the median of the calculated dL/dP estimates (inches per inches Hg) for selected tanks and the weather stations:

Table A.1: dL/dP estimates for selected tanks and weather stations

<i>Station/Tank</i>	<i>AN-103</i>	<i>BX-104</i>	<i>S-106</i>	<i>TX-102</i>
HMS	-0.55	-0.07	-0.38	-1.46
HMS telemetry	-0.57	-0.07	-0.38	-1.39
200E	-0.57	-0.07	-0.39	-1.39
FFTF	-0.57	-0.07	-0.38	-1.38
YAKB	-0.58	-0.07	-0.39	-1.39

The dL/dP estimates are consistent for the 4 other stations. Since the HMS and HMS telemetry measurement devices are adjacent in the same building, and since the two measurements are close (see Figure A.2), the differences observed in dL/dP for the HMS and the other 4 stations must be due to the pattern of available weather measurements. Since the dL/dP values for the 4 widely located stations are consistent, we conclude that the HMS weather station barometric pressure data is as good as a barometric pressure measurement at the tank, for calculating dL/dP for any of the Hanford tanks.

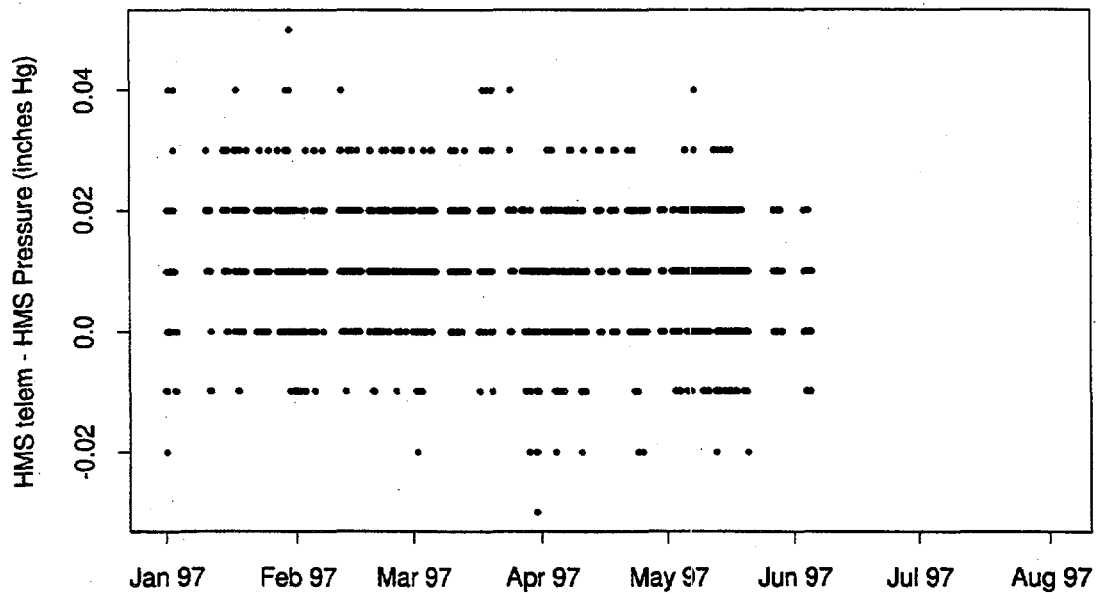
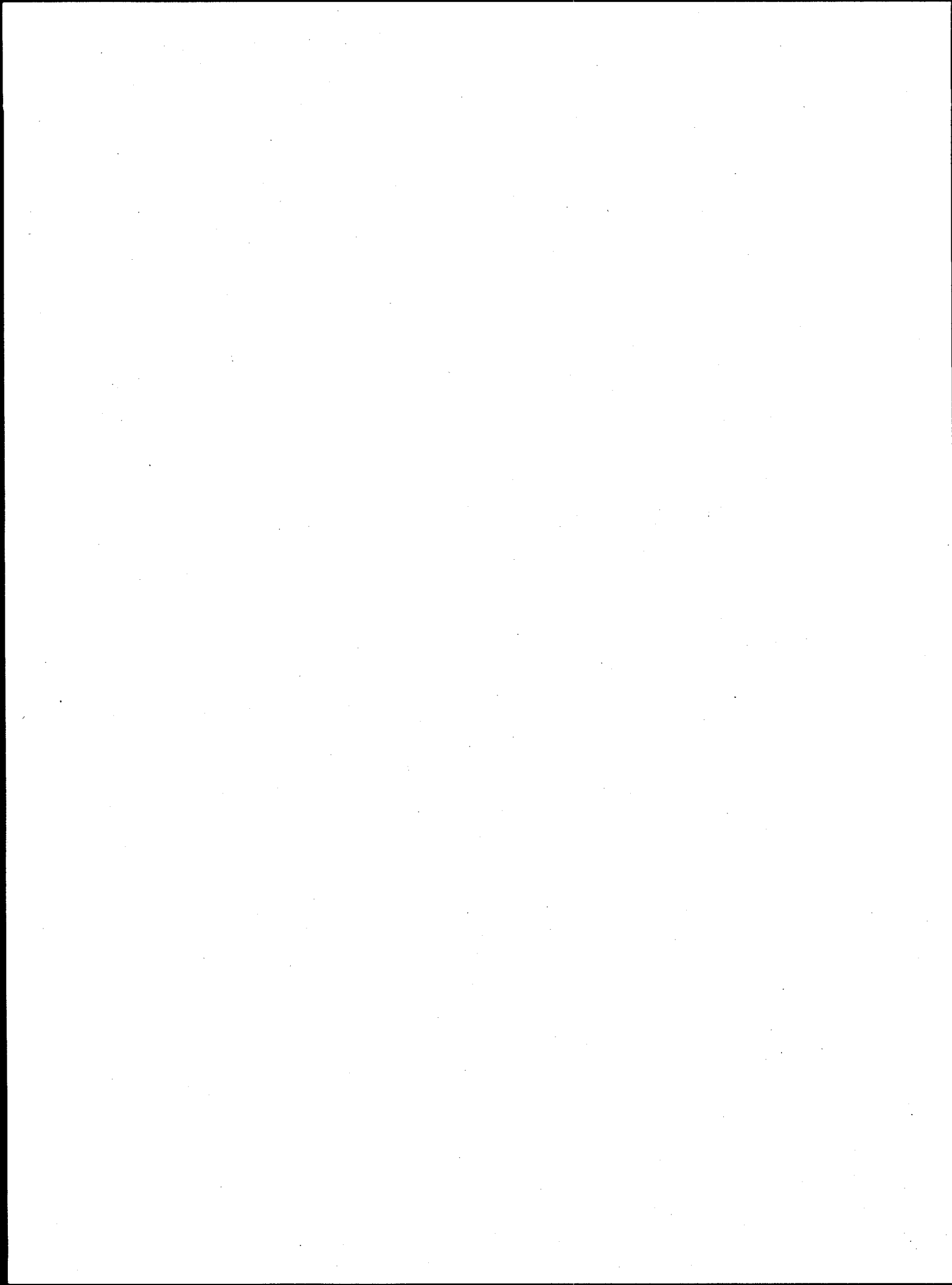


Figure A.2: HMS barometric pressure measurements compared.

Appendix B

Effect of Small Gas Releases on Waste Level in SSTs



Appendix B: Effect of Small Gas Releases on Waste Level in SSTs

We examined whether there was a detectable effect on the waste level measurements as a result of a small release of hydrogen in a single shell tank. Finding an effect would be consistent with the existence of a relation between waste level and retained gas. Our particular hypothesis was:

HYPOTHESIS: The fit of the model is better during periods with no hydrogen gas release as compared to periods during which hydrogen gas is released.

Procedure to Test Hypothesis

Candidate Air Pressure (AP) Intervals

Identify periods of 8-10 days during the winter, for which the air pressure falls over the first half of the period and then rises over the last half of the period, with a total range of about an inch of Hg or more.

Candidate H₂ Gas Release Intervals within Candidate AP Intervals

Identify tanks that appear to have had a gas release during the period of low pressure, within the candidate air-pressure intervals identified above. Periods having a gas release were identified by examination of the standard hydrogen monitoring system (SHMS) data. The gas release signature included a quick rise in hydrogen concentration over a short period (a day or less) and then an exponential decay over a period of several days.

Candidate AP Intervals with no H₂ Gas Release

Identify tanks that do not appear to have had a gas release during the period of low pressure, within the candidate air-pressure intervals identified above.

Discussion of Results

Analysis Periods and Tanks

During the winter of 1995-1996, candidate AP intervals were identified that contained periods both with and without gas releases for the Tanks S-111, U-103, and U-109, see Table B.1. The period containing a gas release for the three tanks was Dec 7 through Dec 18, 1995. The period of no gas release was Feb 29 through Mar 9, 1996.

Table B.1: Time windows centered at pressure low

	<u>Time Window</u>	<u>Date of AP Low</u>	<u>Inches Hg</u>
<u>Gas</u>	Dec 7-Dec 18, 1995	Dec 12, 1995	1.65
<u>No Gas</u>	Feb 29-Mar 9, 1996	Mar 4, 1996	0.95

Comparison of the Fits

For the three tanks studied, both during the periods of gas release and of no gas release, there remains quite a bit of structure in the residuals, indicating a rather poor fit between the data and

the model, see Table B.2. However, we do see a much smaller root mean square error (RMSE) for the residuals during the periods without gas release. The smaller RMSE indicates a better fit of the hysteresis model to the waste level and atmospheric pressure data. Thus, this analysis supports the hypothesis.

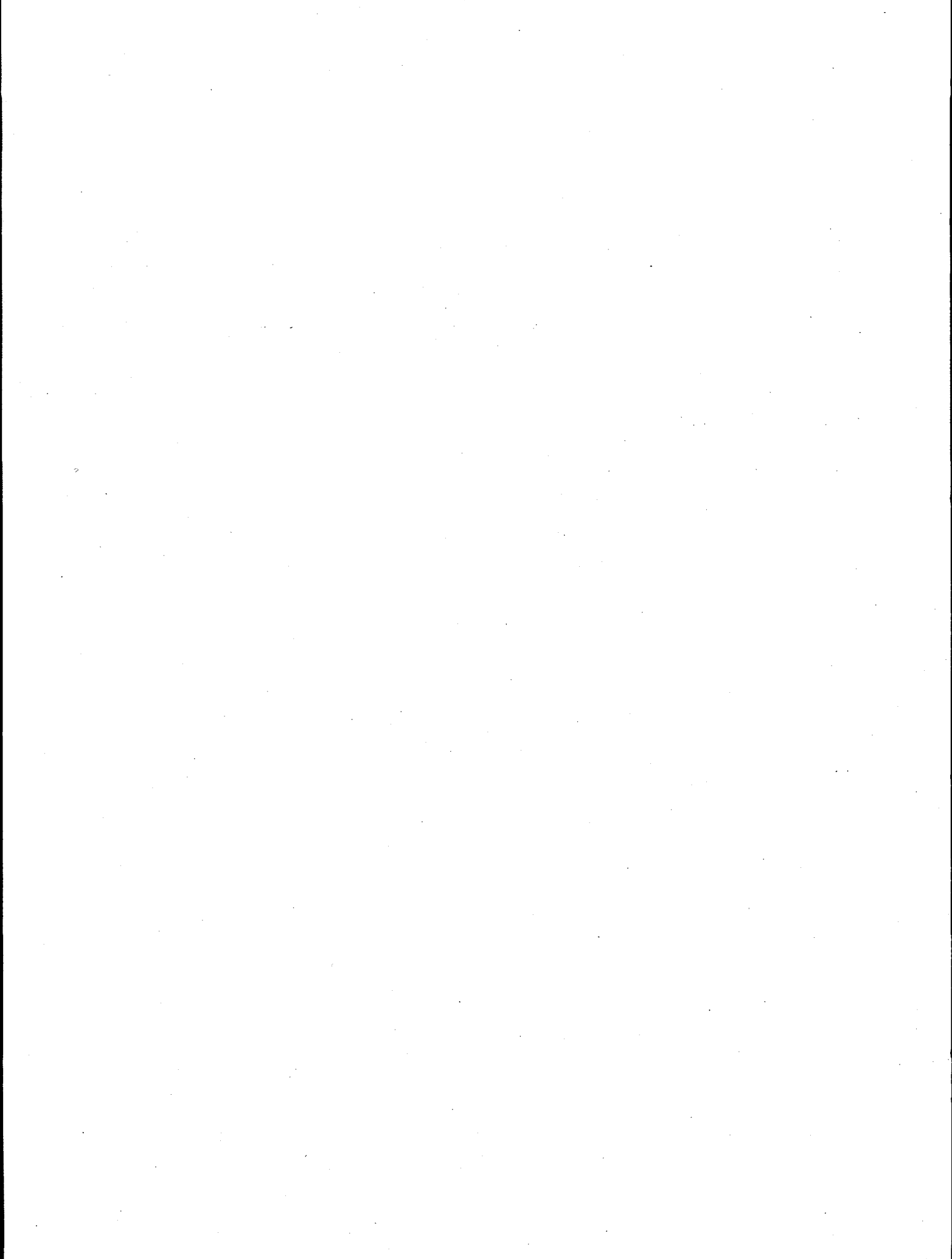
Table B.2: Comparison of waste level model fits for gas release and non-gas release time periods.

Tanks	No Gas RMSE	Gas RMSE
S-111	0.027	0.054
U-103	0.026	0.089
U-109	0.040	0.083

In terms of the magnitude of the residuals, we see degradation in model performance by a factor of two for Tanks S-111 and U-109, and by a factor of about three for Tank U-103.

Appendix C

Information Provided for Tank Evaluations for FY97



Appendix C: Information Provided for Tank Evaluations for FY97

Two types of level/pressure analyses were done for tank level data. The objective of both is to ascertain the extent to which tank waste level and atmospheric pressure are inversely correlated. One analysis is based on breaking the level data into short time intervals (typically 15 days) and performing a regression analysis of tank waste level on the corresponding pressure measurements. The slopes from these regressions are dL/dP estimates and are summarized by a distribution; such as Figure C.2. The quartiles of the distribution, along with the 5th and 95th percentiles are included on each summary. These distribution estimates were discussed in Whitney (1995). A Gaussian distribution is fit to the raw distribution as well, for potential application in Monte-Carlo risk analyses. Another type of summary, typified by Figure C.3, shows the time-history of dL/dP estimates. These estimates are obtained using a Kalman filter methodology described earlier⁹.

Evaluation of Tank 241-BY-103

Two types of level data were analyzed, the interstitial liquid levels estimated from neutron logging and Enraf surface levels. The Enraf levels were read at high frequency via an attached data logger.

Figure C.1 shows the high frequency Enraf levels and the atmospheric pressure measurements. There is no significant relation between the two: the level varies only 0.05 inches while the pressure varies over an inch Hg during the time span.

Figure C.2 shows the summary dL/dP estimates for BY-103 based on the ILL. Six time intervals of ILL data contributed to the calculation: three of the six intervals have negative dL/dP estimates, providing no strong indication of gas retained. A Kalman-filter-based analysis of the ILL data, illustrated in Figure C.3, also shows no indication of level fluctuations with barometric pressure changes.

⁹ "Flammable Gas Data Evaluation Progress Report", WTSFG96.1. P.D. Whitney, N.E. Wilkins, N.E. Miller, P.A. Meyer and M.E. Brewster.

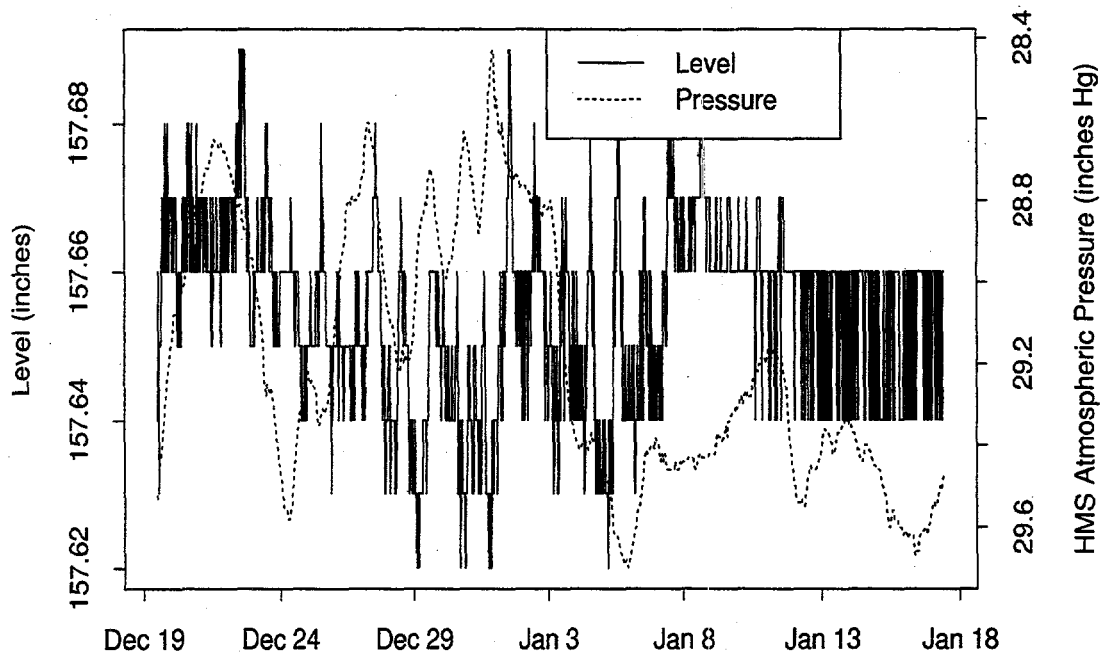


Figure C.1: Comparison of Enraf level measurements and HMS atmospheric pressure for Tank BY-103.

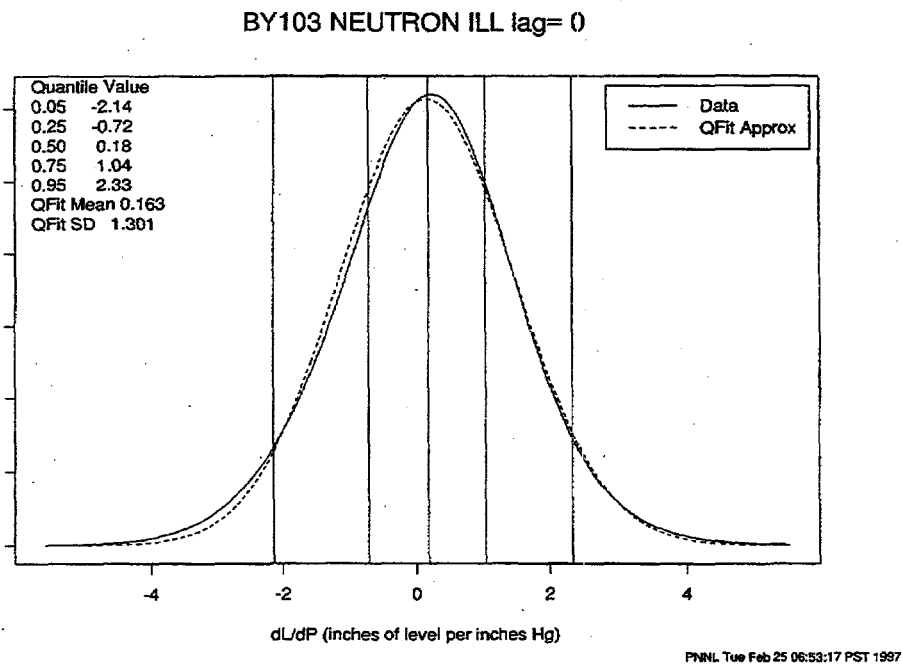


Figure C.2: Summary dL/dP calculation for Tank 241-BY-103 neutron interstitial liquid levels. The units for dL/dP are inches per inches Hg.

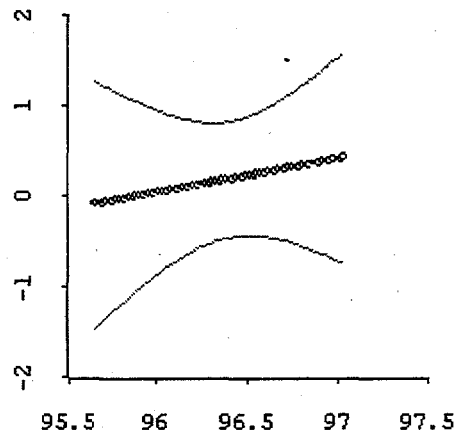


Figure C.3: Estimated dL/dP (cm per kPa) for Tank BY-103 based on the ILL data from November 1, 1995 through January 1, 1997. The center line is the dL/dP estimate and the surrounding lines are approximate 95% confidence limits. Negative dL/dP estimates would indicate retained gas; the analysis summarized in the figure is not strong evidence that gas is present.

Evaluation of Tank 241-S-112

In support of the evaluation of Tank 241-S-112 for flammable gas hazard, the interstitial liquid levels (from 12-93 through 2-97) for this tank were analyzed for correlation with atmospheric pressure. The analyses showed a significant correlation between the ILL's and atmospheric pressure; 16 of the 20 dL/dP estimates calculated were negative, providing strong evidence for retained gas in the tank waste. Figure C.4 shows the dL/dP estimate. Previous work¹⁰ had not shown this tank's waste to contain retained gas. However, far more data are now available, so even though the ILL data is the least accurate level measurement routinely used in the Hanford tanks, it offers one a better chance of detecting retained gas, if present. The Kalman-filter-based analysis of this data, Figure C.5, also shows the presence of retained gas.

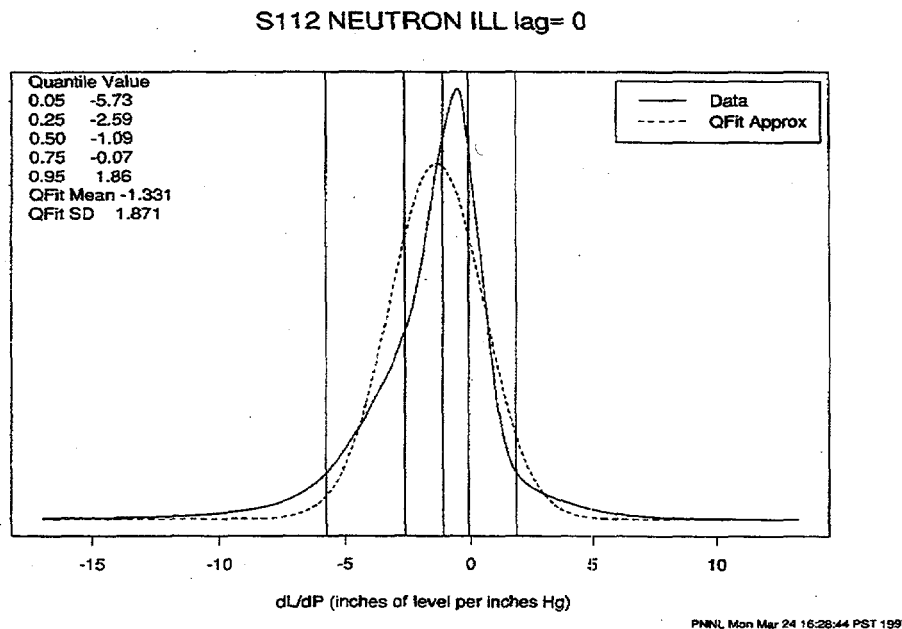


Figure C.4: Summary ILL calculation for Tank 241-S-112. The units for dL/dP are inches per inches Hg.

¹⁰ Whitney PD. 1995. *Screening the Hanford Tanks for Trapped Gas*. PNL-10821, Pacific Northwest National Laboratory, Richland, Washington.

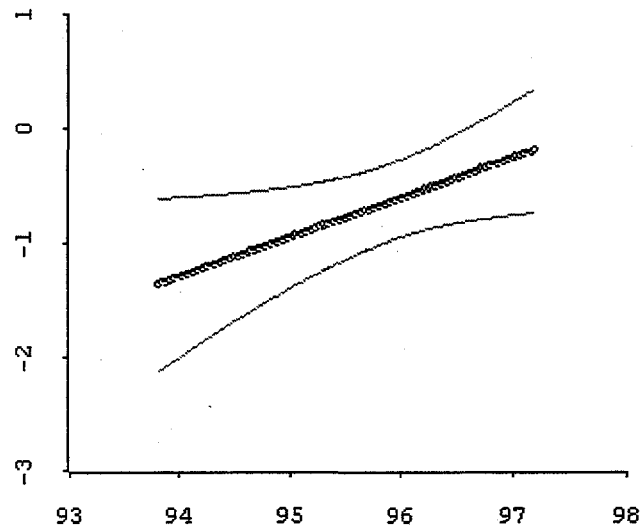


Figure C.5: Estimated dL/dP (cm per kPa) for Tank S-112 based on the ILL data from the beginning of 1994 through February 1997. The centerline is the dL/dP estimate and the surrounding lines are approximate 95% confidence limits. The negative dL/dP estimates are consistent with retained gas.

Evaluation of Tank 241-SX-106

Tank SX-106 (on the flammable gas watch list) data were analyzed for level-pressure correlation. The ILL, Enraf levels and FIC levels, Figures C.6, C.7, and C.8, all clearly indicate the presence of retained gas. Note that the median dL/dP estimates for the FIC and Enraf agree within 5.5%, with the Enraf dL/dP uncertainty estimates being smaller. The Enraf, FIC and ILL dL/dP estimates are consistent: the twenty-fifth and seventy-fifth quantiles of the ILL-dL/dP estimate contain the .05-.95 range for the other two.

SX106 NEUTRON ILL lag= 0

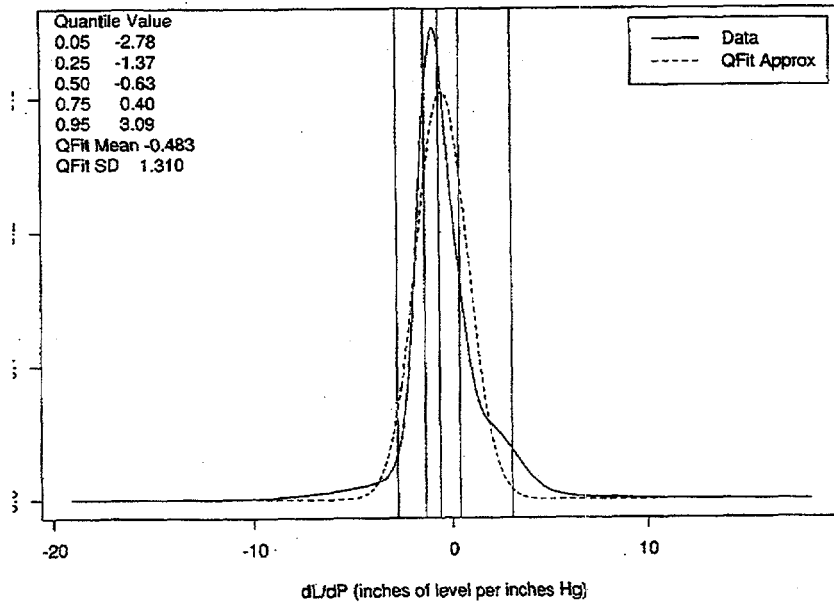
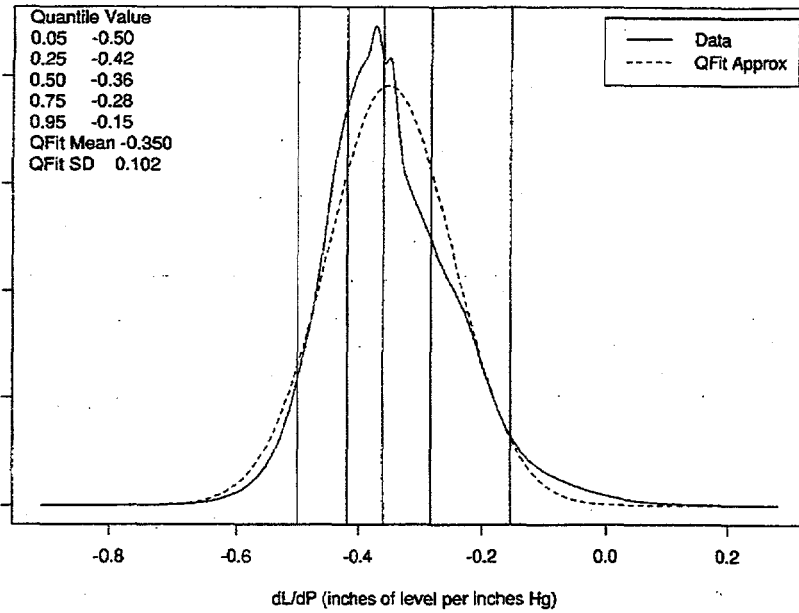


Figure C.6: Summary ILL calculation for Tank 241-SX-106. The units for dL/dP are inches per inches Hg.

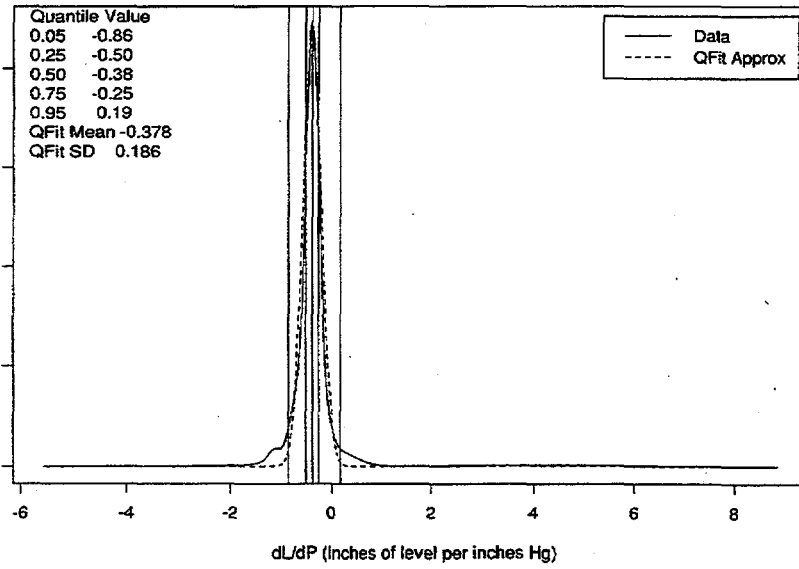
SX106 ENRAF lag= 0



PNNL Tue Apr 29 14:53:07 PDT 1997

Figure C.7: Summary Enraf calculation for Tank 241-SX-106. The units for dL/dP are inches per inches Hg.

SX106 Auto FIC lag= 0



PNNL Tue Apr 29 14:51:26 PDT 1997

Figure C.8: Summary FIC calculation for Tank 241-SX-106. The units for dL/dP are inches per inches Hg.

Evaluation of Tank 241-T-108

Tank T-108 Enraf levels show a strong indication of a small quantity of retained gas. Figure C.9 shows a summary of the dL/dP calculations. This tank was not flagged in an earlier screening (Whitney, 1995), most likely due to the relatively poor level measurements available at the time and the small amount of gas indicated by the dL/dP.

T108 ENRAF lag= 0

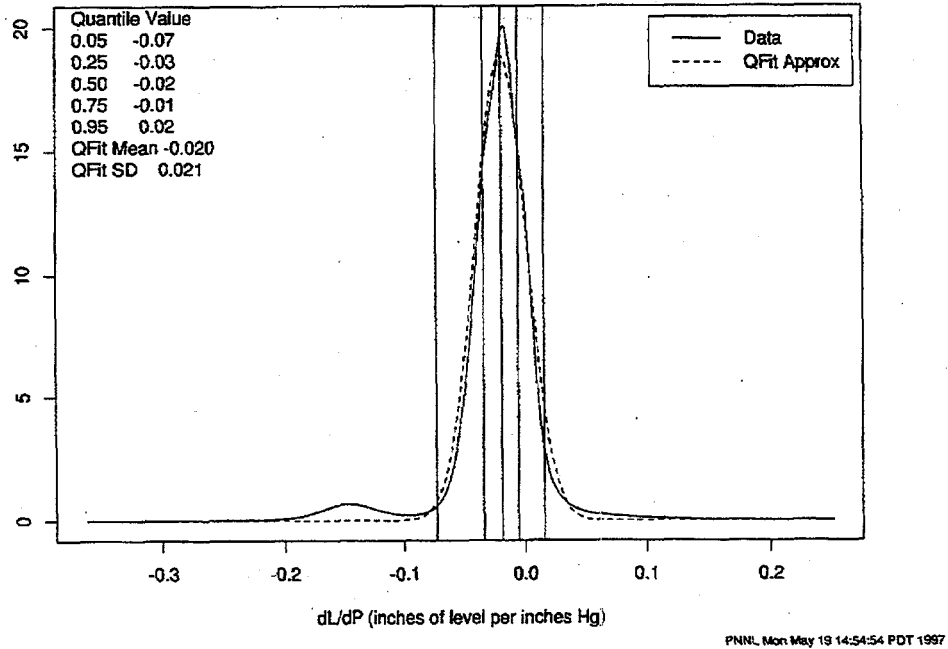


Figure C.9: Summary Enraf calculation for Tank 241-T-108. The units for dL/dP are inches per inches Hg.

Evaluation of Tank 241-T-111

Tank T-111 was salt-well pumped between 5-94 and 2-8-95. The subsequent level measurements (through 4-97) were analyzed to determine whether a significant level/pressure correlation was present. Neither Enraf nor ILL measurements indicate the presence of retained gas, see Figures C.10 and C.11. Note that the dL/dP summaries for the two are consistent, with the Enraf's dL/dP summary distribution (0.25 quantile of -0.01 and 0.75 quantile of 0.03 inch per inches Hg) being more precise than that for the ILL, as expected based on the relative precision of the two level measurements.

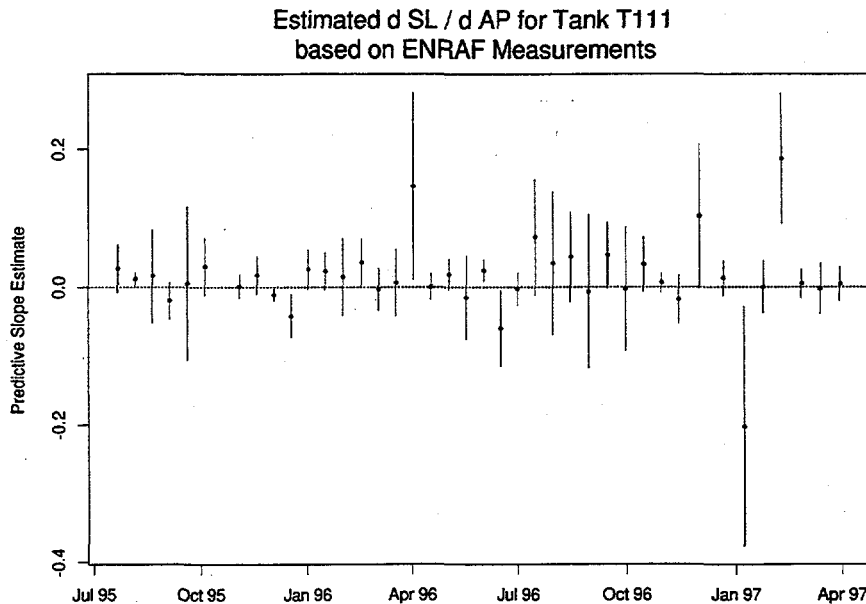


Figure C.10: Summary Enraf calculation for Tank 241-T-111. The units for dL/dP, which is the “predictive slope estimate” are inches per inches Hg. That the majority of dL/dP estimates are positive indicates no detectable retained gas in this tank’s waste.

T111 NEUTRON ILL lag= 0

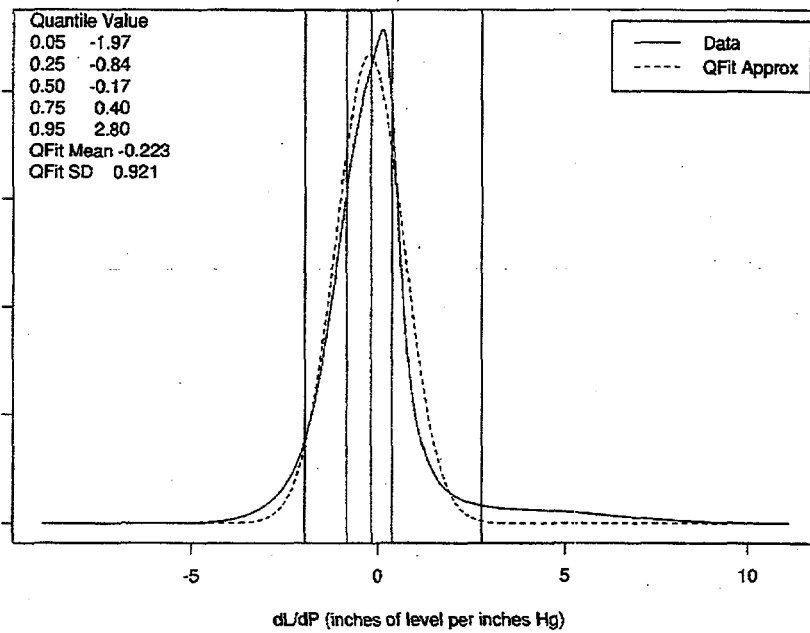


Figure C.11: Summary ILL calculation for Tank 241-T-111. The units for dL/dP are inches per inches Hg.

Distribution

<u>No. of Copies</u>		<u>No. of Copies</u>	
OFFSITE		ONSITE	
2	Los Alamos National Laboratory P.O. Box 1663 Los Alamos, NM 87545 Agnew, S.F. J5-86 Kubic, W.L. K5-75	4	DOE Richland Operations Office C.A. Groendyke S7-54 G.M. Neath S7-51 G.W. Rosenwald S7-54 K. Chen S7-54
1	Sandia National Laboratories Nuclear Facilities Safety Dept. P.O. Box 5800 Albuquerque, NM 87185 Powers, D.A. 0744	25	Hanford Contractors M.J. Bailey T4-07 D.A. Barnes R1-80 G.S. Barney T5-12 W.B. Barton R2-12 R.E. Bauer S7-14 R.J. Cash S7-14 D.B. Engelman L6-37 J.M. Grigsby S7-14 G.W. Hood S7-73 G.D. Johnson (5) S7-14 N.W. Kirch R2-11 C.E. Leach R1-49 J.A. Lechelt R2-11 J.W. Lentsch S2-48 J.E. Meacham S7-14 T.E. Rainey H6-12 R.E. Raymond S7-12 E.R. Siciliano H0-31 L.M. Stock S7-14 R.J. Van Vleet A3-34 N.E. Wilkins R2-12
1	Campbell, D.O. 102 Windham Road Oak Ridge, TN 37830		
1	Hudson, B.C. 202 North Ridge Court Lindsborg, KA 67456		
1	Nuclear Consulting Services, Inc. P.O. Box 29151 Columbus, OH 43229 Kovach, J.L.		
1	Kress, T.S. 102-B Newridge Road Oak Ridge, TN 37830		
1	Larson, T.E. 2711 Walnut Street Los Alamos, NM 87544		
1	Slezak, S.E. 806 Hermosa NE Albuquerque, NM 87110		

**No. of
Copies**

ONSITE (cont'd)

25 Pacific Northwest National Laboratory

J.M. Bates	K7-15
J.W. Brothers (5)	K9-20
S.A. Bryan	P7-25
G. Chen	K5-12
T.A. Ferryman	K5-12
P.A. Gauglitz	P7-41
R.T. Hallen	K2-12
P.G. Heasler	K5-12
P.A. Meyer	K7-15
N.E. Miller	K5-12
L.M. Peurrung	P7-41
B.A. Pulsipher	K5-12
S.D. Rassat	P7-41
K.M. Remund	K5-12
F.M. Ryan	K2-18
C.W. Stewart	K7-15
P.D. Whitney (5)	K5-12
Information Release Office (7)	K1-06